ELSEVIER

Marine Micropaleontology 47 (2002) 17–70

MARINE MICROPALEONTOLOGY

www.elsevier.com/locate/marmicro

Age and paleoenvironment of the Maastrichtian to Paleocene of the Mahajanga Basin, Madagascar: a multidisciplinary approach

S. Abramovich [a,*], G. Keller [a], T. Adatte [b], W. Stinnesbeck [c], L. Hottinger [d], D. Stueben [e], Z. Berner [e], B. Ramanivosoa [f], A. Randriamanantenasoa [g]

[a] *Department of Geosciences, Princeton University, Princeton, NJ 08544, USA*
[b] *Geological Institute, University of Neuchâtel, CH-2007 Neuchâtel, Switzerland*
[c] *Geological Institute, University of Karlsruhe, D-76128 Karlsruhe, Germany*
[d] *Museum of Natural History, CH-4001 Basel, Switzerland*
[e] *Petrography and Geochemistry Institute, University of Karlsruhe, D-76128 Karlsruhe, Germany*
[f] *Musée Akiba, PO Box 652, Mahajanga 401, Madagascar*
[g] *Département des Sciences de la Terre, Université de Mahajanga, Mahajanga, Madagascar*

Received 30 May 2001; received in revised form 1 May 2002; accepted 8 May 2002

Abstract

Lithology, geochemistry, stable isotopes and integrated high-resolution biostratigraphy of the Berivotra and Amboanio sections provide new insights into the age, faunal turnovers, climate, sea level and environmental changes of the Maastrichtian to early Paleocene of the Mahajanga Basin of Madagascar. In the Berivotra type area, the dinosaur-rich fluvial lowland sediments of the Anembalemba Member prevailed into the earliest Maastrichtian. These are overlain by marginal marine and near-shore clastics that deepen upwards to hemipelagic middle neritic marls by 69.6 Ma, accompanied by arid to seasonally cool temperate climates through the early and late Maastrichtian. An unconformity between the Berivotra Formation and Betsiboka limestone marks the K–T boundary, and juxtaposes early Danian (zone Plc? or Pld) and latest Maastrichtian (zones CF2–CF1, *Micula prinsii*) sediments. Seasonally humid warm climates began near the end of the Maastrichtian and prevailed into the early Danian, accompanied by increased volcanic activity. During the late Danian (zones P1d–P2), a change to seasonally arid climates was accompanied by deepening from middle to outer neritic depths.

Keywords: Madagascar; Maastrichtian; Paleocene; age; paleoclimate; paleoenvironment

1. Introduction

Madagascar plays an unique role in the geographic and biological history of the Earth. Ever since its separation from Africa 125–130 Ma ago and its separation from India and the Seychelles

* Corresponding author. Tel.: +1-609-258-4117; Fax: +1-609-258-1671.
E-mail address: sigala@princeton.edu (S. Abramovich).

0377-8398/02/$ – see front matter
PII: S0377-8398(02)00094-4

about 88 Ma ago (e.g. Storey et al., 1997; Rogers et al., 2000), Madagascar developed a unique Gondwana paleofauna, and high endemism in terrestrial and fresh water faunas and floras persisting until today. Late Cretaceous dinosaur-rich vertebrate faunas of the Mahajanga Basin have long been known and there are many recent studies (Forster et al., 1996; Krause and Hartman, 1996; Krause et al., 1997, 1999; Sampson et al., 1998). The uppermost dinosaur faunas appear in the Anembalemba Member of the Maevarano Formation, and are overlain by marine beds of the Berivotra Formation, followed by the Danian Betsiboka limestone. A number of studies have corroborated a Maastrichtian age for the marine sediments of the Berivotra Formation based on sporadic calcareous nannofossil and planktic foraminiferal data (e.g. Perch-Nielsen and Pomerol, 1973; Bignot et al., 1996, 1998; Janin et al., 1996), but no systematic study has been published. Rogers et al. (2000) argued that the terrestrial sequence is time transgressive and of late Maastrichtian age in the Berivotra type area, and therefore contemporaneous with the dinosaur-rich vertebrate faunas recovered from the Deccan basalt sequence of India and dated between 67.5 and 65 Ma.

As part of a broader project aimed at developing a global high-resolution faunal, climatic and environmental history for the late Cretaceous to early Tertiary, we have investigated two sections from the Mahajanga Basin of Madagascar. One is the type section of the Berivotra Formation and the second is a cement quarry near the village of Amboanio. The primary objectives of this study are to determine the biostratigraphy, provide age control for the various rock units, and reconstruct the environmental history of the Mahajanga Basin based on macrofaunas and microfaunas, sedimentology, mineralogy and stable isotopes. Our analytical approach includes: (1) microfossil stratigraphy based on planktic foraminifera and augmented by calcareous nannofossils to determine the age of the marine strata overlying the dinosaur-bearing beds of the Mahajanga Basin; (2) lithology, bulk rock and clay mineral compositions to determine the depositional environment; (3) analysis of planktic foraminifera, larger benthic foraminifera and macrofossil assemblages to characterize the local marine ecosystem and identify paleoceanographic events; (4) stable isotope analysis to evaluate climate and productivity trends; and (5) correlation and comparison of faunal and climatic events with global trends.

2. Methods

Marine Maastrichtian to Danian sections were studied from two localities previously reported by Rogers et al. (2000) in the Mahajanga Basin of northwestern Madagascar (Fig. 1). One is the type locality of the Berivotra Formation near Berivotra village, and the second is in a cement quarry near the village of Amboanio. The sections were measured and described with particular emphasis on bioturbation, trace fossils, macrofossil horizons, hardgrounds and erosion surfaces. At the Berivotra type section, in all 36 samples were collected at approximately 1-m intervals and at 20-cm intervals at the top. At Amboanio, totally 54 samples were collected at 20–50-cm intervals, with the uppermost meter of the Berivotra Formation sampled at 10-cm intervals.

For the micropaleontological studies, marl lithologies were disaggregated in tap water and washed through a >63-μm sieve until clean foraminiferal residues were recovered. The washed samples were oven-dried at 50°C, and sifted through a >150-μm sieve. At the Berivotra section, the >150-μm sieved residues are composed mostly of small benthic foraminifera, larger benthic foraminifera, ostracods, bivalves and bryozoans, with relatively few planktic foraminifera. Therefore, only species census data was obtained from the >63-μm size fraction (Table 1).

Fig. 1. (a). Paleolocation of Madagascar and Site 525A during the late Maastrichtian. Note the similar paleolatitude positions of these two localities. (b). Simplified geographic map of Madagascar Island showing the locality of the Mahajanga Basin. (c). Late Cretaceous geology of the Mahajanga Basin (modified after Rogers et al., 2000) and locations of the two sections analyzed.

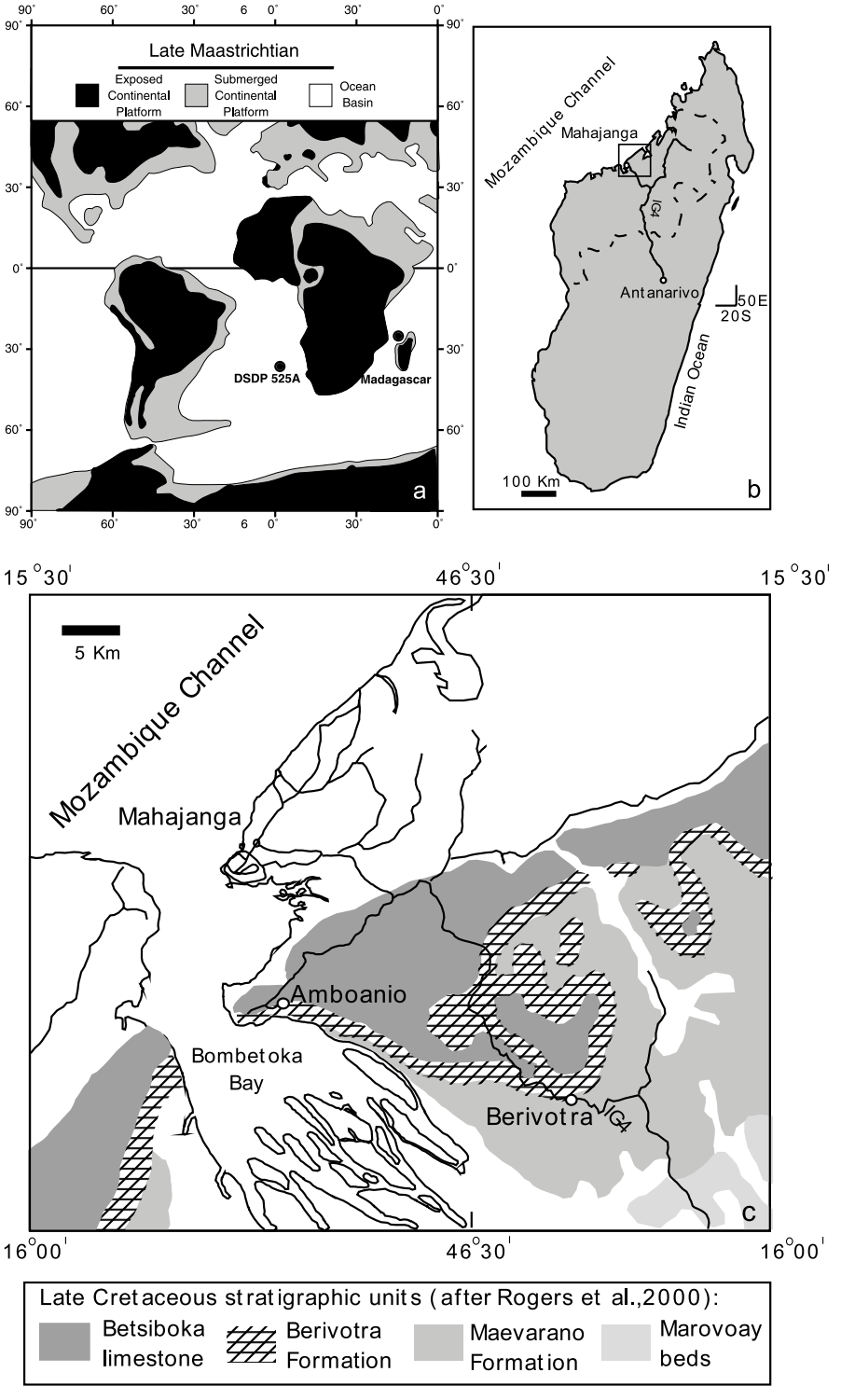
Late Maastrichtian
Exposed Continental Platform
Submerged Continental Platform
Ocean Basin
DSDP 525A
Madagascar
a
Mozambique Channel
Mahajanga
Antanarivo
50E
20S
Indian Ocean
100 Km
b
15°30'
46°30'
5 Km
Mozambique Channel
Mahajanga
Amboanio
Bombetoka Bay
Berivotra
c
16°00'
Late Cretaceous stratigraphic units (after Rogers et al.,2000):
Betsiboka limestone
Berivotra Formation
Maevarano Formation
Marovoay beds

Table 1
Planktic foraminiferal occurrences at the Berivotra section Madagascar

Sample	8	9	10	11	12	13	14	15	16	17	18	19	20	21	22	23	24	25	26	27	28
Depth (m)	5.6	6	6.2	11	12	13	14	15	16	18	19	20	21	22	23	24	25	26	27	28	29
Planktic foraminiferal zones (CF)	CF2–1			CF4					CF5		CF6										
Calcareous nannofossil zones	*Micula prinsii*			*Lithraphidites quadratus* (CC25c)																	
Abathomphalus mayaroensis						x															
Archaeoglobigerina blowi																					x
A. cretacea						x	x							x			x				
Heterohelix dentata	x	x	x	x	x	x	x	x	x	x	x	x	x	x	x	x	x	x	x	x	x
H. globulosa	x	x	x	x	x	x	x	x	x	x	x		x	x	x	x	x	x	x	x	x
H. labellosa		x																			
H. planata										x				x							
H. rajagopalani						x	x		x	x	x			x				x			
Gansserina gansseri																					x
G. weidenmayeri										x											
Globigerinelloides aspera														x							
G. aff. ultramicrus										x											
G. subcarinatus														x							
Globotruncana aegyptiaca	x	x		x	x	x	x	x	x	x	x	x	x	x	x	x	x			x	x
G. arca	x		x	x	x	x	x	x	x	x	x	x	x	x	x	x	x	x	x	x	x
G. bulloides										x									x		
G. duepeblei						x									x				x		
G. esnehensis												x		x						x	
G. falsostuarti				x		x		x	x								x	x			x
G. insignis												x									
G. linneiana										x										x	
G. mariei		x																			
G. orientalis				x	x		x	x	x	x	x		x		x	x	x			x	x
G. rosetta		x			x	x			x		x			x							
G. ventricosa				x	x	x	x	x		x		x	x								
Globotruncanella havanensis							x														
G. petaloidea													x								
Globotruncanita angulata							x	x	x			x		x				x			
G. pettersi																					
G. stuarti				x		x	x		x		x	x	x	x	x	x	x	x		x	x
G. stuartiformis		x		x	x	x	x	x	x	x	x	x	x	x		x		x	x		x
Gublerina cuvillieri					x	x															x
Guembelitria cretacea	x	x	x	x	x	x	x	x	x	x	x	x	x	x	x	x	x	x	x	x	x
G. dammula	x	x	x	x	x	x	x	x	x	x	x	x	x	x	x	x	x	x	x	x	x
Laheviheterohelix glabrans													x								

Table 1 (*Continued*).

Sample	8	9	10	11	12	13	14	15	16	17	18	19	20	21	22	23	24	25	26	27	28
Depth (m)	5.6	6	6.2	11	12	13	14	15	16	18	19	20	21	22	23	24	25	26	27	28	29
Planktic foraminiferal zones (CF)	CF2–1			CF4					CF5		CF6										
Calcareous nannofossil zones	*Micula prinsii*			*Lithraphidites quadratus* (CC25c)																	
Planoguembelina acervulinoides		x							x	x		x				x	x	x	x	x	x
P. brazoensis			x				x			x											
P. carseyae					x								x								
Pseudoguembelina costulata	x	x															x				
P. excolata				x	x	x	x	x	x	x				x					x		
P. hariaensis		x																			
P. kempensis							x														
P. palpebra		x			x														x		
Pseudotextularia deformis	x	x		x	x	x	x	x	x	x	x		x	x	x	x		x			x
P. elegans	x	x	x	x	x	x	x	x	x	x	x	x	x	x	x	x	x	x	x	x	x
P. intermedia	x	x		x	x		x	x	x	x	x		x	x	x		x	x			
Racemiguembelina fructicosa	x							x													
R. powelli		x		x	x	x	x	x	x	x	x	x									
Rosita contusa	x	x				x			x									x			x
R. fornicata																	x				
R. patelliformis												x								x	
R. plicata	x					x		x	x	x				x	x						x
R. plummerae											x		x	x							
R. walfischensis					x	x							x		x		x	x	x		
Rugoglobigerina hexacamerata	x				x	x			x			x	x	x							
R. macrocephala														x				x			
R. milamensis				x	x																
R. pennyi		x		x	x		x			x	x				x	x	x				
R. rugosa	x	x	x	x	x	x	x	x	x	x	x		x	x	x		x			x	
R. scotti	x		x	x	x	x	x		x	x	x	x	x		x		x	x	x		x
R. cf. *Scotti*			x		x					x			x				x				

x = present.

Table 2
Relative percent abundances of planktic foraminifera in the 63–150-μm size fraction at the Amboanio Quarry, Madagascar

Sample	1	2	3	4	5	6	7	8	9	10	11	12	13	14	15	16	18	19	20	22
Depth (m)	0	0.7	1.1	1.5	1.9	2.3	2.7	3.1	3.5	4.02	4.26	4.44	4.6	4.8	5	5.2	5.56	5.72	5.88	6.34
CF zones (planktic foraminifera)	CF4																		CF3	
Calcareous nannofossil zones	*Lithraphidites quadratus* (CC25c)																			
Archaeoglobigerina blowi	1				x		x						x	x		x		x	x	x
A. cretacea			x		x					x							x	x	x	
Hedbergella spp.	6	6	3	2	2	4	5	5	6	2	4	5	7	5	5	5	12	7	10	3
Heterohelix carinata	x	x		x	x	x				x		x			x		x	x	x	x
H. dentata	23	20	33	31	29	36	28	26	18	25	21	20	17	15	16	14	12	18	15	35
H. globulosa	13	20	11	5	7	6	9	6	10	11	6	5	11	18	27	13	12	24	27	27
H. navarroensis	3	4	4	3	2	4	4	6	4	5	5	3	5	5	4	5	8	8	7	9
H. planata	x								x	x	x			x	x			x		
H. rajagopalani								x							x					
Globigerinelloides aspera				x		x		x	x		x					x	2	2	2	x
G. aff. *ultramicrus*																				
G. rosebudensis																	x			
G. subcarinatus	x		x	x		x	x	x	x			x	x			x				
G. yaucoensis	x	x	3	x			2	2	2	3	x	2	x	2	4	3	5	5	3	4
Globotruncana aegyptiaca	x			x	x				x	x						x				
G. arca			x	x						x			2		x					x
G. esnehensis				x																
G. mariei	2					x		x												x
Globotruncanella havanensis																			x	
G. petaloidea		x								x	x				x					x
Globotruncanita angulata																				
Guembelitria cretacea	34	29	38	39	41	33	32	35	38	33	37	35	33	43	22	31	34	14	20	1
G. dammula	9	12	5	12	14	9	10	10	10	12	20	20	14	5	12	21	9	9	10	2
G. trifolia																				
Laeviheterohelix glabrans	2	x	x	x			x	2	2	x		4	x	x	x	x	2		x	x
Pseudoguembelina costulata	3	6		2	3	3	7	6	6	4	3	3	6	4	4	3	3	5	4	10
P. excolata					x															
P. hariaensis																				x
P. kempensis		x		x						x			x							
Pseudotextularia deformis		x		x									x		x					x
P. elegans														x			x	x		x
P. intermedia																				
Rugoglobigerina hexacamerata	x	x	x		x				x		x	x	x	x	x	x				x
R. rugosa	1	x	x	x		2	2	x	x	x	x	x			x	x		2	x	x
R. scotti															x					
Total number counted	253	281	281	422	357	201	256	231	252	278	343	212	223	189	256	346	234	201	279	270

Sample	23	24	25	26	27	28	29	30	31	32	33	34	35	36	37	38	39
Depth (m)	6.6	7	7.2	7.3	7.5	7.7	7.8	7.9	8	8.12	8.22	8.32	8.42	8.5	8.58	8.66	8.76
CF zones (planktic foraminifera)	CF3													CF2–1			
Calcareous nannofossil zones	*Lithraphidites quadratus*			*Micula murus* (CC26a)										*Micula prinsii*			
Archaeoglobigerina blowi	x				x	x	x						x				
A. cretacea	x		2	x		x				x	x				x	x	
Hedbergella spp.	6	8	7	4	3	6	4	6	6	6	6	4	8	7	3	6	9
Heterohelix carinata		4	3	3	2	4	4	3	8	7	4	6	2	5	2	7	4
H. dentata	34	39	36	32	43	38	39	37	42	35	29	30	26	24	19	13	16
H. globulosa	30	15	21	18	20	18	22	9	10	14	11	16	9	9	14	24	14

Table 2 (*Continued*).

Sample	1	2	3	4	5	6	7	8	9	10	11	12	13	14	15	16	18	19	20	22
Depth (m)	0	0.7	1.1	1.5	1.9	2.3	2.7	3.1	3.5	4.02	4.26	4.44	4.6	4.8	5	5.2	5.56	5.72	5.88	6.34
CF zones (planktic foraminifera)	CF4																		CF3	
Calcareous nannofossil zones	*Lithraphidites quadratus* (CC25c)																			
H. navarroensis	7	4	3	7	4	4	3	2	2	5	2	3	8	5	3	6	4			
H. planata		2	x	x	x	x	x	x	x											
H. rajagopalani																				
Globigerinelloides aspera		x	2	3	x		2		x	x		x	2	2	2	5	4			
G. aff. *ultramicrus*		x		2	4	2	2	x	x	x	2	2	x	2	2	3	3			
G. rosebudensis																				
G. subcarinatus		x	x			x						x	x	x						
G. yaucoensis	4	x	3	5	x	x		x	x	2	3	x	x	x	x	2				
Globotruncana aegyptiaca						x									x					
G. arca						x														
G. esnehensis			x																	
G. mariei	x					x	2	x	x	x	x	x	x	x		x	x			
Globotruncanella havanensis					x	x	x		x											
G. petaloidea				x	x			x												
Globotruncanita angulata																				
Guembelitria cretacea	4	10	6	4	3	7	3	26	8	10	20	17	27	18	19	6	8			
G. dammula	3	5	1	2	0	0	3	6	1	5	6	5	6	17	26	9	12			
G. trifolia												x								
Laeviheterohelix glabrans	x	x	x	x	x	x		x		x		x			x					
Pseudoguembelina costulata	5	5	9	14	7	10	9	5	11	12	8	6	7	6	5	11	23			
P. excolata	x																			
P. hariaensis	x		x	x	x	x					x				x	x				
P. kempensis	x		x	x	x	2	x	x	2	x	2	x	x	x	x	x	2			
Pseudotextularia deformis	x		x	x	x			x	x	x	x	x				x				
P. elegans	x	x	x	x	x	x									x					
P. intermedia					x															
Rugoglobigerina hexacamerata	x	x	x		x			x	x	x		x	x	x	x	x				
R. rugosa	x	2	2	4	4	x	3	x	3	2	x	2	x	2	2	3	x			
R. scotti																				
Total number counted	237	238	261	239	212	282	234	276	234	260	209	277	334	320	351	174	170			

x = < 1%.

From each sample of the Amboanio section, about 250–300 planktic foraminifera were picked from random sample splits (using a micro splitter) of two size fractions (> 63 μm and > 150 μm), mounted on cardboard slides and identified (Tables 2 and 3). Planktic foraminifera are well preserved, but partially recrystallized.

Oxygen and carbon isotope analyses of the Berivotra Formation at Amboanio were conducted on 20–30 adult specimens, per sample, of the benthic foraminifer *Cibicidoides pseudoacuta* and of the planktic foraminifer *Rugoglobigerina rugosa*. Stable isotope analyses of the Betsiboka limestone were conducted on whole rock samples. Isotopic data were measured at the stable isotope laboratory of the Geochemistry Department at the University of Karlsruhe, Germany, using a VG Prism II ratio mass spectrometer equipped with a common acid bath (H_3PO_4). The results were calibrated to PDB scale with standard errors of 0.1‰ for $\delta^{18}O$ and 0.05‰ for $\delta^{13}C$ (Table 4).

Whole rock and clay mineral analyses were conducted at the Geological Institute of the University of Neuchâtel, Switzerland, based on X-ray diffraction analyses (SCINTAG XRD 2000 diffractometer). Sample processing followed the procedure outlined by Kübler (1987) and Adatte et al. (1996). Bulk rock contents were obtained using standard semiquantitative techniques based on external standardization (Kübler, 1983, 1987). Total

Table 3
Relative percent abundances of planktic foraminifera in the >150-μm size fraction at the Amboanio Quarry, Madagascar

Sample	1	2	3	4	5	6	7	8	9	10	11	12	13	14	15	16	18	19	20	22
Depth (m)	0	0.7	1.1	1.5	1.9	2.3	2.7	3.1	3.5	4.02	4.26	4.44	4.6	4.8	5	5.2	5.56	5.72	5.88	6.34
CF zones (planktic foraminifera)	CF4																		CF3	
Calcareous nannofossil zones	*Lithraphidites quadratus* (CC25c)																			
Archaeoglobigerina blowi									x	x		x					2		x	x
A. cretacea	+	x	x		x	x	x	x		x		x	x				3	x		x
Heterohelix dentata	2	3	3	3	4	9	8	2	2	3	4	x	5	2		2	x		4	5
H. globulosa	14	20	15	19	14	10	16	16	12	21	13	16	15	15	10	8	8	8	21	17
H. labellosa		x	x	x	3	x		x	x	x			x		3	x			2	5
H. planata			x		2		x		2								2		x	
H. punctulata				x	x			x			x		x				x		x	
H. rajagopalani	3	2	x	x	2	x	x		x		x	x	2	x	x	3	2	x	x	
Gansserina gansseri	x					+		x		x			x			x		+		
G. weidenmayeri									x	x	x	x	x		x	x				
Globigerinelloides aspera			x		x	x	x			x	x		x					x	x	x
G. multispina																				
G. aff. *ultramicrus*																			x	
G. rosebudensis																				
G. subcarinatus	x			x				x		x										
G. yaucoensis				x	x	x	x		x	x		x								x
Globotruncana aegyptiaca	3	8	10	8	4	4	5	8	11	7	5	8	8	6	4	5	5	3	x	2
G. arca	26	17	23	18	23	19	18	18	17	14	20	19	19	26	14	18	19	16	3	6
G. duepeblei	x			x					x					x						
G. esnehensis	2	3	3	3	x	2	4	5	3	3	5	2	2	4	8	6	7	10	10	5
G. falsostuarti				+	x	x														x
G. insignis															x					
G. mariei	3	x	2	3	x	x	2	2	5	2	3	4	3	5	4	5	5	5	8	7
G. orientalis	2	2	2	2	3	3	7	6	5	x	2	x	3		3	3	2	4	2	x
G. rosetta	x			x		x	2	x	x				x		x			x	x	2
G. ventricosa	x	x		x	2	2		+	x					x		x		x		
Globotruncanella havanensis		x			x		x		x										x	
G. petaloidea			x	x		x		x				x						x		x
Globotruncanita angulata	x		x	>	x	x				x	x				x	x	x			
G. pettersi	x					x														
G. stuarti	+		x	+		2	x	x	x	x	x	x	x	x		x	x	x		x
G. stuartiformis	6	3	2	3	2		3	2	3	4	3	3	4	5	3	5	5	3	5	x
Gublerina cuvillieri		x						x	x			x	x	x		x		x		
Laheviheterohelix glabrans	x	x	2	x	x		x	x			x		x		x					
Planoguembelina acervulinoides						x							x							x
P. brazoensis												x								x
P. carseyae											x						x	x	x	

Table 3 (*Continued*).

Sample	1	2	3	4	5	6	7	8	9	10	11	12	13	14	15	16	18	19	20	22
Depth (m)	0	0.7	1.1	1.5	1.9	2.3	2.7	3.1	3.5	4.02	4.26	4.44	4.6	4.8	5	5.2	5.56	5.72	5.88	6.34
CF zones (planktic foraminifera)	CF4																		CF3	
Calcareous nannofossil zones	*Lithraphidites quadratus* (CC25c)																			
P. riograndensis																				
Pseudoguembelina costulata	2		x	x	5	3	2	3	x	2	3	x	x		x	x	3	2	x	3
P. excolata	4	3	2		x		2	x	x	x	3	2	x	4	x	2		2		
P. hariaensis														x			x		2	3
P. kempensis																				
P. palpebra				x	x	x			x	x					x	x	2			3
Pseudotextularia deformis	5	9	4	7	8	7	4	5	6	6	8	7	3	5	3	7	8	3	7	3
P. elegans	9	8	13	13	11	15	11	18	15	10	9	8	7	6	5	6	3	4	7	8
P. intermedia	x	2	x	x	3	4	x	x	2	x	2	3	2	2	2	2	3	2	3	3
Racemiguembelina fructicosa	x	x	x	+					x	x	x	x						x		x
R. powelli	x	2	3	x	2	3	x	x	2	3	3	2	x	3	2	5	x	x	x	3
Rosita contusa						x														
R. fornicata				x								x	x	x	x		x	x		
R. patelliformis			x								x	x								
R. plicata	x	x		x		x	x		x		x									x
R. walfischensis								x							x	x				
Rugoglobigerina hexacamerata	x	2	x	4	3	x	3	2	x	3	2	6	4	5	9	5	6	3	2	3
R. macrocephala				x								x	x							
R. milamensis																				
R. pennyi		x		x	x	x	x	x	x			x			x		x	x		
R. rotundata											x	x			x					
R. rugosa	13	8	5	2	2	4	4	3	3	10	4	4	9	4	10	9	11	17	13	10
R. scotti	x	x	x	x	x	x	x	x	2	x	2	3	5	5	7	2	2	4	2	4
R. cf. *Scotti*	x		x	x	x						x		x	2	2	2	x	2		
Total number counted	280	233	286	239	314	181	245	279	294	291	278	249	305	257	291	239	252	213	276	232

Sample	23	24	25	26	27	28	29	30	31	32	33	34	35	36	37	38	39	40
Depth (m)	6.6	7	7.2	7.3	7.5	7.7	7.8	7.9	8	8.12	8.22	8.32	8.42	8.5	8.58	8.66	8.76	8.82
CF zones (planktic foraminifera)	CF3													CF2–1				
Calcareous nannofossil zones	*Lithraphidites quadratus*			*Micula murus* (CC26a)										*Micula prinsii*				
Archaeoglobigerina blowi	x	x																
A. cretacea	x				x	x		x		x								
Heterohelix dentata	5	x	2	5	x	5	x	4	x	4	4	2	7	11	4	5	3	
H. globulosa	15	16	20	15	23	24	21	22	25	24	26	22	21	20	34	21	20	x
H. labellosa		3	3	x		x	3	2				x	2	3	x	7	3	
H. planata	x		2	x	3			3	3	2	x							
H. punctulata	x	x		x					x									

Table 3 (*Continued*).

Sample	23	24	25	26	27	28	29	30	31	32	33	34	35	36	37	38	39	40
Depth (m)	6.6	7	7.2	7.3	7.5	7.7	7.8	7.9	8	8.12	8.22	8.32	8.42	8.5	8.58	8.66	8.76	8.82
CF zones (planktic foraminifera)	CF3													CF2–1				
Calcareous nannofossil zones	*Lithraphidites quadratus*			*Micula murus* (CC26a)										*Micula prinsii*				
H. rajagopalani	x	x		x	x			x		x		x	x			x		
Gansserina gansseri																		
G. weidenmayeri																		
Globigerinelloides aspera	x	x	x				x	x		x	x		x				x	
G. multispina				x					x									
G. ultramicrus	x	x		2					x		x	x			x			
G. rosebudensis			x											x				
G. subcarinatus																		
G. yaucoensis					x		x	2	x	x	x	x	x	x	2	x		
Globotruncana aegyptiaca	2	2	2	3	3	x	2	4	3	4	x	x	2	6	x	5	3	
G. arca	3	12	4	5	7	6	9	6	6	9	8	11	2	2	2	2	10	x
G. duepeblei																		
G. esnehensis	3	3	3	2	x	2	3	x	x	x	x	x	x	2	x	2		
G. falsostuarti			x															
G. insignis					x				x				x	2	x		x	
G. mariei	7	4	4	2	6	4	5	5	3	5	5	5	5		2	5		
G. orientalis	4	x	2	2	x	3	x	x	2	x	x	x	x		x			
G. rosetta	2	2	2		x	x	x		x	x			x		x	x		
G. ventricosa																		
Globotruncanella havanensis						x	x	x	x		x	x	x	x	x			
G. petaloidea			x	x	x					x				x				
Globotruncanita angulata	x		x	x						x								
G. pettersi							x											
G. stuarti	x	x	x	x	x	x								x			x	
G. stuartiformis	4	4	3	2	3	x	3	3	3	x	2	2	x	x	x	x		x
Gublerina cuvillieri						x												
Laheviheterohelix glabrans	x												x	x				
Planoguembelina acervulinoides	x	x	3				x	x		x		x		x	x			
P. brazoensis			x	x	2						x	x	x			x		
P. carseyae		x	x	x	x		x	x	x	x	x	x	x	x	x	x		
P. riograndensis									x	x								
Pseudoguembelina costulata	x	3	2	4	x	2	2	2	x	x	x	x	x	3	2	x	x	
P. excolata												0				x		
P. hariaensis	7	7	9	8	4	9	7	6	8	8	12	11	9	12	8	13	6	
P. kempensis				x		x		x		x		x			x	x	x	
P. palpebra	3	4	4	2	3	x	3	2	2	2	4	2	x	x	x		5	x
Pseudotextularia deformis	6	7	6	8	6	7	8	7	7	5	5	5	5	4	3	4	8	x

Table 3 (*Continued*).

Sample	23	24	25	26	27	28	29	30	31	32	33	34	35	36	37	38	39	40
Depth (m)	6.6	7	7.2	7.3	7.5	7.7	7.8	7.9	8	8.12	8.22	8.32	8.42	8.5	8.58	8.66	8.76	8.82
CF zones (planktic foraminifera)	CF3													CF2–1				
Calcareous nannofossil zones	*Lithraphidites quadratus*			*Micula murus* (CC26a)										*Micula prinsii*				
P. elegans	9	9	6	12	11	11	9	7	13	9	8	12	11	6	10	4	7	x
P. intermedia	3	2	3	2	3	2	2	2	2	x	x	2	2	x	x		x	
Racemiguembelina fructicosa	x								x									
R. powelli	3	3	2	2	2	x	x	x	x	x	2	x	x	x	x	x		
Rosita contusa								x										
R. fornicata		x		x														
R. patelliformis		x							x									
R. plicata	x	x			x	x	x	x		x	x			x		x	x	
R. walfischensis				x														
Rugoglobigerina hexacamerata	4	2	x	2	x	3	3	4	2	3	3	5	2	7	2	6	6	x
R. macrocephala		x											x		x			
R. milamensis									x					x				
R. pennyi	x		x		x	x					x							
R. rotundata		x							x			x			x	+		
R. rugosa	7	6	11	9	8	8	9	7	8	8	6	6	13	11	17	15	18	x
R. scotti	4	2	5	4	x	3	2	3	2	x	2	4	4	2	5	2	3	
R. cf. *Scotti*		x		x	x	x		x	x	x	3	x	x		x	x		
Total number counted	303	269	265	305	224	215	290	286	344	289	297	396	334	304	583	212	143	

x = < 1%; + = rare species.

Table 4
Oxygen and carbon isotope values of *Rugoglobigerina rugosa* (planktic), *Cibicidoides pesudoacuta* (benthic), and bulk rock of the Amboanio Quarry, Madagascar

Amboanio Quarry		*Cibicidoides pseudoacuta*		*Rugoglobigerina rugosa*	
Samples	Depth	$\delta^{13}C$(‰)	$\delta^{18}O$(‰)	$\delta^{13}C$(‰)	$\delta^{18}O$(‰)
1	0	1.32	−3.48	1.13	−5.06
2	0.7	1.33	−3.59	1.05	−5.02
3	1.1	1.30	−3.78	1.30	−5.27
4	1.5	1.20	−3.84	1.47	−5.05
5	1.9	1.27	−3.82	1.15	−5.20
6	2.3	1.47	−3.95	1.58	−4.91
7	2.7	not analyzed		1.11	−5.43
8	3.1	1.36	−3.79	1.42	−5.31
9	3.5	1.22	−3.90	1.43	−5.52
10	4.02	1.13	−3.54	1.23	−5.51
11	4.26	1.13	−3.70	1.54	−5.43
12	4.44	1.18	−3.55	1.61	−4.78
13	4.6	not analyzed		1.06	−4.74
14	4.8	1.07	−3.31	1.16	−4.68
15	5	1.08	−3.63	2.18	−4.42
16	5.2	0.88	−3.72	1.31	−4.56
18	5.56	0.75	−3.35	not analyzed	
19	5.72	0.48	−3.02	0.95	−4.42
20	5.88	0.32	−4.06	0.27	−4.96
22	6.34	1.26	−4.16	0.81	−5.63
23	6.6	0.88	−4.01	1.03	−5.35
24	6.96	0.77	−4.13	not analyzed	
25	7.2	0.74	−4.31	0.64	−5.67
26	7.32	0.52	−4.17	0.54	−5.50
27	7.5	0.86	−4.79	0.69	−5.49
28	7.74	0.66	−4.48	0.91	−5.64
29	7.84	0.56	−4.56	0.57	−5.31
30	7.92	0.78	−4.50	0.86	−5.45
31	8	0.64	−4.67	not analyzed	
32	8.12	0.35	−4.61	0.52	−5.55
33	8.22	0.69	−4.60	0.91	−5.60
34	8.32	0.42	−4.83	1.14	−5.19
35	8.42	0.64	−4.49	0.60	−5.45
36	8.5	0.17	−4.30	0.72	−4.59
37	8.58	0.78	−4.45	0.84	−5.43
38	8.66	0.12	−4.24	1.04	−4.30
39	8.76	−0.77	−4.13	1.17	−3.66
Sample	Depth	Whole rock	Whole rock		
41	8.9	−2.125	−5.306		
42	8.95	−1.601	−5.273		
43	9.5	−1.114	−4.807		
44	9.9	−1.612	−4.522		
45	10.9	−1.491	−4.780		
46	11.5	−3.037	−4.500		
47	12	−2.471	−7.482		
48	12.5	−1.032	−4.595		
49	12.7	−1.579	−4.167		
50	13	−2.978	−4.208		

organic carbon (TOC) analysis was performed with a Rock Eval 6 pyrolyser on powdered bulk samples, based on the analytical methods of Espitalié et al. (1986) and Lafargue et al. (1996).

2.1. Principles of mineralogical interpretation

For mineralogical interpretations of the clay mineral species we follow Chamley (1989, 1998), Weaver (1989), Robert and Chamley (1991), Debrabant et al. (1992a,b), and Deconinck and Chamley (1995). Clay minerals and their relative abundances may record information on climate, eustasy, burial diagenesis, or reworking. Deep burial diagenesis affects clay minerals (e.g. smectite recrystallizes to illite–smectite mixed layers, kaolinite disappears) at depths >2000 m in sediments other than permeable sandstones (Weaver, 1989; Chamley, 1998). In the Mahajanga Basin, where Tertiary sediments do not exceed 1000 m, there is no deep burial diagenesis, as shown by the presence of smectite and the co-existence of smectite with high kaolinite throughout the section. Detrital input is the dominant factor responsible for the clay mineral distribution in marine sediments. Illite, illite–smectite mixed layers, chlorite, associated quartz and feldspars typically constitute terrigenous species (Chamley, 1998). These clay minerals generally develop in areas of steep relief where active mechanical erosion limits soil formation, particularly during periods of enhanced tectonic activity (Millot, 1970; Chamley, 1998). They can also form in cold and/or desert regions where low temperatures and/or low rainfall reduce chemical weathering (Millot, 1970; Chamley, 1998).

Although smectite can form due to hydrothermal weathering of volcanic rocks, it is generally of detrital origin and can issue from soils developed under a warm to temperate climate characterized by alternating humid and dry seasons (Chamley, 1998). Maximum amounts of smectite frequently coincide with sea-level highstands (Deconinck, 1992). During the Maastrichtian to early Danian, the Madagascar sections were located in a coastal to outer neritic environment which experienced little hydrodynamic activity and hence little mineral segregation that could mask or exaggerate the climate signal (Adatte and Rumley, 1989; Chamley, 1989; Monaco et al., 1982). Kaolinite develops typically in tropical soils, which are characterized by warm, humid climates, well-drained areas with high precipitation and accelerated leaching of parent rocks (Robert and Chamley, 1991). However, increased kaolinite can also result from increased erosion during sea-level regressions or transgressions (Robert and Kennett, 1994; Thiry, 2000; Chamley, 1998).

3. Lithology and mineralogy

The Berivotra type locality and the Amboanio section are here described based on field observations, including lithology, hardgrounds, macrofossils, trace fossils and bioturbation, and laboratory analysis of thin sections, bulk rock and clay minerals that provide paleoenvironmental interpretations.

3.1. Berivotra

The Berivotra type locality is near Berivotra village, approximately 80 km southeast of Mahajanga along the Mahajanga–Antananarivo national road IG4 (Fig. 1). The section was sampled about 500 m beyond the village along an uphill trail on the right side of the road. A small limestone quarry is on the flat hilltop (Fig. 2). In this area, the marine sediments of the Berivotra Formation overlie white sandstones with exceptionally abundant dinosaur and other vertebrate remains (Figs. 2a,b and 3; Forster et al., 1996; Krause and Hartman, 1996; Krause et al., 1997, 1999). Rogers et al. (2000) defined this terrestrial layer as Facies 1 of the Anembalemba Member that forms the top of the Maevarano Formation in the Berivotra type area. They interpret this sandstone facies to have accumulated aggradationally in a shallow, broad system of ephemeral flood channels cut into a low-lying alluvial plain. In our study, bulk rock analysis of the top 2 m of the Anembalemba Member (Fig. 4) shows that the clastic sediments are dominated by quartz (45%), K-feldspar (33%) and plagioclase (23%), phyllosilicates (2–7%) and calcite (22%). The phyl-

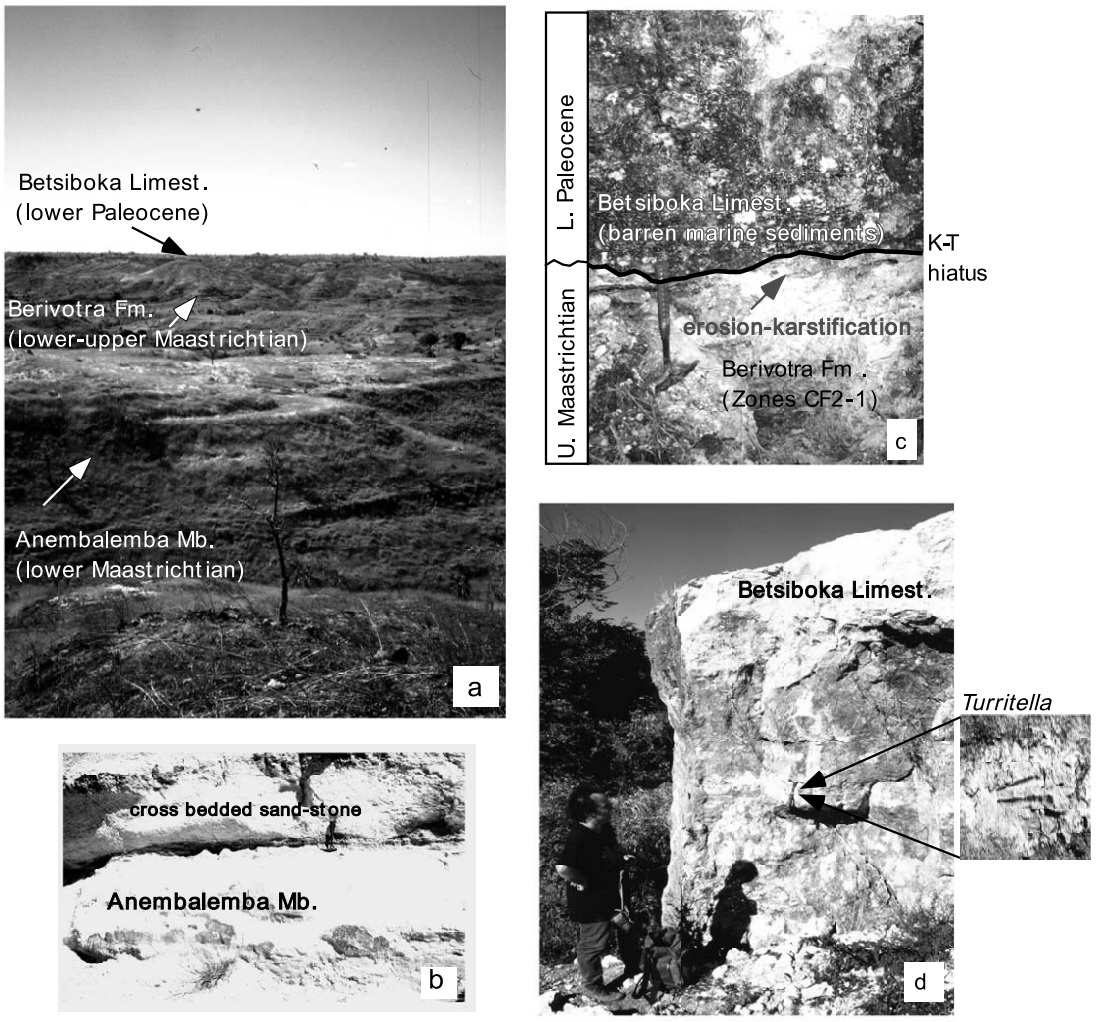

Fig. 2. (a). Overview of the Berivotra type locality showing the terrestrial Anembalemba Member of the Maevarano Formation, the marine Berivotra Formation, and the Betsiboka limestone. (b). Close-up of cross-bedded sandstone (Facies 1 of Rogers et al., 2000) of the upper Anembalemba Member. (c). Contact between the Berivotra Formation and the Betsiboka limestone showing a karstic erosional unconformity that marks the K–T boundary. (d). Betsiboka limestone with 10 cm long *Turritella* molds (see inset) 3 m above the base of the limestone.

losilicates show decreasing smectite and chlorite (Fig. 5).

A 30-cm thick microconglomerate disconformably overlies these terrestrial sediments, and contains rounded clasts (<3 mm in diameter), monocrystalline quartz, and minor chert in a sandy calcareous matrix. This microconglomerate is overlain by marginal marine yellow to brown

Fig. 3. Lithology, biostratigraphy, macrofossils, and inferred paleoenvironmental and sea-level changes at the Berivotra type locality. The onset of marine conditions is marked by a 30-cm-thick microconglomerate (ravinement surface) that overlies the terrestrial sequence of the Anembalemba Member and underlies shoreface deposits of sandstone with abundant macrofossils. A rising sea level reached middle neritic depth during the early and late Maastrichtian but shallowed near the end of the Maastrichtian. During the early Paleocene a shallow neritic environment is indicated by the absence of marine plankton.

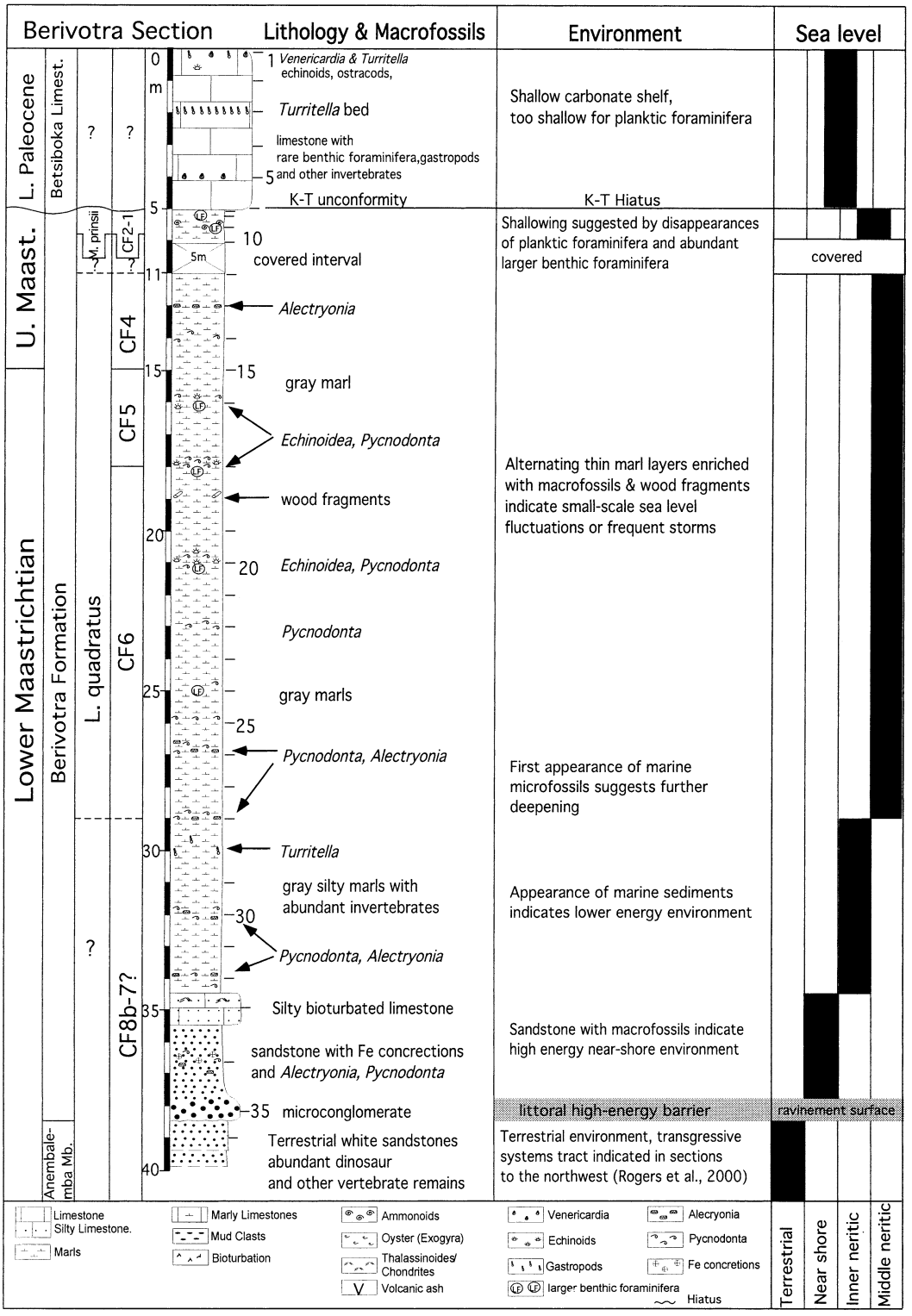
Berivotra Section
Lithology & Macrofossils
Environment
Sea level
L. Paleocene
U. Maast.
Lower Maastrichtian
Betsiboka Limest.
Berivotra Formation
Anembale-mba Mb.
L. quadratus
M. prinsii
CF2-1
CF4
CF5
CF6
CF8b-7?
0 m
5
10
11
15
20
25
30
35
40
1 Venericardia & Turritella echinoids, ostracods,
Turritella bed
limestone with rare benthic foraminifera,gastropods and other invertebrates
5
K-T unconformity
5m
covered interval
Alectryonia
15
gray marl
Echinoidea, Pycnodonta
wood fragments
20
Echinoidea, Pycnodonta
Pycnodonta
gray marls
25
Pycnodonta, Alectryonia
Turritella
gray silty marls with abundant invertebrates
30
Pycnodonta, Alectryonia
Silty bioturbated limestone
sandstone with Fe concrections and Alectryonia, Pycnodonta
35 microconglomerate
Terrestrial white sandstones abundant dinosaur and other vertebrate remains
Shallow carbonate shelf, too shallow for planktic foraminifera
K-T Hiatus
Shallowing suggested by disappearances of planktic foraminifera and abundant larger benthic foraminifera
Alternating thin marl layers enriched with macrofossils & wood fragments indicate small-scale sea level fluctuations or frequent storms
First appearance of marine microfossils suggests further deepening
Appearance of marine sediments indicates lower energy environment
Sandstone with macrofossils indicate high energy near-shore environment
littoral high-energy barrier
Terrestrial environment, transgressive systems tract indicated in sections to the northwest (Rogers et al., 2000)
covered
ravinement surface
Limestone
Silty Limestone.
Marls
Marly Limestones
Mud Clasts
Bioturbation
Ammonoids
Oyster (Exogyra)
Thalassinoides/ Chondrites
Volcanic ash
Venericardia
Echinoids
Gastropods
larger benthic foraminifera
Alecryonia
Pycnodonta
Fe concretions
Hiatus
Terrestrial
Near shore
Inner neritic
Middle neritic

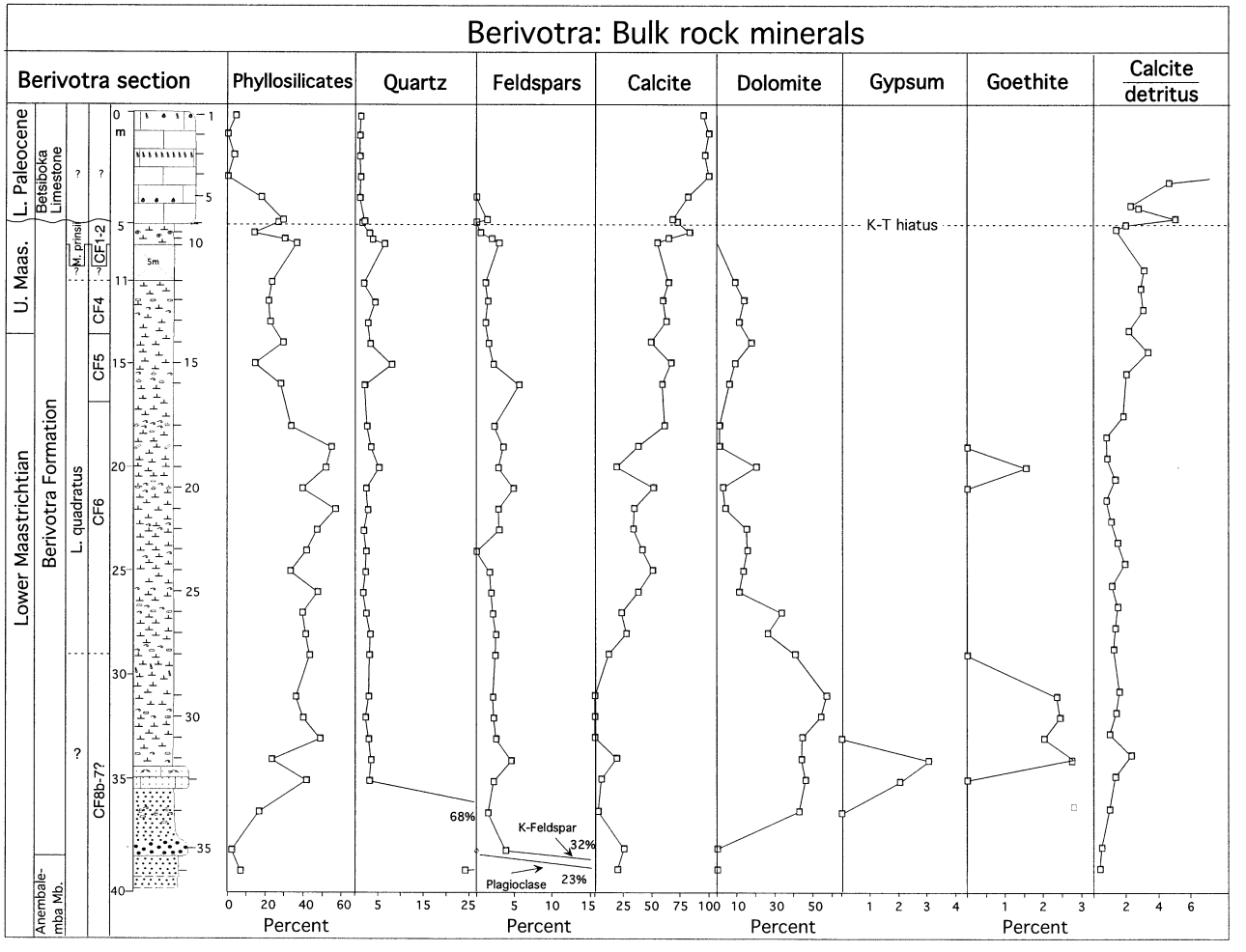

Fig. 4. Bulk rock composition of the Berivotra section. The transition between the terrestrial Anembalemba Member and the marine Berivotra Formation is marked by decreased clastic input and increased dolomite. Abundant dolomite in the lower part of the Berivotra Formation (zones CF8B–7?) indicates shoreface conditions. Decreased abundance of dolomite and increased calcite in zone CF6 reflects a rising sea level. Low abundance of clastic minerals in the lower Betsiboka limestone indicates the temporary shutdown of clastic supply. Key to lithology in Fig. 3.

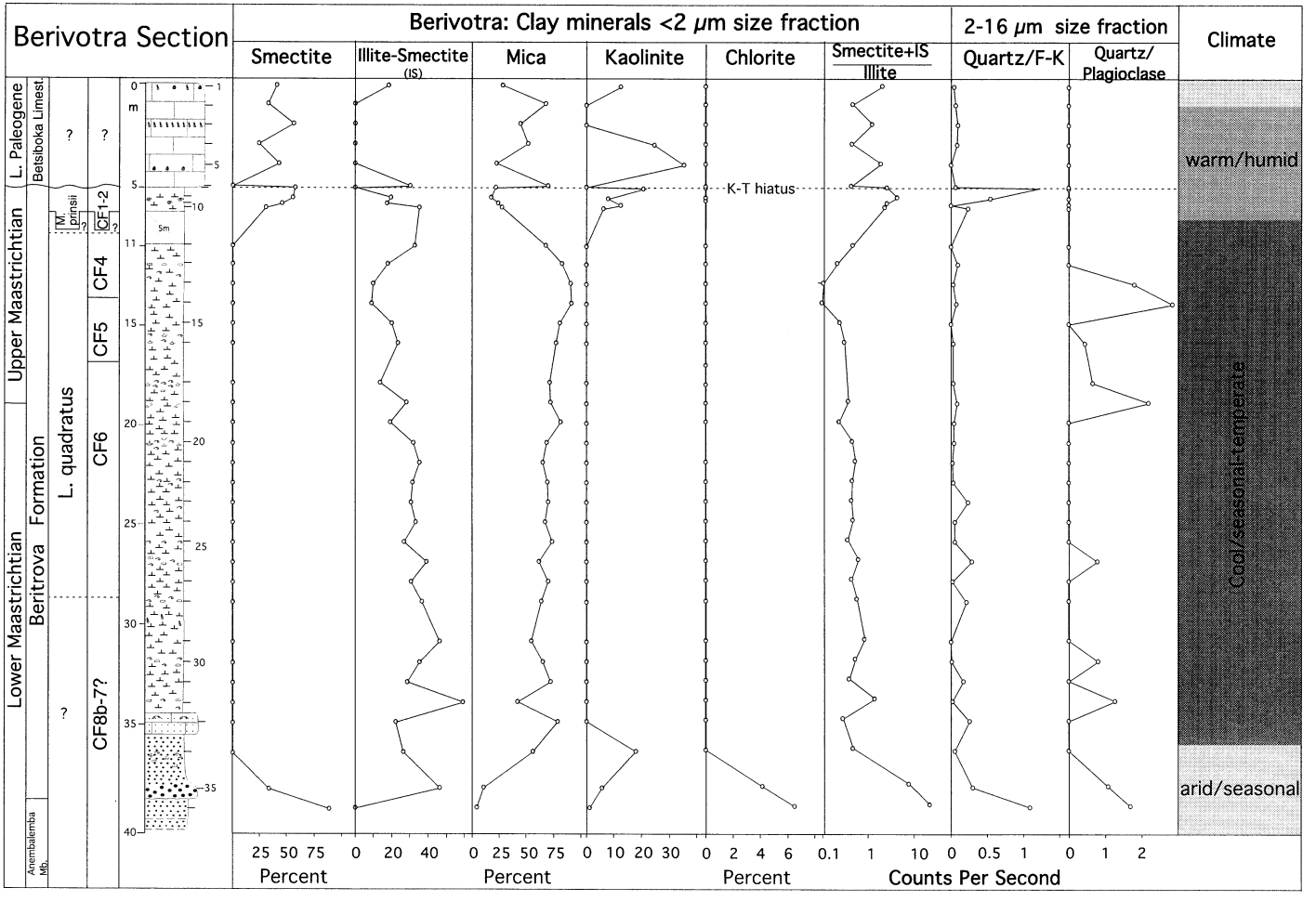

Fig. 5. Clay mineral composition in the <2-μm and the 2–16-μm size fractions of the Berivotra section. The high abundance of smectite and kaolinite in the earliest Maastrichtian, latest Maastrichtian and early Paleocene indicate warm/humid climates (see key to lithology in Fig. 3).

sandstone with small iron concretions and marine oysters (e.g. *Pycnodonta vesicularis*, *Agerostrea ungulata*, *Alectryonia* spp. Fig. 3). The dolomitic sandstone is characterized by low quartz (2–3%), K-feldspar (2–4%) and calcite (0–20%), abundant dolomite (42–46%), increased phyllosilicates (20–40%), significant gypsum (2–3%) and goethite (2–3%; Fig. 4). Mica and illite–smectite replace smectite and kaolinite among the phyllosilicates (Fig. 5). Above the sandstone is a 20-cm thick layer of white unfossiliferous limestone that consists of lime mud with small dolomite rhombs. The top of this sandstone is strongly bioturbated by *Chondrites*. Mottled fossiliferous gray–green marls with *Pycnodota vesicularis*, *Agerostrea ungulata* and other macrofossils overlie the limestone horizon. The base of the marl contains small dolomite rhombs, but lacks microfossils. The gray–green marls grade upwards into gray marls (bioclastic wackestones) rich in benthic foraminifera and sparse, but diverse, planktic foraminiferal and calcareous nannofossil assemblages (Fig. 3). This part of the section is characterized mineralogically by dolomite, low quartz and K-feldspar, disappearance of gypsum and goethite, and increased calcite and phyllosilicates, of which the latter are mainly illite–smectite and mica (Figs. 4 and 5).

The overlying sediments consist of 1–2-m-thick gray marl layers rich in planktic foraminifera and calcareous nannofossils, but poor in macrofossils. These marl layers are periodically interrupted by thin, more fossiliferous horizons with *Pycnodota vesicularis*, *Agerostrea ungulata*, other oysters (e.g.

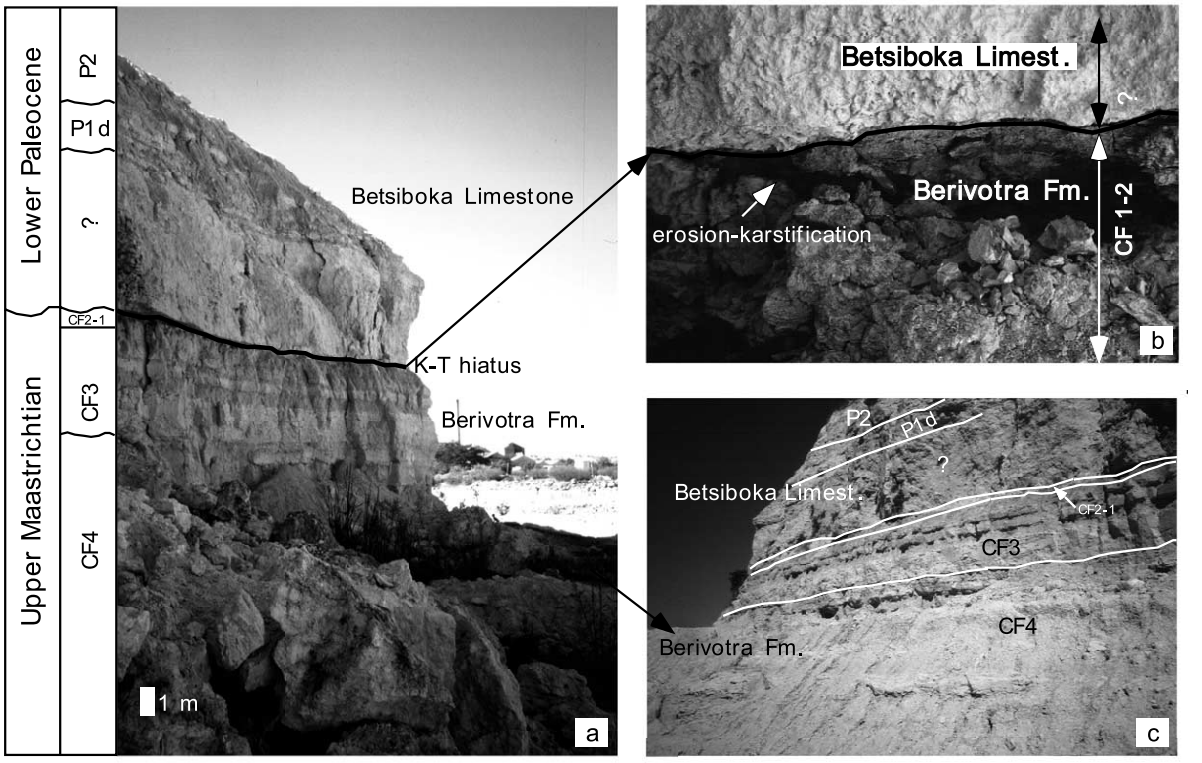

Fig. 6. (a). Amboanio Quarry walls showing sediments of the upper Berivotra Formation and the Betsiboka limestone, prominently separated by a 20-cm-thick brown clay layer that marks the K–T unconformity. (b). Close-up view of the K–T unconformity, which is marked by an erosion surface, karstification, abundant mudclasts, and volcanic ash. (c). Overview of the late Maastrichtian and early Paleocene biostratigraphy of the Berivotra Formation and lower Betsiboka limestone. Note the rhythmic alternation between marls and limestone layers in zones CF4 and CF3 that indicate small-scale sea-level fluctuations.

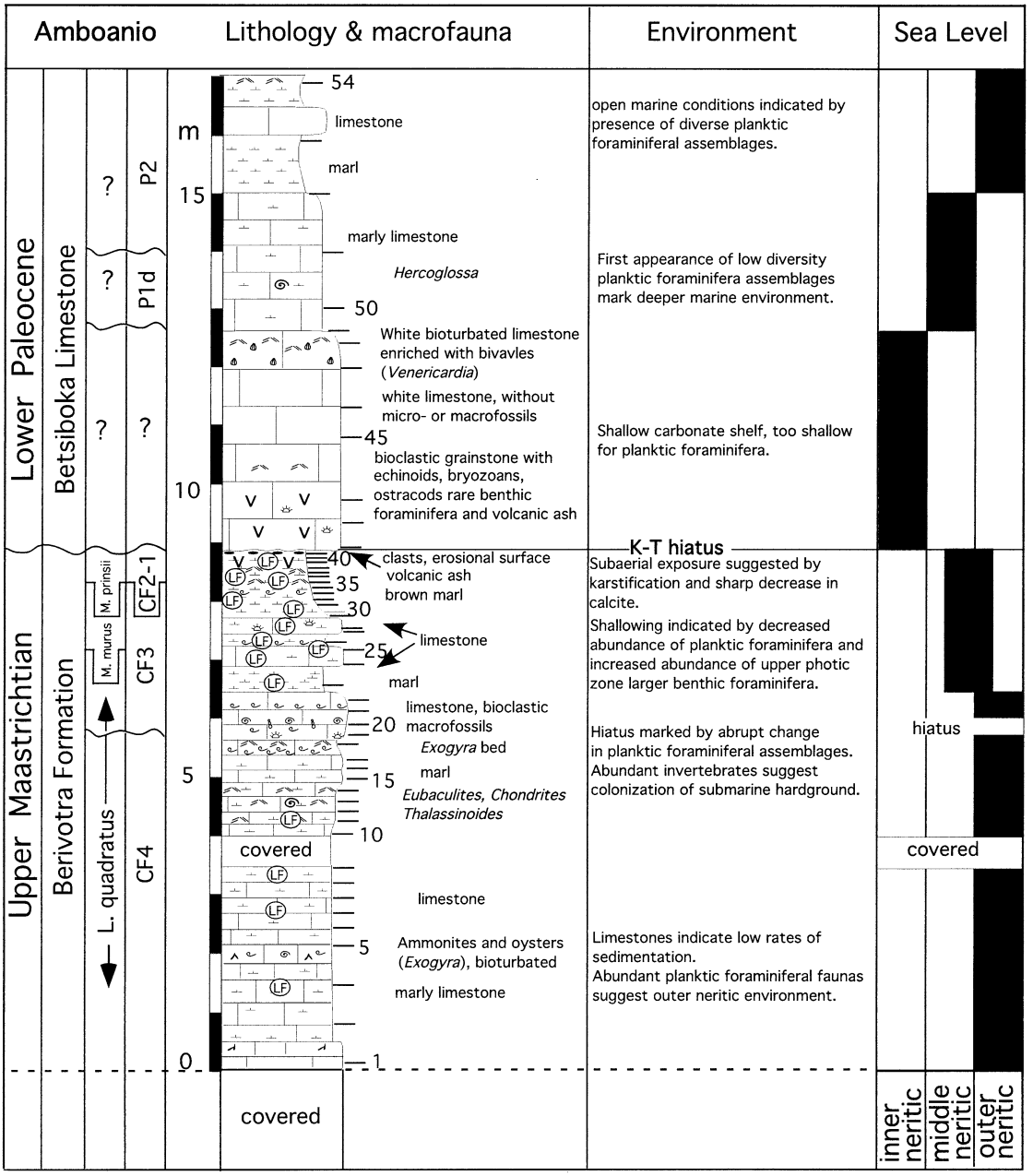

Fig. 7. Lithology, biostratigraphy, macrofossils, and inferred paleoenvironmental and sea-level changes at Amboanio. The oldest sediments exposed in the quarry are of late Maastrichtian zone CF4 age (68.3 Ma) and indicate an outer neritic environment. Horizons of shell concentrations may represent colonized submarine hardgrounds. A hiatus is present at the CF4–CF3 transition (~67 Ma), as indicated by an *Exogyra* bed and abrupt changes in planktic foraminiferal assemblages. Shallowing during the latest Maastrichtian (upper CF3 and CF2–CF1) culminates at the K–T unconformity marked by a karstic erosional surface enriched with mudclasts. Above the K–T unconformity, the shallow neritic environment deepens to hemipelagic outer neritic depths in the late Danian (see key to lithology in Fig. 3).

Rastellum), larger and small benthic foraminifera and wood fragments. In addition, *Isocrania costata*, echinoid spines, bryozoans, gastropods (e.g. *Campanile*) and shark teeth are frequent components (Fig. 3). Increased calcite, decreased dolomite and subsequently decreased phyllosilicates characterize this part of the section (Fig. 4). Near the top of the Berivotra Formation a slump covers about 5 m of the outcrop. Above this interval is 1.2-m-thick brown-gray marl with larger benthic foraminifera. A single baculitid ammonite (aff. *Eubaculites simplex*) was found 50 cm below the top of the Berivotra Formation (Fig. 3). The upper contact is represented by residual brown clay that is barren of microfossils and composed primarily of smectite and kaolinite, and overlies a karstic erosional surface (Figs. 2c and 5).

A small quarry is at the top of the Betsiboka limestone formation. The limestone in this quarry consists of peloidal packstone and grainstones with abundant bioclasts, recrystallized shells, or interior molds of bivalves (*Venericaria*, rare oysters), and gastropods (e.g. turritellids). Echinoids, bryozoans and benthic foraminifera (especially miliolids) are also abundant, but planktic foraminifera and calcareous nannofossils are absent (Fig. 3). A shell bed with *Turritella* molds up to 10 cm long is present 3 m above the base of the limestone in the older part of the quarry (Fig. 2d). Calcite is the dominant mineral with kaolinite rapidly increasing (Figs. 4 and 5).

3.2. Amboanio

The Amboanio section is located in the cement quarry near the village of Amboanio, approximately 28 km south of the city of Mahajanga and close to the northern end of the Bay of Bombetoka (Fig. 1). The lower part of this quarry exposes 9 m of marls and marly bioclastic limestone of the upper Berivotra Formation. The upper part of the quarry consists of 15 m of thick-bedded chalky limestone of the Betsiboka Formation (Fig. 6a,c). A prominent 20-cm-thick dark brown clay layer marks the disconformity between the Berivotra and Betsiboka Formations (Fig. 6b).

The Berivotra Formation consists of light colored marl, marly limestone and interlayered bioclastic horizons (Fig. 7). Calcite dominates (up to 80%), followed by phyllosilicates (illite–smectite and illite) and minor quartz (Figs. 8 and 9). The marl and marly limestone layers are rich in planktic foraminifera and calcareous nannofossils. Sediments are generally mottled with *Chondrites* and *Thalassinoides* burrows recognizable. Burrows are frequently present at the base of marly limestone layers where they penetrate down into the softer marls. Thin sections show the bioclastic limestones to be wackestones and minor packstones. Fossils are abundant in these layers and include diverse oysters (e.g. *Aetostreon*, *Agerostrea*), gastropods (e.g. *Gyrodes*, *Ampullina* and other naticids, turritellids, *Epitonium*), bryozoans (e.g. *Lunulites*), bivalves (e.g. *Chlamys*), echinoids (e.g. cidarids), terebratulid brachiopods, rare ammonites (e.g. *Eubaculites labyrithicus*, *Eubaculites* aff. *simplex*, *Pachydiscus*), low diversity assemblages of larger benthic foraminifera, and planktic foraminifera (Fig. 7). A prominent bioturbated *Exogyra* bed is present at 5.5 m. Overlying the *Exogyra* bed is 1 m of bioclastic limestone with abundant macrofossils and microfossils (e.g. oysters, echinoids, gastropods, ammonites, benthic and planktic foraminifera).

Above this interval, marl and marly limestone layers again alternate between horizons dominated by benthic taxa (e.g. oysters, larger benthic foraminifera), abundant trace fossils (e.g. *Chondrites*, *Thalassionides*) and rare planktic foraminifera. The last meter is characterized by brown marl bioturbated by *Thalassinoides* and *Chondrites*, with echinoids, small oysters, larger and smaller benthic foraminifera, and mostly fragmented mollusc shells that appear to be transported. Volcanic ash is common to abundant in the top 10 cm of the brown marl and also present within the overlying 1.2 m of the Betsiboka limestone. Calcite is significantly reduced in the brown marl, phyllosilicates dominate, and quartz and feldspar increase (Fig. 8). Kaolinite, illite–smectite and minor chlorite represent the clays (Fig. 9).

An undulose and erosive surface characterizes the unconformity between the brown marl at the top of the Berivotra Formation and white chalk of the overlying Betsiboka limestone (Fig. 6b). Below the erosional surface, the brown marl con-

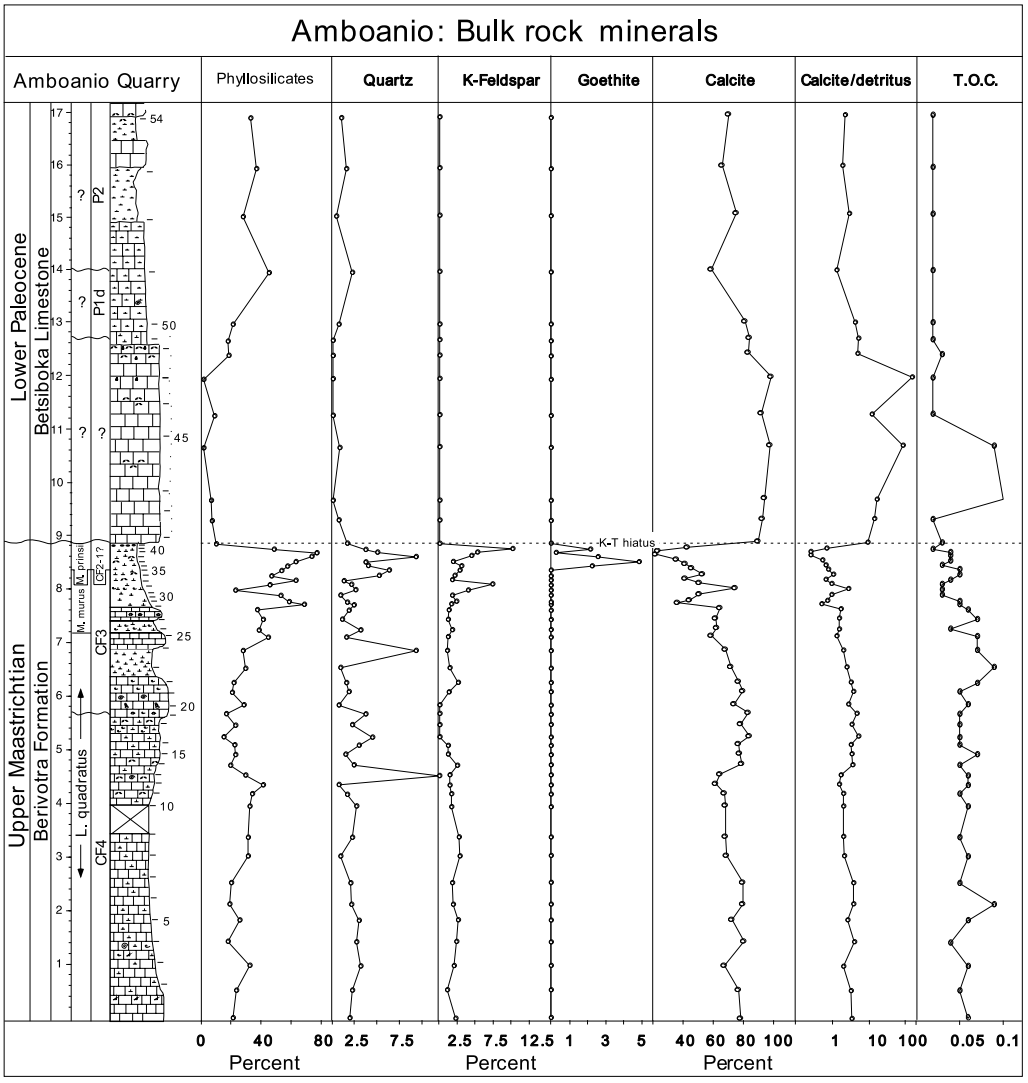

Fig. 8. Bulk rock composition and TOC of the Amboanio section. The increased phyllosilicates and decreased calcite in the CF3–CF1 interval indicate shallowing. The decrease in phyllosilicates in the lower 3 m of the Betsiboka limestone reflects the temporary shutdown of clastic supply, as also observed in the Berivotra section (see key to lithology in Fig. 3).

tains abundant well-rounded mudclasts, fragmented oyster shells, common volcanic ash, wood fragments, iron concretions, phosphatic pellets and rare planktic foraminifera. Above the unconformity, the first 1.2 m consists of white bioclastic grainstone or packstone with volcanic ash in the lower part and diverse macrofossils, including bryozoans, echinoids, oysters and ostracods (Fig. 7). A 1.5-m-thick white limestone devoid of micro- or macrofossils overlies this interval, followed by bioturbated limestone enriched with bivalves (e.g. *Venericardia*), gastropods (e.g. *Turritella*), rare corals, abundant larger foraminifera, small benthic foraminifera, ostracods and common wood fragments. *Ophiomorpha*, *Thalassinoides* and *Chondrites* trace fossils are abundant in some intervals in the limestone. Notably absent are marine plankton (planktic foraminifera and calcareous nannofossils) in the basal 3.8 m of the Betsiboka limestone. This part of the section

is dominated by calcite with phyllosilicates nearly absent, increased kaolinite, chlorite and smectite to the detriment of illite and illite–smectite (Figs. 8 and 9).

The white marly limestone, wackestones and packstones above this interval bear similar macrofossil assemblages, though wood fragments are very rare, and planktic foraminifera are present. Near the top of the section, white marly limestone layers alternate with white marl layers with abundant planktic foraminifera and calcareous nannofossils, and the nautilid *Hercoglossa* occurs 4.6 m above the base (Fig. 7). Calcite is abundant in this part of the section, followed by phyllosilicates and quartz, whereas kaolinite disappears and smectite dominates (Figs. 8 and 9).

TOC values at the Amboanio Quarry section are very low (<0.1 wt%) and average 0.06 wt% (Fig. 8). These TOC values are too low to determine the type (I, II or III) of organic matter or Tmax. Nevertheless, pyrolysis data suggest a terrigenous source (Type III or IV). Post-depositional alteration is indicated by the low hydrogen index (50–60 HC/g TOC) and extraordinarily high oxygen index (300–880 mg CO_2/g TOC) values.

3.3. Paleoenvironmental interpretations

Rogers et al. (2000) viewed the marine section of the Berivotra Formation as a transgressive sequence that overlies the lowland terrestrial section of the Anembalemba Member. Inner shelf conditions, interpreted from coarse-grained clastics and shallow water macrofossils, deepen to more offshore conditions as indicated by finer grain sizes and presence of planktic foraminifera and ammonites. The subsequent alternations of claystone and marl layers are considered to reflect small-scale relative sea-level fluctuations. They interpret maximum flooding around the K–T transition, and assumed that flooding of clastic sources accounts for the nearly pure limestone of the overlying Betsiboka limestone. They thus considered the Berivotra/Betsiboka contact as gradational. This interpretation differs considerably from that of Papini and Benvenuti (1998) who considered the entire section to be restricted and lagoonal in nature.

Our findings are in substantial agreement with the transgressive sequence proposed by Rogers et al. (2000) for the early to late Maastrichtian, but differ significantly for the K–T transition and early Danian as discussed below. Although in general two sections are insufficient for a regional systems tract subdivision, some significant markers are apparent. For example, the fluviatile sandstones that underlie the Berivotra Formation appear to be part of the transgressive system tract (Fig. 4). These sandstones contain clastics formed under seasonal warm/arid conditions, as indicated by abundant smectite and low illite, chlorite and kaolinite contents (Fig. 5). The overlying microconglomerate unit indicates passage through the littoral high-energy barrier, and may represent part of a ravinement surface. The facies transition suggests that this horizon is not necessarily a regional unconformity. The shoreface deposit and the near-shore sands and silts above it indicate passage of the transgressive cycle through the energetic zone, as indicated by a resistant marine molluscan faunal assemblage. Clay minerals include increasing kaolinite, indicative of marine reworking and erosion (Fig. 4).

Continued deepening and lower energy environments are indicated upsection as dolomitic sediments are replaced by calcite, and deposition of predominantly gray carbonate marl lithologies. Open marine pelagic microfaunas appear 9 m above the first marine horizon, indicating deepening well beyond accommodation in this transgressive tract, and proximity to the maximum flooding level (Fig. 3). The main part of the Berivotra Formation at the type locality consists of 20 m of hemipelagic marls. The same lithofacies appears at the Amboanio section (Fig. 7). Open marine shelf macrofaunas are present throughout the Berivotra section, but concentrations may indicate colonized marine hardground facies. At Amboanio similar hardground facies may be represented by intensely burrowed horizons with *Thalassinoides* and *Chondrites* (Fig. 7). In some of these burrowed horizons the presence of transported material, such as wood fragments, broken bioclasts, and possibly some larger foraminifera, suggests that distal storm concentrates may be present. Dominant phyllosilicates are mica and

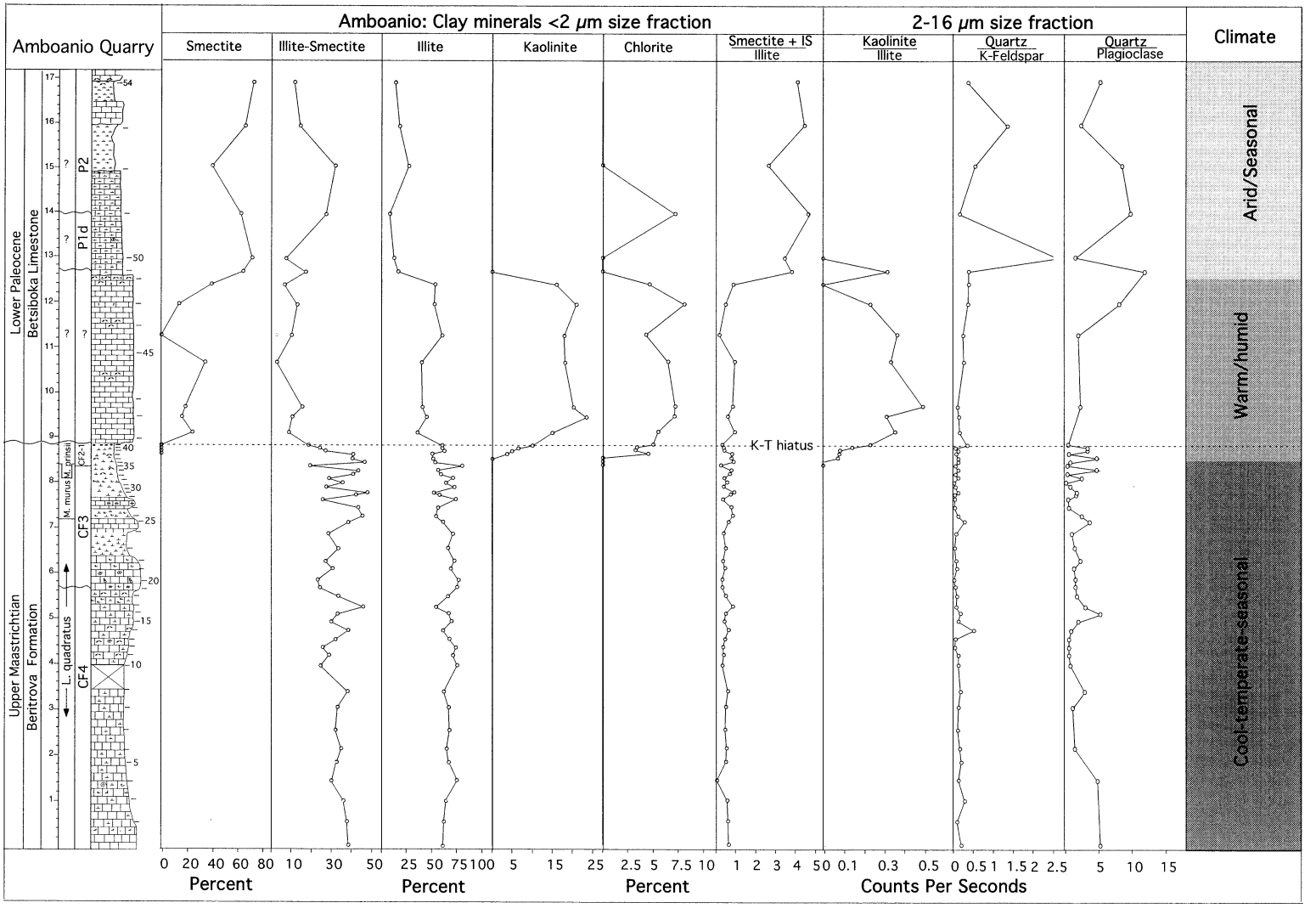

Fig. 9. Clay mineral composition in the <2-μm and the 2–16-μm size fractions of the Amboanio section. The high abundance of kaolinite, chlorite and smectite in the latest Maastrichtian and early Paleocene indicate warm/humid climatic conditions (see key to lithology in Fig. 3).

illite–smectite of distal origin, which suggests drier and cooler environments in the absence of kaolinite and smectite (Fig. 9). There are no erosional surfaces or facies shifts to support significant sea-level falls within this part of the sections.

The upper meters of the Berivotra Formation are more calcareous and best exposed at the Amboanio locality (the coeval strata at the Berivotra type locality are mostly covered). Burrowed horizons and *Exogyra* beds, and decreased influx of fine clastics indicate low rates of sedimentation (Fig. 7). Shell concentrations without particular indicators for transport (e.g. wood fragments) may represent colonized submarine hardground surfaces, with larger benthic foraminifera possibly one component of this colonization. These lithological and paleontological characteristics suggest a maximum sea-level highstand in the upper part of the Berivotra Formation (Fig. 7).

An environmental change is indicated in the uppermost 1.6 m of the Berivotra Formation at Amboanio by significant decreases in calcite and planktic foraminifera, and increases in phyllosilicates and benthic foraminifera, suggesting shallowing (Fig. 7). The erosional surface at the top of this interval marks the Berivotra/Betsiboka Formation contact and suggests a significant sea-level fall and subaerial exposure, as indicated by sediment karstification and a major hiatus documented by biostratigraphic data (see discussion below). This event is probably also responsible for the dissolution of calcite that is evident in the uppermost 20 cm of the Berivotra Formation.

The overlying 3.8 m of the Betsiboka limestone represent a new sedimentary cycle with the establishment of shallow marine conditions in the Mahajanga Basin, as indicated by diverse macrofaunal assemblages, but absence of microfossils (Fig. 7). Within this interval, the appearances of smectite and kaolinite are particularly noteworthy. The appearance of smectite coincides with the presence of ash layers in the top 10 cm of the Maastrichtian and the overlying lower part of the Betsiboka limestone (1.2 m), and appears to reflect hydrothermal weathering of volcanic rocks (Figs. 5 and 9). The increased kaolinite in the uppermost part of the Berivotra Formation and lower Betsiboka limestone suggests relatively warm/humid climatic conditions. Throughout the lower 3 m of the Betsiboka limestone phyllosilicates are rare and record a temporary shutdown of the clastic supply, which may be related to the earlier sea-level fall and changes in riverine transports that decreased terrestrial influx.

The top of the basal 3.8-m-thick limestone is marked by a submarine hardground surface as indicated by shell concentrations (mainly bivalves). Above this hardground, hemipelagic conditions were reintroduced as indicated by the gradual re-appearance of planktic foraminifera, followed by abundant and diverse assemblages that indicate a re-establishment of fully marine conditions in the Mahajanga Basin. A major increase in smectite during this interval also suggests a rising sea level, whereas the disappearance of kaolinite reflects more seasonally/arid conditions.

4. Biostratigraphy

Biostratigraphic correlation and age determinations of the Mahajanga Basin sections are primarily based on planktic foraminifera and augmented by calcareous nannofossils. The deeper water lithofacies is rich in calcareous microfossils, which permits correlation within Madagascar and to low and middle latitude sections globally (Fig. 10). Age determinations could not be obtained from shallow water or terrestrial intervals with rare or no calcareous microplankton, though in some cases ages could be interpolated from well-dated faunas above and/or below barren intervals. Taxonomy of planktic foraminifera in this study follows Smith and Pessagno (1973), Robaszynski et al. (1983–1984), Caron (1985) and Nederbragt (1991), with selected species illustrated in Plates I and II, and range charts provided in Tables 1–3.

The Maastrichtian stage is generally divided into three planktic foraminiferal zones, i.e. *Globotruncana aegyptiaca*, *Gansserina gansseri*, and *Abathomphalus mayaroensis* (Caron, 1985; Fig. 10). Recently, Li and Keller (1998a) subdivided this zonal scheme into nine Cretaceous Foraminiferal (CF) zones labeled CF1 to CF9 and cali-

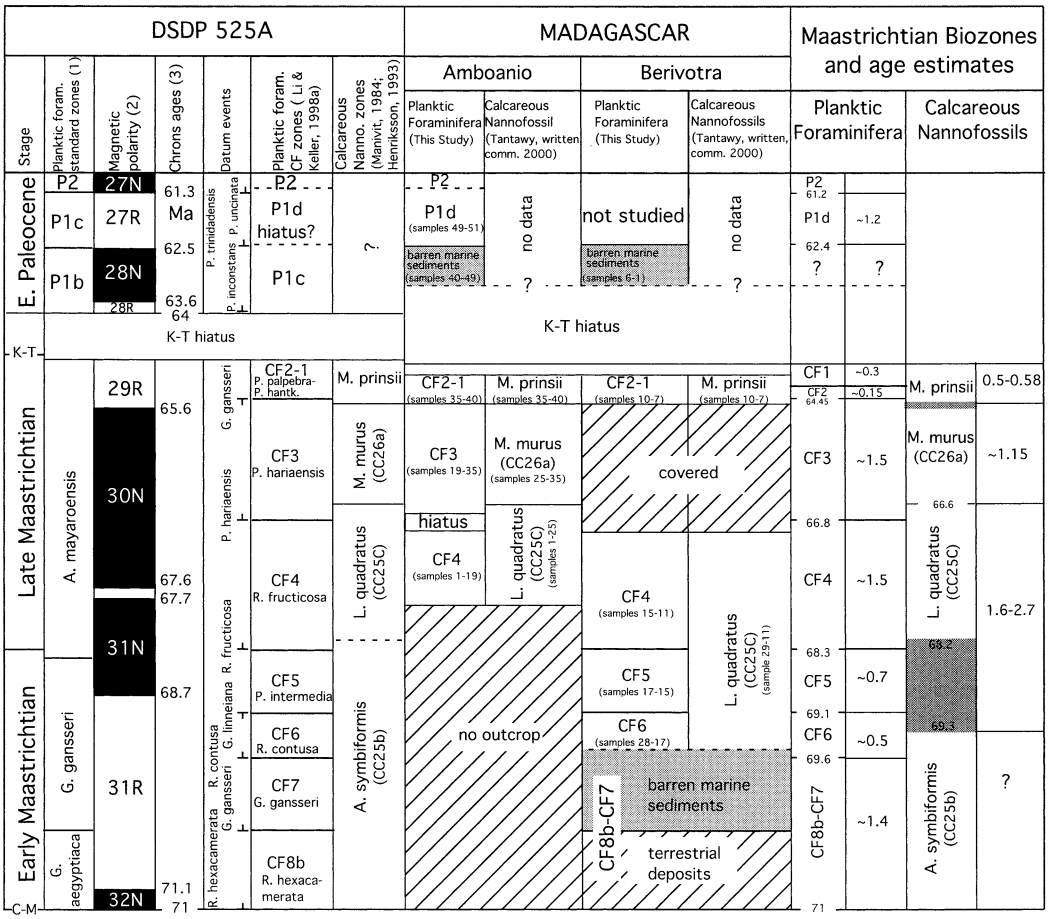

Fig. 10. Biozones of planktic foraminifera and calcareous nannofossils in the Berivotra and Amboanio sections and their correlation with biozones and the paleomagnetic record of DSDP Site 525A. Age estimates for planktic foraminiferal zones are from Li and Keller (1998a). Correlation with calcareous nannofossil zones are based on Site 525A (Manivit, 1984) and other South Atlantic deep sea sites (Henriksson, 1993). The paleomagnetic record of the Danian at Site 525A is revised based on our re-examination of Danian planktic foraminiferal assemblages. Note that at Berivotra the oldest marine sediments that contain microfossils are in zone CF6 (69.6–69.1 Ma) or *Lithraphidites quadratus* zone. The transition from terrestrial to marine sediments occurred between 71 and 69.6 Ma. The K–T hiatus probably spans the early Danian (zones P0, Pla, Plb and possibly Plc?) as well as part of the latest Maastrichtian CF2–CF1 interval. Key references: (1) Caron (1985), Berggren et al. (1995); (2) Chave (1984), Manivit (1984), this study; (3) Chave (1984), Berggren et al. (1995).

brated them to the paleomagnetic time scale of DSDP Site 525A. This new zonal scheme was subsequently applied successfully to sections in Tunisia (Li and Keller, 1998b; Li et al., 1999, 2000; Abramovich and Keller, 2002), Bulgaria (Adatte et al., 2002), and Egypt (Tantawy et al., 2002; Keller, 2002). The new zonal scheme is particularly applicable to the Madagascar planktic foraminiferal assemblages because it was originally based on South Atlantic DSDP Site 525A, located at the same paleolatitude as Madagascar (Fig. 1). For the Lower Tertiary part of the section the subdivision of the Danian used by Keller (1993) and Keller et al. (1995) was used.

4.1. Planktic foraminiferal zones

Rosita contusa (CF6) zone, (69.1–69.6 Ma): this zone is defined by the first appearance (FA) of *R.*

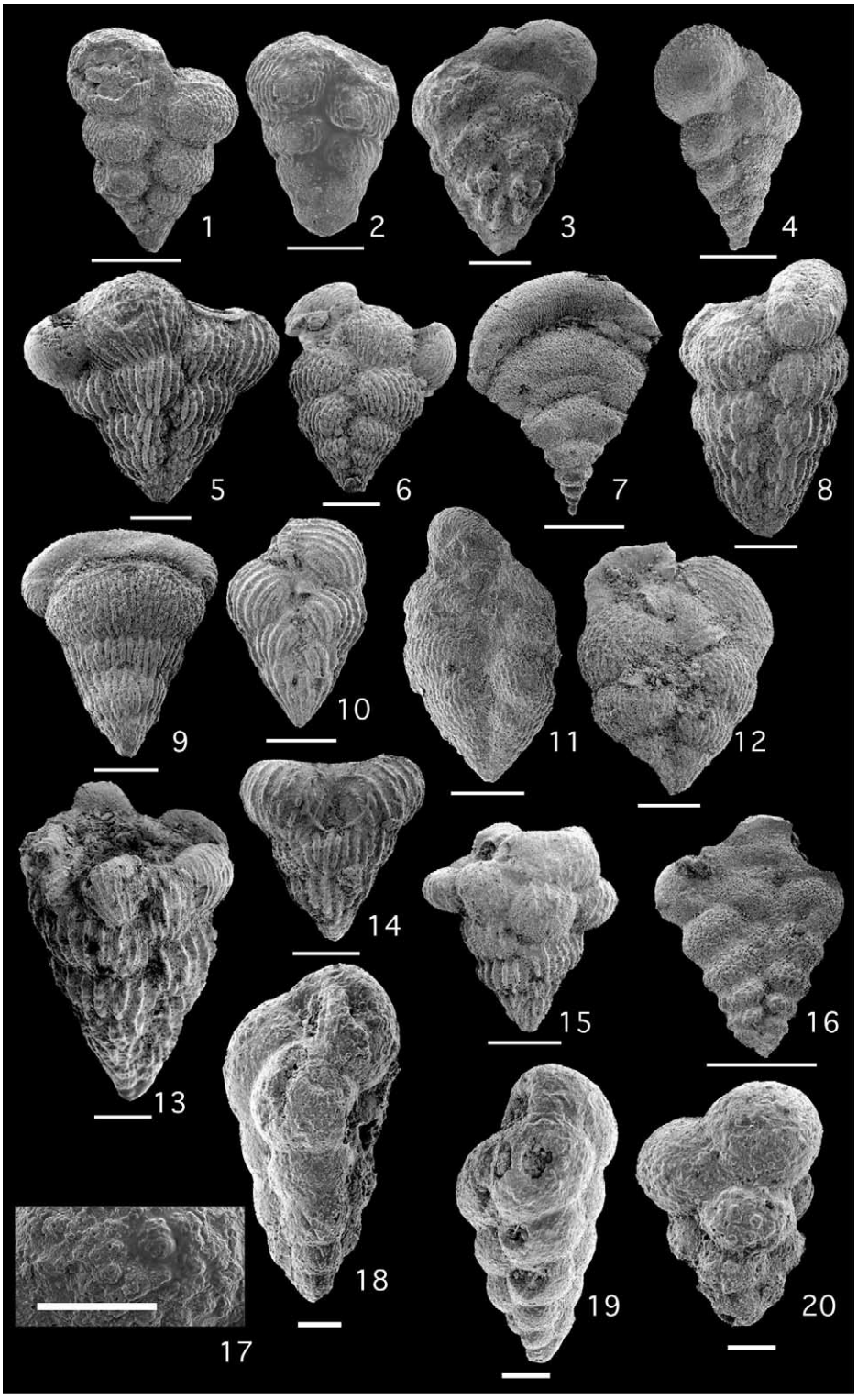

Plate I.

contusa at the base and the last appearance (LA) of *Globotruncana linneiana* at the top. At the Berivotra section, zone CF6 spans 11 m (samples 28–17; Figs. 10 and 11), although the lower part may extend into the underlying barren interval.

Pseudotextularia intermedia (CF5) zone (68.3–69.1 Ma): this zone is defined by the LA of *Globotruncana linneiana* at the base and the FA of *Racemiguembelina fructicosa* at the top. At the Berivotra section zone CF5 spans 3 m (samples 17–15; Figs. 10 and 11).

Racemiguembelina fructicosa (CF4) zone (66.8–68.3 Ma): this zone is defined by the FA of *R. fructicosa* at the base and the FA of *Pseudoguembelina hariaensis* at the top. At the Berivotra section zone CF4 spans 4 m (samples 15–11; Figs. 10 and 11). A slump covers the interval between 11 and 6.5 m, which probably includes the upper part of zone CF4. At the Amboanio section, *R. fructicosa* (Plate I) is relatively common, particularly in the lower 1 m of the section, and zone CF4 spans 5.7 m (from sample 1 to 19; Figs. 10 and 12). The basal part of the zone may be missing due to the limited exposure of the Berivotra Formation at the base of the quarry.

Pseudoguembelina hariaensis (CF3) zone (64.45–66.8 Ma): this zone is defined by the FA of *P. hariaensis* at the base and the LA of *Gansserina gansseri* at the top. Zone CF3 cannot be identified at the Berivotra section, as it is probably within the 5-m-covered interval. *Pseudoguembelina hariaensis* (Plate I) is relatively abundant in the Amboanio section and therefore the base of zone CF3 can be easily recognized. However, *G. gansseri* is rare and the top of zone CF3 was therefore not recognized based on planktic foraminifera.

Pseudoguembelina palpebra (CF2) and *Plummerita hantkeninoides* (CF1) zones (65.0–65.45 Ma): the *Pseudoguembelina palpebra* zone is defined by the LA of *Gansserina gansseri* at the base, and the FA of *Plummerita hantkeninoides* at the top. The *P. hantkeninoides* zone is defined by the total range of the index taxon, plus the last appearances of all tropical species that mark the K–T boundary mass extinction. The zonal index taxa *G. gansseri* and *P. hantkeninoides* are very rare or absent in middle to higher latitude regions, including Madagascar (Pardo et al., 1996; Li and Keller, 1998a). In the absence of these index species, the uppermost Maastrichtian in the Berivotra and Amboanio sections is recognized by the age equivalent nannofossil *Micula prinsii* zone (see discussion below).

Early Paleocene: no biostratigraphic control could be obtained from the lowermost 3.8 m of the Betsiboka limestone because planktic forami-

Plate I.

1. *Heterohelix globulosa* (Ehrenberg), Amboanio, sample 29, bar = 100 μm.
2. *Heterohelix navarroensis* (Loeblich), Amboanio, sample 8, bar = 50 μm.
3. *Heterohelix rajagopalani* (Govindan), Amboanio, sample 3, bar = 100 μm.
4. *Laeviheterohelix glabrans* (Cushman), Berivotra, sample 20, bar = 50 μm.
5. *Planoguembelina brazoensis* (Martin), Amboanio, sample 26, bar = 100 μm.
6. *Planoguembelina carseyae* (Plummer), Amboanio, sample 3, bar = 100 μm.
7. *Pseudotextularia elegans* (Rzehak), edge view, very wide terminal chamber, Amboanio, sample 19, bar = 200 μm.
8,9. *Pseudotextularia deformis* (Kikoine), Amboanio, sample 3, bar = 100 μm and 200 μm, respectively.
10. *Pseudoguembelina costulata* (Cushman), Amboanio, sample 8, bar = 100 μm.
11. *Pseudoguembelina hariaensis* (Nederbragt), Amboanio, sample 26, bar = 100 μm.
12. *Pseudoguembelina palpebra* (Brönnimann and Brown), Amboanio, sample 6, bar = 100 μm.
13. *Racemiguembelina fructicosa* (Egger), Amboanio, sample 10, bar = 100 μm.
14. *Pseudotextularia intermedia* (De Klasz), Amboanio, sample 4, bar = 100 μm.
15. *Racemiguembelina powelli* (Smith and Pessagno), Amboanio, sample 6, bar = 200 μm
16. *Gublerina cuvillieri* (Kikoine), Amboanio, sample 2, bar = 200 μm
17. Detail of Guembelitria dammula test surface with pore mounds, Amboanio, sample 8, bar = 10 μm.
18,19. *Guembelitria dammula*, (Voloshina), Amboanio, sample 8, bar = 20 μm. Specimens with 5–6 serial chambers and slow increase in chamber size.
20. *Guembelitria cretacea* (Cushman), Amboanio, sample 8, bar = 20 μm.

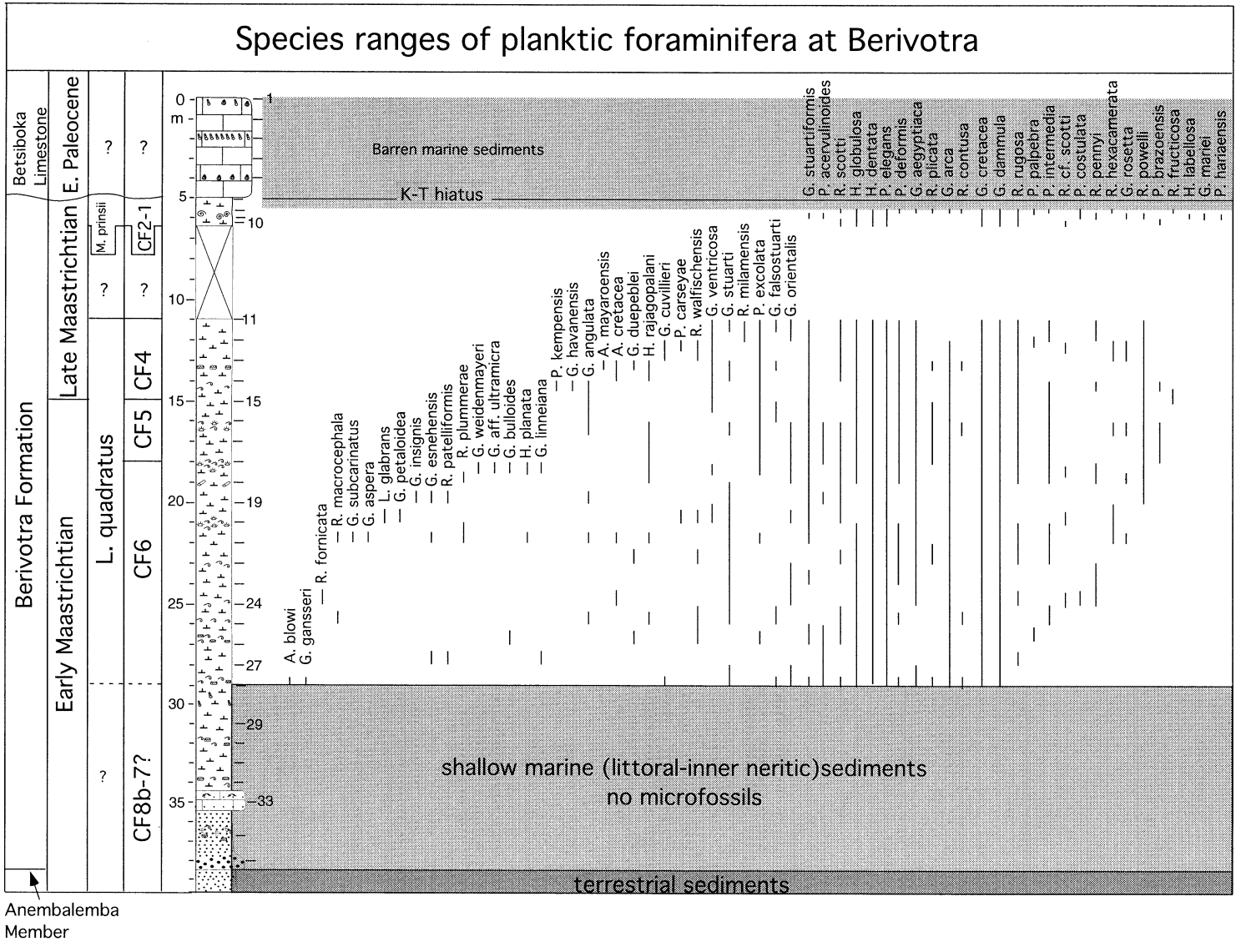

Fig. 11. Biostratigraphic ranges of planktic foraminifera (>63 μm) at the Berivotra section. Planktic foraminifera first appear 9 m above the base of the Berivotra Formation and indicate a zone CF6 assemblage. Both species diversity and relative abundances remain low and sporadic throughout the Maastrichtian and indicate shallow water environments. The Betsiboka limestone contains no plankton (see key to lithology in Fig. 3).

nifera and calcareous nannofossils are absent. However, the age of this interval is probably early Paleocene, as suggested by the Pld age of the overlying limestone (Figs. 10 and 12). However, the age could be anywhere between zones Pla (*Parvularugoglobigerina eugubina*) and Plc.

Rare planktic foraminifera first appear in sample 49 at Amboanio and include *Eoglobigerina pentagona*, *Parasubbotina pseudobulloides*, *P. varianta*, *Praemurica inconstans* and the index species *P. trinidadensis* for the Danian zone Pld (Fig. 12). The first diverse planktic foraminiferal assemblage appears in sample 51 and includes the zone P2 index species *Praemurica uncinata*. The faunal assemblage also includes *P. inconstans*, *Parasubbotina pseudobulloides*, *P. varianta*, *Subbotina triloculinoides*, *Eoglobigerina edita*, *E. trivialis*, *Globoconusa daubjergensis*, *Guembelitria dammula*, *G. cretacea*, *Chiloguembelina crinita*, and *C. morsei* (Fig. 12).

4.2. Calcareous nannofossil zones

Calcareous nannofossil biostratigraphy of the Berivotra and the Amboanio Quarry sections was conducted by Tantawy (written commun., 2000). Nannofossil data were also reported by Bignot et al. (1996, 1998). Taxonomy and definition of zones follow Martini (1971).

Lithraphidites quadratus zone: this zone is defined by the FA of *Lithraphidites quadratus* at the base and the FA of *Micula murus* at the top. At Berivotra the *L. quadratus* zone spans 18 meters (samples 28–11; Figs. 10 and 11). At Amboanio, the *L. quadratus* zone spans the basal 7.2 m of the section (samples 1–25; Figs. 10 and 12).

Micula murus zone: this zone is defined by the FA of *M. murus* at the base and the FA of *Micula prinsii* at the top. *Micula murus* co-occurs in samples 10–8 at Berivotra with *Micula prinsii*, the index taxon for the *M. prinsii* zone (see also Bignot et al., 1996, 1998). This suggests that the *M. murus* zone could be within the underlying covered interval. At the Amboanio section the *M. murus* zone spans 1.22 m (samples 25–35; Figs. 10 and 12).

Micula prinsii zone: this zone is defined by the FA of *M. prinsii* at the base and the FA or increased frequency of *Thoracospharea* sp. at the K–T boundary (Henriksson, 1993). At Berivotra, the *M. prinsii* zone spans the last 1.2 m of the Berivotra Formation, but the uppermost samples (60 cm) are barren probably due to dissolution (Fig. 11). At Amboanio the *M. prinsii* zone spans the uppermost 40 cm of the Berivotra Formation (Figs. 10 and 12). The presence of *M. prinsii* in the Berivotra Formation was also reported by Perch-Nielsen and Pomerol (1973) and Bignot et al. (1998).

Early Paleocene: no calcareous nannofossils were recovered by Tantawy (written commun., 2000) from the Betsiboka Formation. However, Bignot et al. (1998) tentatively identified zones NP1 and NP2 in the upper part of this unit, but report poor preservation and therefore could not identify the index species.

4.3. Age and correlation of microfossil zones

The planktic foraminiferal zonation, augmented by nannofossil stratigraphy, and applied to sections from the Mahajanga Basin, provides a firm basis for correlation with other Maastrichtian and Lower Tertiary pelagic sections (Fig. 10). The lowermost dated horizon within the marine sediments of the Berivotra Formation is within zone CF6, which spans from 69.1 to 69.6 Ma. Zone CF6 corresponds to the lower part of the *Lithraphidites quadratus* nannofossil zone at Berivotra, as also observed at El Kef, Tunisia (Pospichal, written commun., 1993; Li and Keller, 1998b) and Egypt (Tantawy et al., 2002). Though Manivit (1984) placed the FA of *Lithraphidites quadratus* near the base of planktic foraminiferal zone CF4 at DSDP Site 525A (stippled interval, Fig. 10), a discrepancy that may be due to diachronous first appearance of the index taxon, different taxonomic concepts, and/or low sample resolution at Site 525A. In the Mahajanga Basin, the *L. quadratus* zone spans zones CF4–CF6 at Berivotra, in agreement with the correlation of these zones in the Tethys. Only zone CF4 and the upper part of zone *L. quadratus* were recovered at Amboanio.

A hiatus marks the zone CF4–CF3 transition at Amboanio, as noted by the abrupt change in

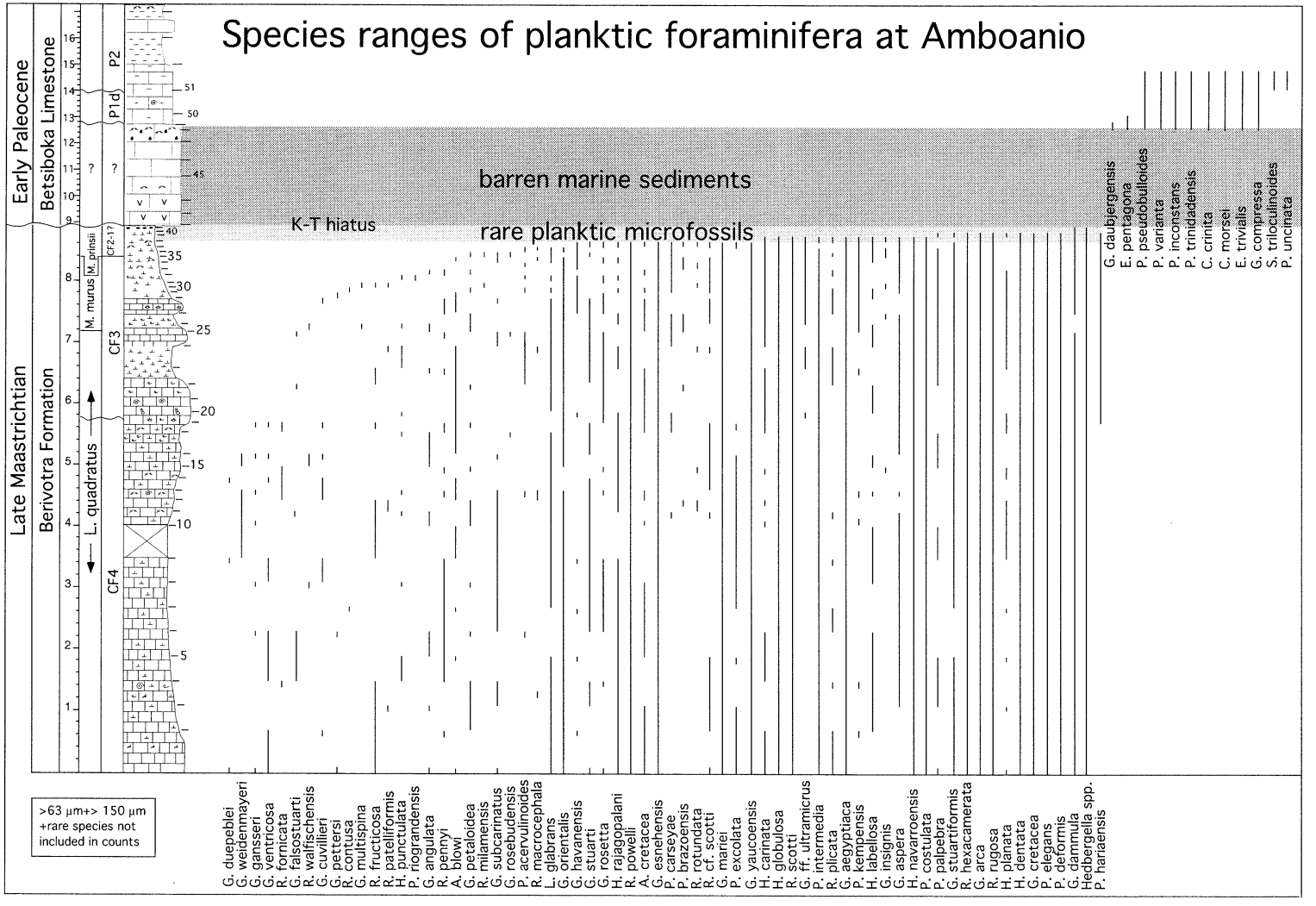

Fig. 12. Biostratigraphic ranges of planktic foraminifera at the Amboanio section (based on 63–150-µm, >150-µm size fractions, and rare species). Note the gradual decline of species between the upper zone CF4 through CF1, and low diversity near the top of the Maastrichtian. Planktic foraminifera are absent in the lower part of the Betsiboka limestone, similar to the Berivotra section and the first early Danian (P1d) species appear 3.8 m above the K–T unconformity (see key to lithology in Fig. 3).

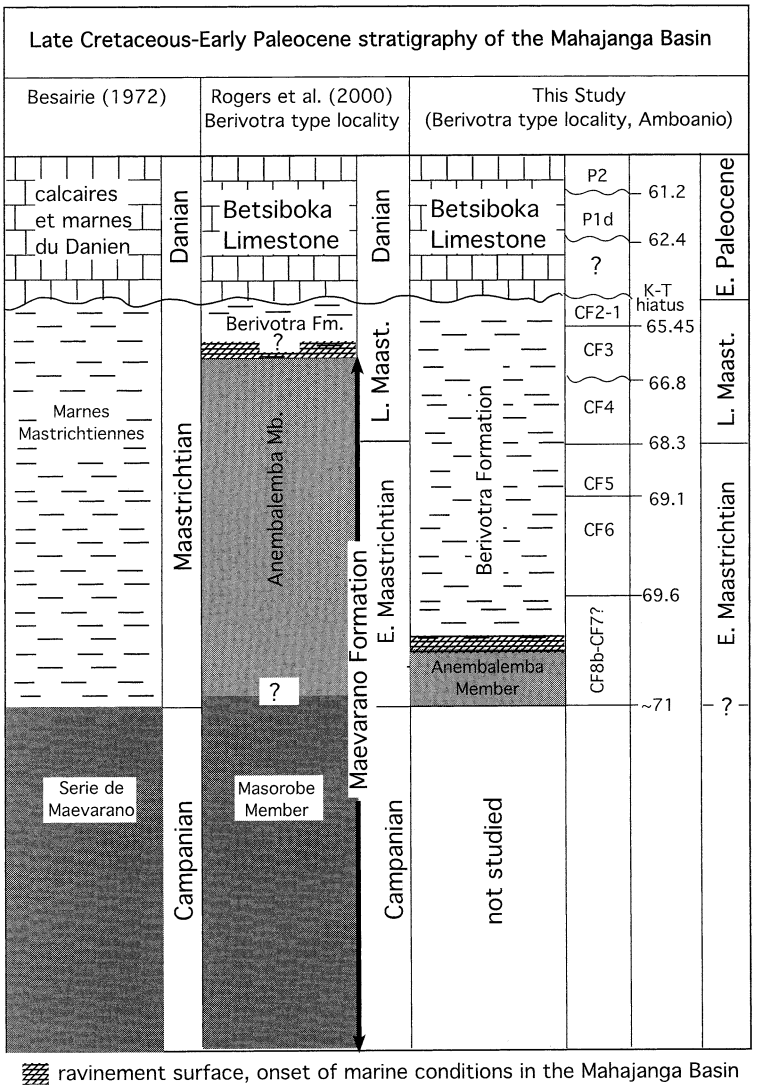

Fig. 13. Stratigraphic nomenclature and biostratigraphy of the late Cretaceous of the Mahajanga Basin based on Besairie (1972), our interpretation of Rogers et al. (2000) for the Berivotra type locality, and this study for the same locality and Amboanio. The stratigraphic nomenclature of Rogers et al. (2000) is adopted in this study. Age estimates for Maastrichtian and early Paleocene rock units and lithostratigraphic boundaries are based on the high-resolution planktic foraminiferal biostratigraphy by Li and Keller (1998a,b). In the Berivotra type locality the Anembalemba Member–Berivotra Formation transition is within the early Maastrichtian CF8b–CF7? interval, or between 71 and 69.6 Ma (see text for discussion), rather than in the late Maastrichtian as suggested by Rogers et al. (2000).

planktic foraminiferal abundances (see discussion below; Fig. 16). An age for this hiatus can be estimated from the microfossil zonations. Sediments overlying the hiatus are of zone CF3 age, and the *Micula murus* zone begins 1.5 m above it (Fig. 12). Since the base of the *M. murus* zone correlates to near the base of planktic foraminiferal zone CF3 (Fig. 10), we can assume that most or all of zone CF3 is present, which would place the hiatus below the 66.8 Ma age of the base of zone CF3.

Age estimates can also be obtained for the lat-

est Maastrichtian based on planktic foraminiferal and nannofossil zones. Henriksson (1993) observed that the range of *Micula prinsii* begins just above the base of magnetochron C29R in a number of Atlantic and Pacific sites, as also observed at Agost, Spain (Pardo et al., 1996) and DSDP Site 525 (Li and Keller, 1998a). Similarly, the range of planktic foraminiferal zones CF2–CF1 (LA of *Gansserina gansseri* to La of *Plummerita hantkeninoides*) begins just above the FA of *M. prinsii* and above the base of C29R in these sections. C29R spans the last ~580 ky of the Maastrichtian (65.6–65.00 Ma; Berggren et al., 1995), whereas CF2–CF1 zones are estimated to span 450 kyr with the base of *M. prinsii* slightly older (Fig. 10). The close correlation of the base of CF2 and *M. prinsii* zones allows the identification of the latest Maastrichtian time interval at both Amboanio and Berivotra. However, since the contact with the overlying Betsiboka Formation is erosional, we assume that the upper part of the *M. prinsii* and CF2–CF1 zones is removed.

The K–T boundary clay was not recovered. An erosional surface and some karstification marks the unconformity between the top of the Berivotra Formation and the overlying Betsiboka limestone formation which is barren of microfossils in the basal 3.8 m. The first planktic foraminiferal assemblage above this interval is of zone P1d age. This suggests that the hiatus spans at least part of the early Danian zones P0–Plc. Hiatuses of this magnitude have been observed in many shallow marine sequences in low to middle latitudes (Fig. 7; MacLeod and Keller, 1991a,b; Stinnesbeck et al., 1997; Keller et al., 1998). The return to carbonate sedimentation after the K–T event begins in the world oceans in planktic foraminiferal zone Plc, more than 500 000 kyr after the K–T boundary (Keller, 1988; Zachos et al., 1989; D'Hondt et al., 1994). It is possible that the shallow water limestone above the K–T unconformity is of zone P1c age, though this cannot be confirmed.

4.4. Age of rock units

The late Cretaceous to early Tertiary of the Mahajanga Basin is lithostratigraphically divided into the terrestrial deposits of the Maervarano Formation, which consists of the Masarobe, Anembalemba and Miadana Members, and the marine deposits of the Berivotra Formation, and Betsiboka limestone (Fig. 13; Rogers et al., 2000). The Miadana Member is not present in the Berivotra type area or at Amboanio. Rogers et al. (2000) observed that the Miadana and Anembalemba Members are time transgressive, with the terrestrial facies becoming younger from northwest to southeast.

Since the 1970s the entire Maevarano Formation has generally been considered to be of Campanian age (Besairie, 1972). Recently, Rogers et al. (2000) argued for a possible late Maastrichtian age for the top of this formation, coeval with the Deccan volcanic province of India estimated between 65 and 67.5 Ma. Our study does not support this assumption for the Berivotra type area. Since the Maevarano Formation consists of terrestrial sediments, a relative age can be inferred based on age diagnostic fossils of the overlying marine sediments of the Berivotra Formation. Biostratigraphic data indicate that the marine sediments that contain diagnostic microplankton in the Berivotra Formation of the type area span from the early Maastrichtian planktic foraminiferal zone CF6 (69.6 Ma) and nannofossil *Lithraphidites quadratus* zone to the K–T boundary unconformity (Fig. 10). The lowermost 9 m of the Berivotra Formation are barren of microfossils due to the very shallow marine environment, but their stratigraphic position indicates an age older than zone CF6. The underlying terrestrial Anembalemba Member must therefore be older also, and a late Maastrichtian age can be ruled out for this unit in the Berivotra type area.

A precise age for the top of the Anembalemba Member in the Berivotra type area is difficult to establish, but since the fossiliferous marine strata are of zone CF6 age (69.6 Ma), the intervening 9-m barren interval may be as old, or older than zones CF7–CF8b. A further age inference can be derived from global sea-level changes based on the assumption that the onset of the marine incursion in the Mahajanga Basin is related to a general rise in the global sea level. A major sea-level rise is widely documented in the earliest

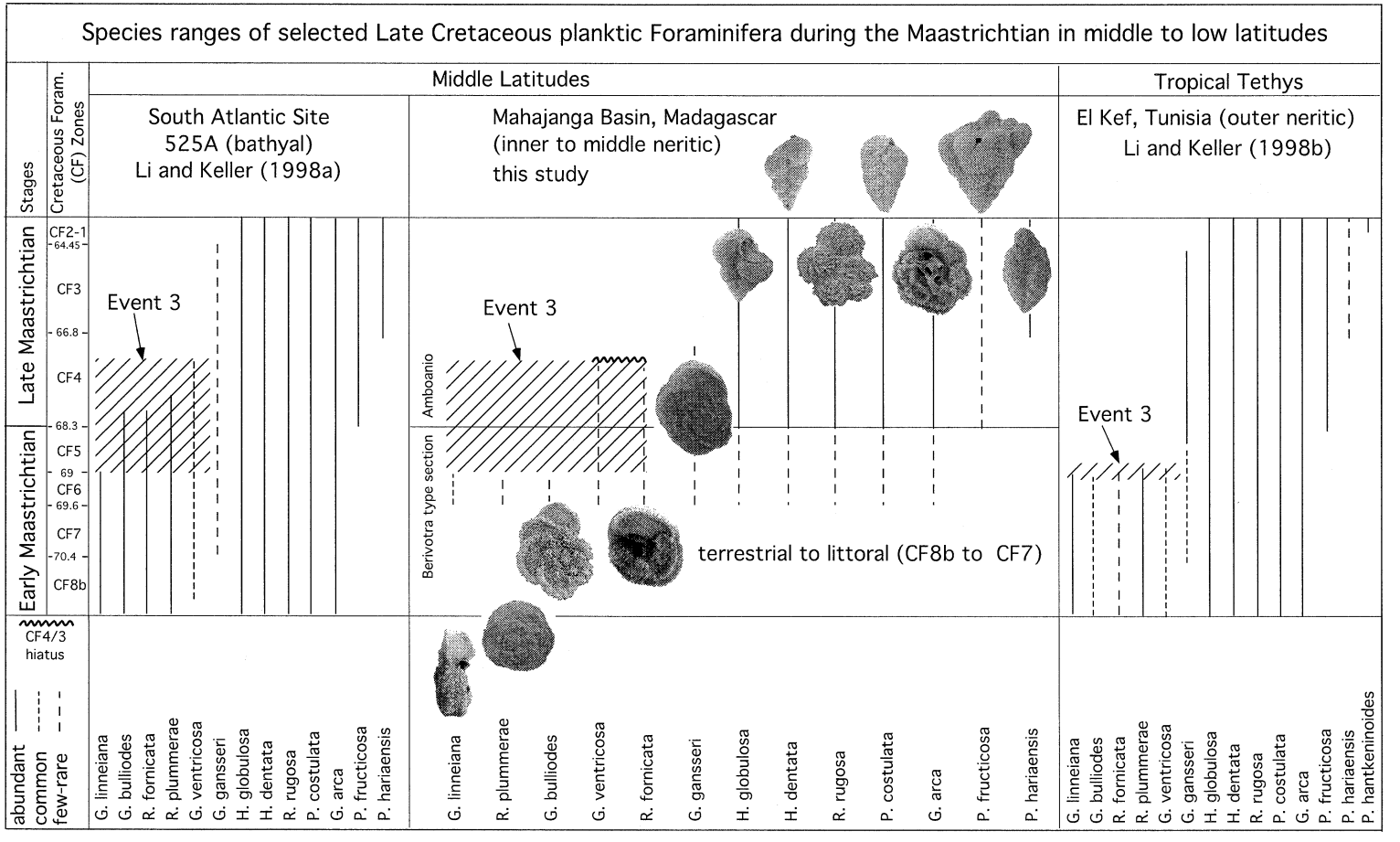

Fig. 14. Stratigraphic ranges of selected planktic foraminiferal species in Madagascar (this study), El Kef, Tunisia (Li and Keller, 1998b), and DSDP Site 525A (Li and Keller, 1998a). Note that the globally recognized Maastrichtian extinction Event 3 is detected in Madagascar. The rarity of *Gansserina gansseri* and other keeled species in Madagascar reflects inhospitable environmental conditions for these species.

Maastrichtian at about ~71 Ma (Haq et al., 1987; Li et al., 1999), following a major global cooling and sea-level lowstand (Barrera et al., 1997; Li and Keller, 1998a). This global cooling occurs near the Campanian–Maastrichtian transition as defined by Gradstein et al. (1995), 71.6 ± 0.7 Ma, and Odin (2001), 72 Ma, which correlates with the base of subzone CF8b (Li et al., 1999).

In the Berivotra type area, it is likely that the first diverse marine assemblages in zone CF6 reflect establishment of fully marine conditions as the sea-level rise reached this area, and that the underlying microfossil-barren sediments reflect the nearshore environment of the early part of this transgression, preceded by the marine and coastal plain sandstones of the underlying Anembalemba Member. By this reasoning, the base of the Berivotra Formation and the Anembalemba Member in the Berivotra type area are of earliest Maastrichtian age (possibly as old as CF7–CF8b; Fig. 13). The Maastrichtian age proposed by Rog-

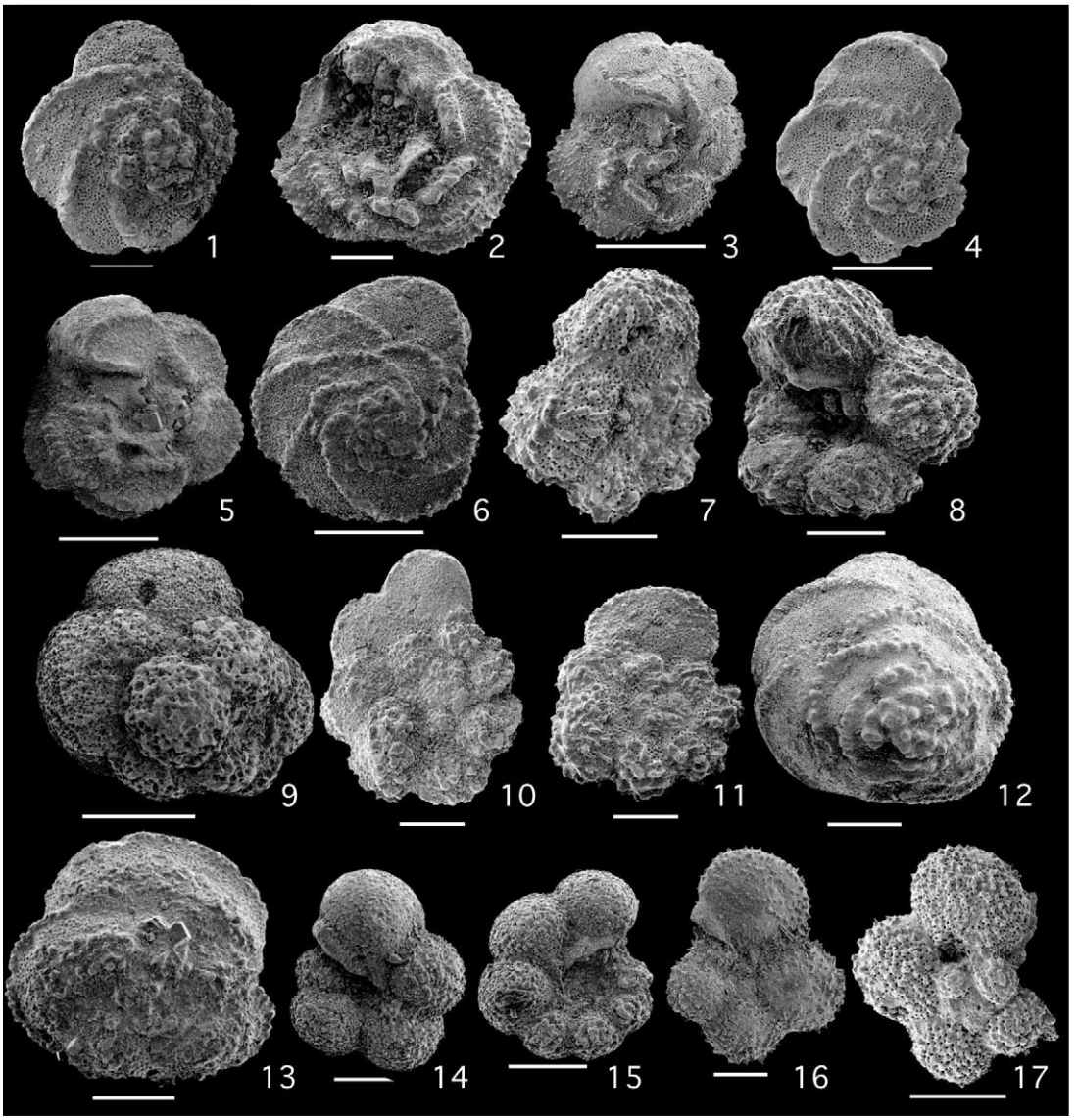

Plate II.

ers et al. (2000), based on the presence of a gastropod morphotype somewhat below the top of the Anembalemba Member, is substantiated, but should be considered very early in the Maastrichtian.

The unconformity between the top of the Berivotra and the Betsiboka Formations marks the K–T boundary (Besairie, 1972; Rogers et al., 2000; Bignot et al., 1996, 1998; Janin et al., 1996). The presence of the latest Maastrichtian *Micula prinsii* and CF2–CF1 zones indicates that the top of the Berivotra Formation is of very latest Maastrichtian age. However, because of the unconformity the precise age of the Berivotra–Betsiboka transition is unknown. As noted above, we estimate that the base of the Betsiboka limestone is of early Danian age, possibly zone Plc? or Pld (Figs. 10 and 13).

5. Planktic foraminiferal faunal analysis

The evolutionary ranges of Maastrichtian planktic foraminifera from the Indo–Pacific province are still poorly understood and the relative abundances of their species populations largely unknown. The Mahajanga Basin of Madagascar provides a unique opportunity to evaluate these planktic foraminiferal parameters within the middle latitude environment of the Indo–Pacific Ocean. This record is further compared with similar records from the middle latitude South Atlantic DSDP Site 525A and various localities of the Tethys Ocean. Quantitative documentation and comparison of species abundances, diversity, evolution and extinctions across latitudes is a necessary prerequisite to understanding regional as well as global patterns of major biotic events.

5.1. Species census data

A total of seventy-one planktic foraminiferal species were identified from Maastrichtian sediments of the Berivotra and Amboanio sections (Figs. 11 and 12). Among these species are 24 biserial or multiserial taxa of the *Heterohelicidea* family, 28 taxa of the trochospiral family *Globotruncanidea*, 10 taxa of the trochospiral family *Rugoglobigerinidea*, six taxa of the planispiral family *Globigerinelloidea*, and three taxa of the triserial genus *Guembelitria*.

At the Berivotra section, planktic foraminifera are rare or sporadically present from the onset of hemipelagic conditions in zone CF6 (69.6 and 69.1 Ma) to the top of the section (Fig. 11). This suggests that full pelagic conditions were not established during the Maastrichtian in this region. However, at Amboanio to the northwest, more diverse and continuous late Maastrichtian (68.3–~65 Ma) planktic foraminiferal assemblages indicate a pelagic paleoenvironment. The differences between these two paleoenvironments are

Plate II.

1,2. *Globotruncana arca* (Cushman), Amboanio, samples 6 and 4 respectively, bar = 100 μm.
3. *Globotruncana orientalis* (El Naggar), Amboanio, sample 4, bar = 200 μm.
4. *Globotruncana linneiana* (D'Orbigny), Berivotra, sample 23, bar = 100 μm.
5. *Globotruncana linneiana* (D'Orbigny), Berivotra, sample 27, bar = 200 μm.
6. *Globotruncanita stuarti* (De Lapparent), Amboanio, sample 9, bar = 200 μm.
7,8. *Rugoglobigerina rugosa* (Plummer), Amboanio, sample 29, bar = 100 μm.
9. *Rugoglobigerina milamensis* (Smith and Pessagno), Amboanio, sample 23, bar = 200 μm.
10. *Rugoglobigerina* cf. *Scotti*, specimen with 7 1/2 chambers in the last whorl and compressed final two chambers, Amboanio, sample 7, bar = 100 μm.
11. *Rugoglobigerina scotti* (Brönnimann), Amboanio, sample 11, bar = 100 μm.
12. *Rosita contusa* (Cushman), Berivotra, sample 25, bar = 200 μm
13. *Rosita plummerae* (Gandolfi), Berivotra, sample 25, bar = 100 μm.
14. *Globigerinelloides aspera* (Ehrenberg), Amboanio, sample 24, bar = 100 μm.
15. *Globigerinelloides* aff. *ultramicra* (Subbotina), with relict apertural flaps, sample 24, bar = 100 μm.
16. *Globigerinelloides subcarinatus* (Brönnimann), Amboanio, sample 8, bar = 50 μm.
17. *Globotruncanella havanensis* (Voorwijk), Amboanio, sample 29, bar = 100 μm.

apparent in the greater Maastrichtian species richness at Amboanio, with 67 species as compared with 61 at Berivotra, their more continuous presence, and the overall higher abundance at Amboanio (Figs. 11 and 12). In both localities, biserial or trochospiral taxa dominate, whereas keeled trochospiral and multiserial taxa are sporadically present. This is consistent with Tethyan shelf regions in general, e.g. Tunisia (Li and Keller, 1998b; Abramovich and Keller, 2002; Keller et al., 2002; Luciani, 2002), Israel (Abramovich et al., 1998), Egypt (Keller, 2002) and Bulgaria (Adatte et al., 2002), whereas in deep sea environments trochospiral and multiserial taxa tend to be more common (e.g. Li and Keller, 1998a, 1999). Therefore, their sporadic occurrence in the Mahajanga Basin suggests that the shallow water environment was the primary limiting factor. In addition, biogeography was a limiting factor as suggested by the absence of the tropical–subtropical Tethyan species *Plummerita hantkeninoides*, and the sporadic occurrence of *Gansserina gansseri*.

In general, the last appearance datum (LAD) of a species either represents the extinction or disappearance from a particular region due to inhospitable environmental conditions. Such conditions are indicated in the Maastrichtian of the Mahajanga Basin by the early disappearances and sporadic occurrences of tropical and deeper water dwelling species. For example, the tropical index taxon for zone CF1, *Plummerita hantkeninoides*, is very common in the late Maastrichtian Tethys Ocean (e.g. Spain, Italy, Tunisia, Egypt, and Israel; Pardo et al., 1996; Luciani, 1997; Li and Keller, 1998b; Abramovich et al., 1998; Abramovich and Keller, 2002; Tantawy et al., 2002; Keller, 2002), but generally absent in middle latitudes including Madagascar (e.g. Site 525, Bulgaria, Kazakhstan, Denmark; Schmitz et al., 1992; Li and Keller, 1998a; Pardo et al., 1999; Adatte et al., 2002). The index taxon for zone CF2, *Gansserina gansseri*, disappeared in zone CF6 at Berivotra and in CF4 at Amboanio, or about 1–2 million yr earlier than in low or middle latitudes (e.g. Tunisia, Israel, Egypt, Site 525A; Figs. 11 and 12). Species disappearances that are coeval in Madagascar and the Tethys (e.g. Tunisia, Israel, Spain, Egypt) include *G. bulloides*, *G. linneiana* and *R. plummerae* (Plate II), the marker species for the CF6–CF5 transition (~69 Ma) and the first Maastrichtian extinction event (Event 3 of Li and Keller, 1998a; Fig. 13). However, at the middle latitude Site 525A only *G. linneiana* occurs in this interval, whereas *G. bulloides*, *R. plummerae* ranged into the base of zone CF4 (~68 Ma). Compared with the tropics *R. fornicata* and *G. ventricosa* also survived longer in middle latitude Site 525 and Madagascar (Fig. 14). Though, the expanded occurrence of these two species at Amboanio (CF4–CF3 transition; Fig. 9), as compared to Site 525A (middle CF4), suggests that the upper part of CF4 is missing at this locality (Fig. 14). The diachronous disappearances of species in low and middle latitude environments reflect: (1) the expanded evolutionary range of temperate species in middle latitudes and shortened range in lower latitudes; (2) the expanded evolutionary range of tropical–subtropical species in low latitudes and shortened range in middle latitudes; and (3) the limiting depth habitat of shallow continental shelves (Madagascar), as compared with open marine environments.

5.2. Relative abundance patterns in the 63–150-μm size fraction

The scarcity of planktic foraminifera in the Berivotra type section prevents quantitative analysis, though such data are obtained from the Amboanio section from two size fractions (63–150 μm and >150 μm; Figs. 15 and 16, Tables 2 and 3).

At the Amboanio section the 63–150-μm size fraction contains 35 species but only four of these dominate the assemblages (Fig. 15). The dominant taxa include two biserial species, *Heterohelix dentata* and *Heterohelix globulosa* and two triserial species *Guembelitria cretacea* and *Guembelitria dammula* (Plate I). The remaining species are less abundant, though sporadically present in the upper Maastrichtian, except for *Hedbergella* spp. and *Pseudoguembelina costulata*, which are continuously present with low abundances (<10%; Fig. 15). The dominant species populations are characterized by simple shell morphology, generally thin test walls and unadorned tests.

The heterohelicids *Heterohelix globulosa* and

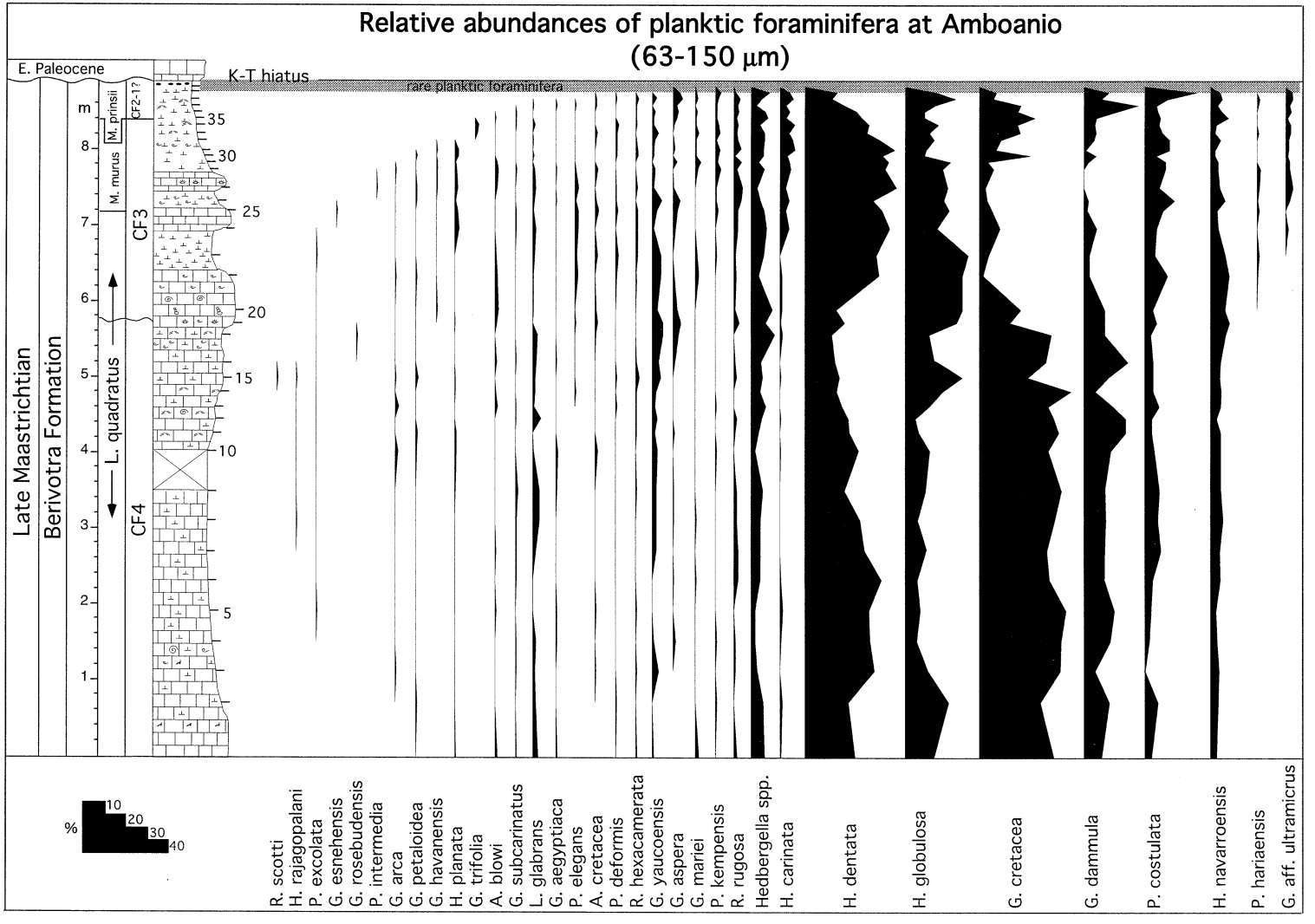

Fig. 15. Relative species abundances of planktic foraminifera in the 63–150-µm size fraction at Amboanio. Note that these low diversity assemblages are dominated by only four species, all of them ecological generalists. The temporary decrease in the relative abundance of *Guembelitria* and the increase in abundance of *Heterohelix dentata* in the lower to middle part of zone CF3 reflect adverse environmental conditions (see text for discussion; key to lithology in Fig. 3).

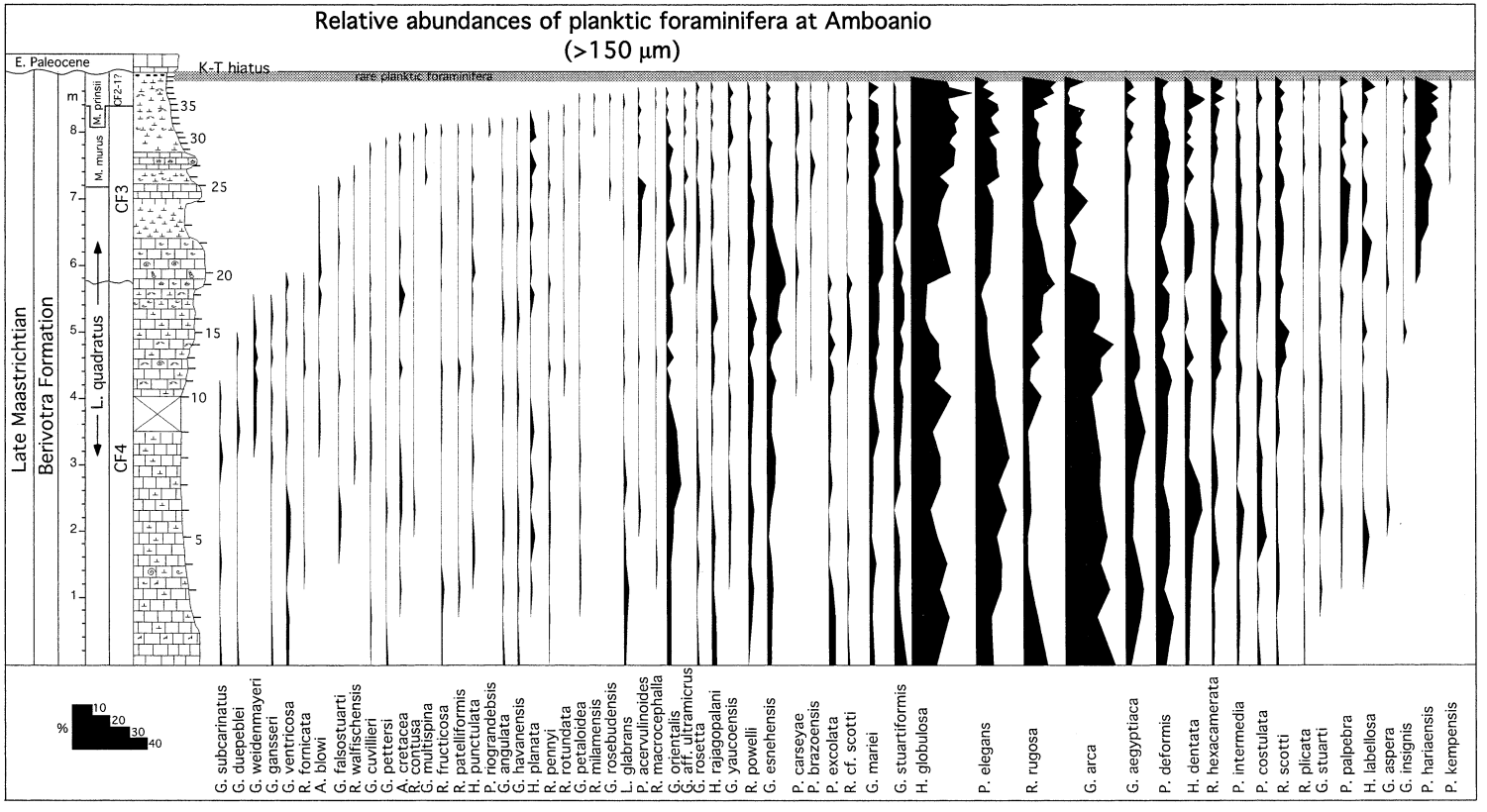

Fig. 16. Relative species abundances of planktic foraminifera in the >150-µm size fraction at Amboanio. Note that the gradual decline of species in the late Maastrichtian CF3–CF1 interval marks environmental changes related to global cooling and local paleodepths. The sharp decrease in the relative abundance of *Globotruncana arca* and increase in *Heterohelix globulosa* at the CF3–CF4 transition may be an artifact of the CF3–CF4 hiatus (key to lithology is in Fig. 3).

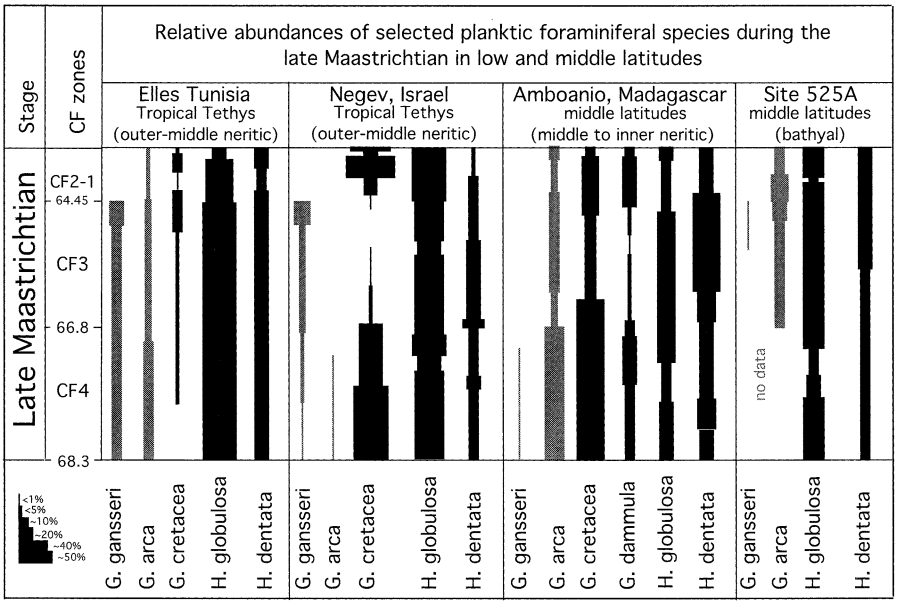

Fig. 17. Relative abundances of selected late Maastrichtian planktic foraminiferal species of Madagascar compared with DSDP Site 525A (Li and Keller, 1998a) and the eastern Tethys, i.e. Negev, Israel (Abramovich et al., 1998); Elles, Tunisia (Abramovich and Keller, 2002). Note that similar *Guembelitria* abundance patterns in Madagascar and the Negev suggest similar responses to high-stress late Maastrichtian conditions; the zone CF3 *Gansserina gansseri* abundance peak appears restricted to lower latitudes; the *Globotruncana arca* decrease in the upper CF4 zone (~67.5–66.8 Ma) may reflect a high-stress shelf environment for this species; and the greater abundance of *Heterohelix dentata* relative to *Heterohelix globulosa* in Madagascar compared with the reverse in continental shelf sections of Tunisia and Israel, suggests *H. dentata*'s ecological preference for shallower depths.

Heterohelix dentata tend to dominate in continental shelf environments such as in the eastern Tethys, as well as in deeper marine environments (e.g. Site 525A) where *H. globulosa* is typically more abundant than *H. dentata* (Fig. 17). However, in Madagascar *H. dentata* is significantly more abundant than *H. globulosa* (Figs. 15 and 17). A similar pattern is observed in the shallow environment of the Seldja section in southern Tunisia (Keller et al., 1998). These abundance patterns suggest that *H. dentata* thrived in shallower neritic environments.

A major faunal change occurs above the CF4–CF3 transition where the relative abundance of *Guembelitria cretacea* and *Guembelitria dammula* decrease to less that 10% from their earlier dominance of >50% (Fig. 15). The relative abundance of *Guembelitria* remains low through zone CF3. At the same time the abundance of the biserial *Heterohelix dentata* and *Heterohelix globulosa* increases significantly (40 and 30%, respectively), and *Pseudoguembelina costulata* increases to 10%. In the upper part of CF3 the relative abundance of *Guembelitria* species increases to ~30% and remains high through the CF2–CF1 interval, except at the top (samples 38 and 39) where *Guembelitria* decreases (<20%) and *H. globulosa* and *P. costulata* increases (24% and 23% respectively).

The high abundance of *Guembelitria* in the Amboanio section is of significant ecological importance. They are interpreted as ecological opportunists mainly due to the *Guembelitria* bloom in the early Danian following the K–T mass extinction (Smit, 1982, 1990; Keller and Benjamini, 1991; Schmitz et al., 1992; Keller, 1988; Keller et al., 1993, 1995; MacLeod, 1993; Pardo et al., 1996). However, *Guembelitria* species are generally abundant in shallow neritic environments of the Maastrichtian, as studies have shown from Denmark (Schmitz et al., 1992; Keller et al., 1993), Kazakhstan (Pardo et al., 1999), Tunisia

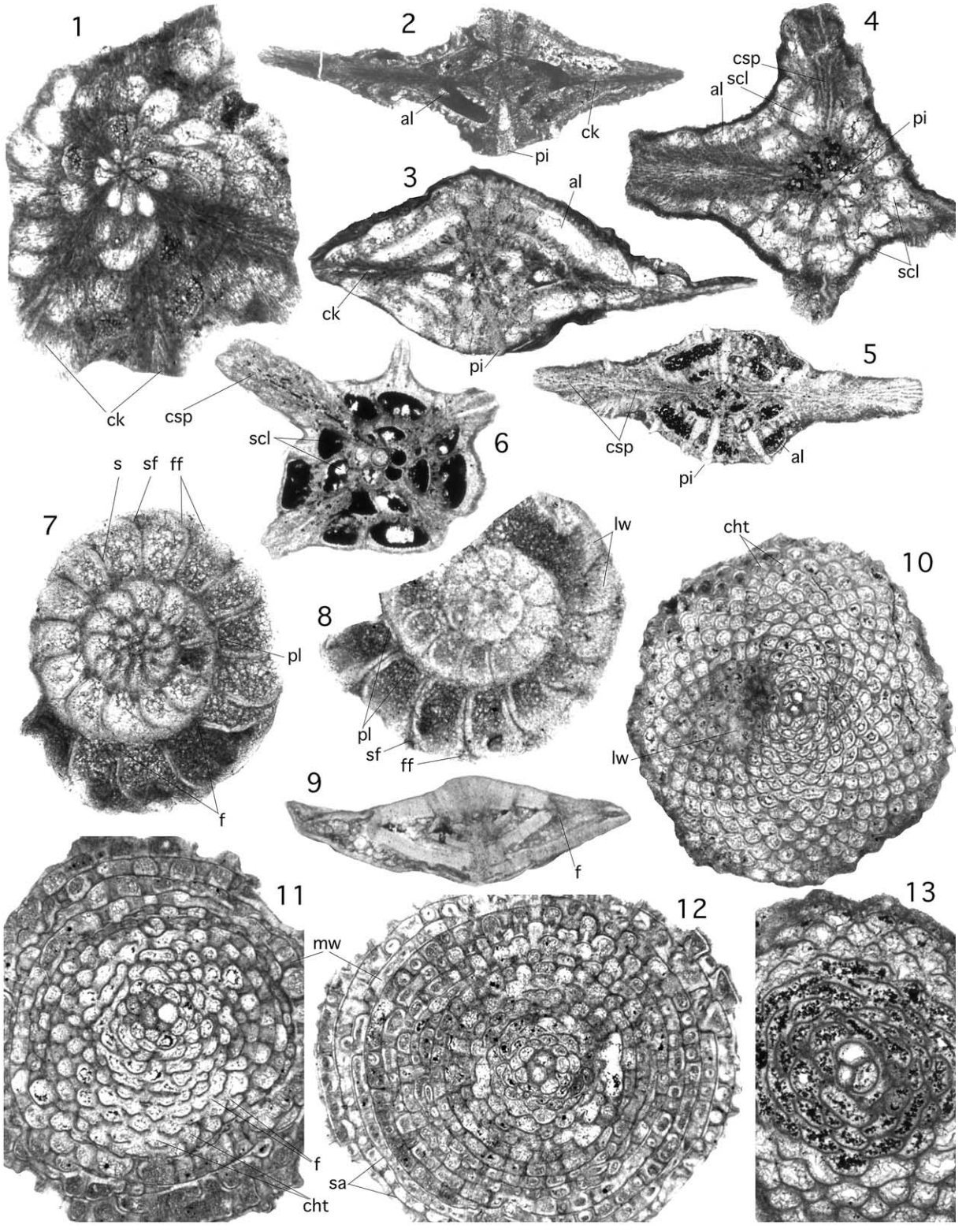
1
ck
csp
2
al
ck
pi
3
al
ck
pi
4
csp
scl
al
pi
scl
5
csp
al
pi
6
scl
7
s
sf
ff
pl
f
8
lw
pl
sf
ff
9
f
10
cht
lw
11
mw
f
cht
12
sa
13

Plate III.

(Keller et al., 1998, 2002) and Texas (Keller, 1989). Abundant *Guembelitria* are also observed in the uppermost Maastrichtian (CF2–CF1 zones) of the deeper outer shelf–upper bathyal environment of the northern Tethys, e.g. Bulgaria (Adatte et al., 2002) as well as Israel (Abramovich et al., 1998) and Egypt (Keller, 2002). A second *Guembelitria* bloom (>60%) is observed in the upper Maastrichtian CF5–CF4 interval in the Negev, Israel (Fig. 17). *Guembelitria* tends to thrive in high stress and predominantly near-shore environments, though the specific environmental parameters are still unclear.

Peak *Guembelitria* abundances in the Amboanio section correlate with those observed in the Negev of Israel (Fig. 17) and suggest times of widespread high-stress conditions, possibly due the shallow water environment. However, at Amboanio these *Guembelitria* blooms span a longer time interval (CF4–CF3) than in the Negev (upper CF4 to lower CF3) and suggest prolonged high-stress conditions. Another major difference between the two regions is the presence of *Guembelitria dammula* at Amboanio and its absence in the Negev or Egypt. *G. dammula* is distinguished from all other *Guembelitria* species by having a larger elongate test and very regularly stacked chambers, similar to its smaller relative *Guembelitria danica* (Plate I). This species was originally described from the late Maastrichtian and early Danian of Bjala, Bulgaria (Rögl et al., 1996; Adatte et al., 2002). Similar morphotypes of this species are rarely present in Tunisia, Israel and Egypt where they are generally included with *G. danica*. *G. danica* was originally described from the Danian of Denmark where this morphotype is abundant. It is still unclear to which degree *G. danica* and *G. dammula* may be ecological variants of the same species. Nevertheless, the relatively high abundance of large *Guembelitria* (e.g. *G. dammula* or *G. danica*) in Madagascar and Bulgaria suggests an ecological preference for middle latitudes.

5.3. Relative abundance patterns in the >150–μm size fraction

Populations of planktic foraminiferal species in

Plate III.

1–3. *Siderolites denticulatus* (Douvillé). Magnification ×25. Amboanio, sample 28.
1. Not quite centered equatorial section showing canalicular keel (ck) extended over the entire equatorial plane, separating the main spiral chambers into two alar chamberlets.
2,3. Axial sections, more or less well centered, showing equatorial separation of spiral chambers by median canalicular keel (ck) after the second volution of the spire.
4,5. *Siderolites calcitrapoides* (Lamarck). Magnification ×25. Berivotra, sample 16.
4. Subequatorial, slightly oblique section showing two canalicular spines rising from early interseptal spaces and covered laterally by alar prolongations (al) of spiral chambers (scl). Umbilical piles (pil) lack any canals and insert on the proloculus wall.
5. Axial section cutting two opposite canalicular spines (csp). Umbilical piles (pil) do not bear canals.
6. Small specimen considered as juvenile of *S. calcitrapoides*. Magnification ×50. Berivotra, sample 16. Well centered equatorial section showing details of the origin of the canalicular spines in relation to the early spiral chambers.
7–9. Novum genus 1, nova species A. Magnification ×50. Amboanio, sample 28.
7,8. Not quite centered equatorial sections. Note submarginal position of intercameral foramen (f) as well as septal furrow (sf) and faint sutural feathering (fs) below spiral periphery. The significance of the 'plate' (pl) is not clear and needs further investigation.
9. Axial section showing perfectly evolute dorsal side, the most unusual adaxial ventral alar prolongations (val) and the submarginal position of the intercameral foramen (f).
10. *Orbitoides concavatus* (Rahaghi). Magnification ×25. Berivotra, sample 8. Equatorial section of slightly distorted specimen that reaches the lateral chamberlet walls not far from the shell center.
11,12. *Omphalocyclus macroporus* (Lamarck). Magnification ×25. Berivotra, sample 8. Equatorial sections. Note median walls separating the two main layers of regular orbitoidal chamberlets and the foramen (f) connecting them.
13. *Omphalocyclus macroporus* (Lamarck). Juvenile specimen. Magnification ×50. Berivotra, sample 8. Details of nepiont: embryonic apparatus not oriented in the median plane of the adult.

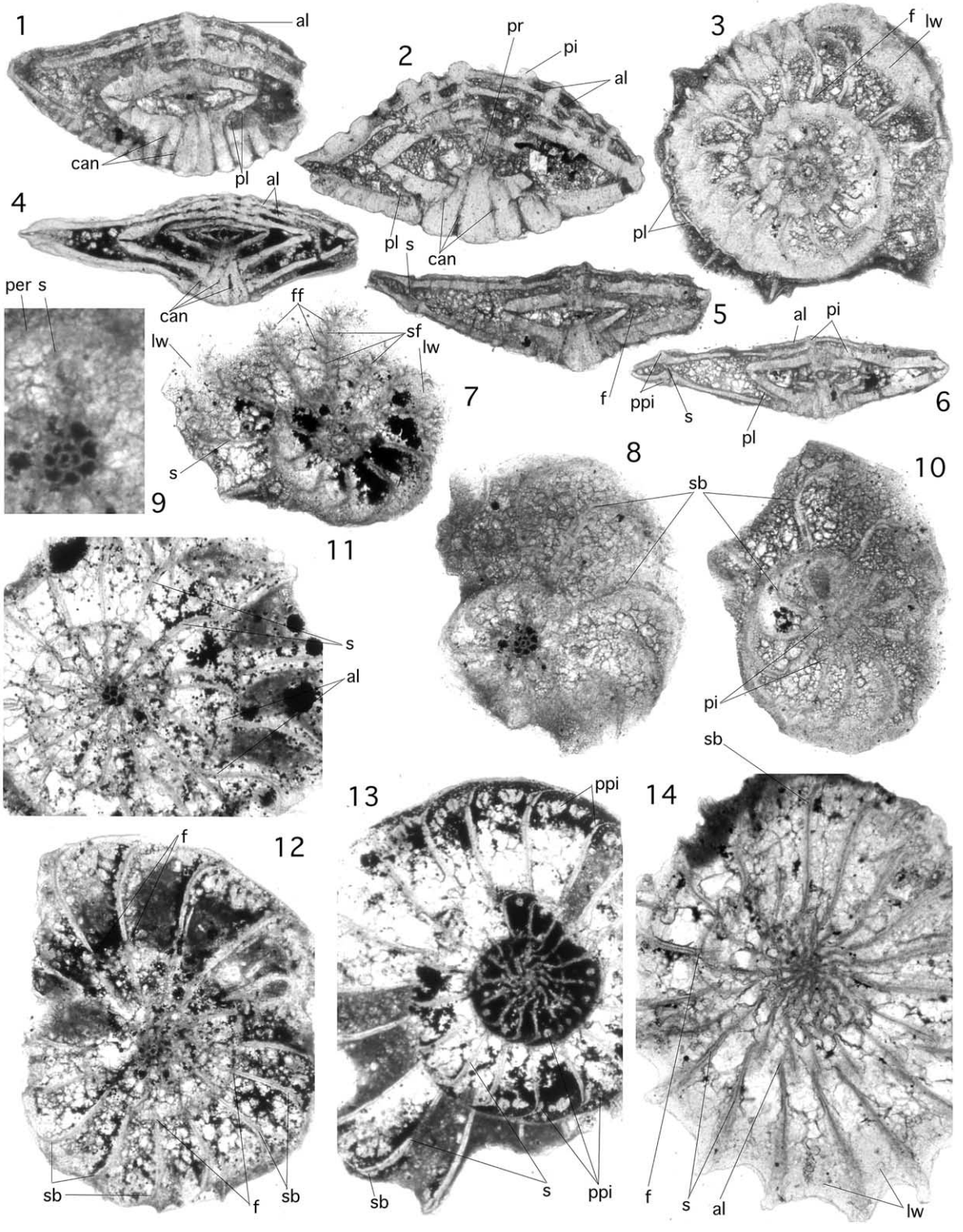
1
al
can
pl
al
2
pr
pi
al
pl
s
can
3
f
lw
pl
4
al
can
per
s
ff
sf
lw
lw
s
9
7
5
al
pi
f
ppi
s
pl
6
8
sb
10
pi
11
s
al
sb
13
ppi
14
12
f
sb
f
sb
sb
s
ppi
f
s
al
lw

Plate IV.

the >150–μm size fraction of the Amboanio section are more diverse as compared with the smaller 63–150–μm size fraction, and consist of 61 species (Fig. 16). Within these assemblages, nine species dominate with abundances >10% (*Heterohelix globulosa*, *Pseudotextularia deformis*, *Pseudotextularia elegans*, *Pseudoguembelina hariaensis*, *Rugoglobigerina rugosa*, *Globotruncana aegyptiaca*, *Globotruncana arca*; Plates I and II). *Pseudoguembelina hariaensis* is common only in the uppermost Maastrichtian (Fig. 16). The rest of the species are either less abundant or sporadically present (Fig. 12). A major faunal change characterizes the transition between the CF4–CF3 zones, where the relative abundances of *G. arca* and *G. aegyptiaca* drop sharply (from 16 to 3% and from 5 to 0% respectively), and the relative abundance of *H. globulosa* increases from 8 to 21%. This abrupt faunal change coincides with a lithological change between marly limestone/limestone and marks a hiatus between these rocks units. In zone CF3 *G. arca* (Plate II) increases to about 10%. This increase is not observed in the Tethys where *G. arca* continues to decline throughout the rest of the Maastrichtian (Fig. 17). However, at Site 525A the relative abundance of *G. arca* is similar to that observed in Madagascar, demonstrating *G. arca*'s ecological preference for middle latitude environments.

Between the upper part of CF3 and the top of the Maastrichtian 15 species gradually decline (e.g. *Globotruncana arca, G. orientalis, G. rosetta*, *Globotruncanita stuarti*, *G. insignis Archaeoglobigerina blowi*, *A. cretacea*, *Heterohelix rajagopalani*, *H. planata Pseudogeumbelina excolata*, *Planoglobulina acervulinoides*, *P. brazoensis Globigerinelloides*. aff. *ultramicra*, *Racemiguembelina powelli*, and *Pseudotextularia intermedia*; Fig. 16). The decline and disappearance of these species in the Mahajanga Basin can be attributed to the local shallowing that reduced plankton habitats during the latest Maastrichtian.

6. Selected larger benthic foraminifera with complex structures

Larger benthic foraminifera with complex test structures are common only in selected Maastrichtian intervals of both the Berivotra and Amboanio sections, and rare or absent in the early Paleocene. A preliminary study of these species is

Plate IV.

1–3. *Sirtina orbitoidiformis* (Brönnimann and Wirz). Magnification ×50. Berivotra, sample 16.
1. Subaxial section showing dorsal alar prolongations (al) and umbilical canal system (can).
2. Axial section showing umbilical plate (up), – or umbilical wall?
3. Equatorial section showing intercameral foramen (f) immediately below spiral periphery.
4, 11–14. *Sirtina* nova sp. B. Magnification ×50. Berivotra, sample 16.
4. Subaxial section of specimen infiltrated by iron oxide.
11. Equatorial section with nepiont infiltrated by iron oxide.
12. Subequatorial section, slightly oblique, shows position of intercamaeral foramen (f) below spiral periphery.
13. Subequatorial section immediately above equatorial plane showing adaxial alar prolongations and dorsal piles in early whorls. Note peripheral rows of piles (ppi) standing over the peripheral backward bend (sb) of septa. No lateral chamberlets.
14. Oblique section near equatorial plane showing position of intercameral foramen (f) below spiral periphery (left) and dorsal alar prolongations (right). Lateral walls (lw) of late spiral chambers pushed into the chamber lumen by sediment compaction.
5–10. *Daviesina fleuriausi* (d'Orbigny). Magnification ×50, except (9) where magnification is ×100. Berivotra, sample 17.
5,6. Axial sections showing at least one layer of dorsal. adaxial alar prolongations (al) supported by dorsal piles (pi). The plate (pl) might be an umbilical wall of the spiral chamber and needs additional investigation.
7. Tangential section cutting the ventral lateral wall (lw) of the spiral chambers, showing furrow and feathering of ventral septal sutures.
8. Centered equatorial section showing backward bend of septa (sb) at about mid height of the spiral chambers.
9. Enlarged detail of (8) showing early chambers filled with iron oxide.
10. Subequatorial section through dorsal part of shell showing dorsal piles (pi) supporting adaxial alar prolongations (al)

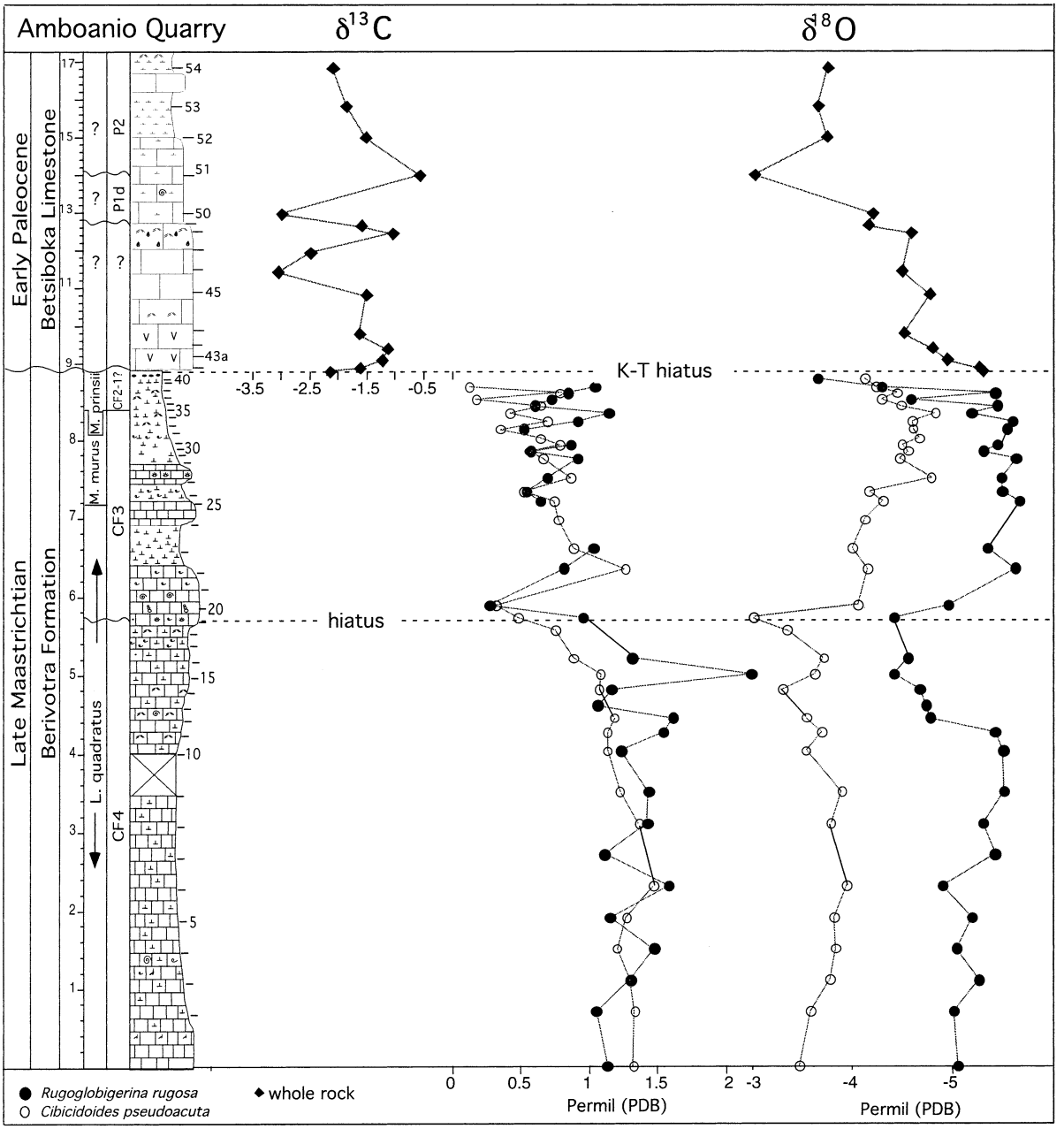

Fig. 18. Stable isotope records ($\delta^{18}O$ and $\delta^{13}C$) of the surface dwelling planktic foraminifer *Rugoglobigerina rugosa* and benthic foraminifer *Cibicidoides pseudoacuta* at Amboanio. Note the positive shift of benthic and planktic $\delta^{18}O$ values in zone CF4 that suggests cooler temperatures. The decreases in $\delta^{18}O$ values and the surface-to-deep gradient above the CF4–CF3 hiatus suggest warmer bottom water temperatures possibly due to shallowing. $\delta^{13}C$ values suggest decreased surface productivity above the CF4–CF3 hiatus. The Berivotra–Betsiboka unconformity is marked by 2‰ $\delta^{13}C$ shift that characterizes the global drop in surface productivity in the early Danian (see key to lithology in Fig. 3).

presented here based on thin-sections and taxonomic identification following Rahaghi (1976) and Wannier (1983). Common species are illustrated in Plates III and IV.

In the modern ocean most foraminiferal species with complex test structures, and of more or less large size, live in the photic zone because most of them have symbionts. Larger foraminifera most frequently are preserved in cemented limestone from where they have to be identified in random thin-sections. Most information about their stratigraphic and paleoenvironmental ranges comes from the stratigraphic relationship of cemented hard rock. In the Madagascar sections, larger foraminifera are occasionally present as free specimens in residues of washed, marly sediments where their external morphology reveals their specific identity, but rarely their generic characters. Therefore, free specimens of larger foraminifera must still be documented by appropriate thin sections, which are comparable to random sections in hard rock.

In the Berivotra section, low diversity larger benthic foraminiferal assemblages are present in silty marl layers rich in macrofossils and small benthic foraminifera. These larger foraminiferal assemblages generally consist of one dominant and a few rare species. For example, in samples br 20, 17 and 16 (planktic foraminiferal zones CF6 and CF5) either *Daviesina fleuriausi* is dominant and *Sirtina* n. sp. B rare, or the reverse prevails. Additional species present include *Sirtina orbitoidiformis*, *Siderolites calcitrapoides*, *Palmula* sp. and *Goupillaudina* sp. (Plates III and IV). At the top of the Maastrichtian (*Micula prinsii* zone) *Omphalocylus* cf. *macroporus* is frequent and few specimens of *Orbitoides concavatus* are present (Plate III).

At Amboanio, sediments in the lower part of the section (upper Maastrichtian zone CF4) contain normal outer neritic to epibathyal small benthic foraminiferal assemblages (e.g. lenticulinids, marginulinids, *Flabellinella* gr. *africana*), and macrofossils are common only in a few limestone layers. Larger benthic foraminifera are common only in the limestone layers of zone CF3 that are rich in macrofossils (e.g. oysters, abundant trace fossils *Chondrites*, *Thalassinoides*). The monogeneric larger benthic foraminiferal assemblage present consists of *Siderolites denticulatus* and various morphologic variants (Plate III).

The larger foraminiferal fauna from the Mahajanga Basin of Madagascar is characterized by a surprising absence of late Cretaceous orbitoidiforms (i.e. *Orbitoides*, *Hellenocyclina* and *Lepidorbitoides*). Elsewhere, for instance in southwestern France, facies dominated by *Omphalocyclus* and/or *Siderolites* have at least some orbitoidiform representatives that mark the local end-members of shallowing trends within the photic zone. On the other hand, *Sirtina* and their consorts in southern France and in the Subbetic realm in southern Spain characterize the lower part of the photic zone where the siderolitids are thin and compressed and where *Orbitoides* is replaced by *Lepidorbitoides* and *Hellenocyclina*. The discorbinid *Praestorrsella roestae* (Visser, 1951) is another typical representative in these deeper photic facies (Hottinger and Caus, 1993) that is absent in the Madagascar faunas.

Thus the Madagascar faunas observed in the late Maastrichtian interval at Amboanio section represent a deeper photic environment, taking into account not only the extreme flattening of the *Siderolites denticulatus*, but also the constant presence of lenticulinids and marginulinids. The latter are known to range in recent tropical seas from the epibathyal realm into the lowermost photic zone (Reiss and Hottinger, 1984). In the Berivotra section, the top of the Berivotra Formation is dominated by *Omphalocyclus macroporus*, reached the upper photic zone whereas the earlier deposits, dominated by *Syrtina* and *Daviesina fleuriausi*, represent a deeper neritic environment. It is possible that the paleoecological gradient reflected by the faunal changes is not a simple depth gradient (due to the absorption of sunlight in the water column), but also to a cline in nutrient concentration. This is supported by the presence of the *Flabellinella africana* group in sample am 11 that characterizes late Cretaceous upwelling conditions on the continental shelf in Morocco (Hottinger, 1966).

The species identified in Madagascar are also present in southern India, Iran, southeastern Turkey, Libya, Pyrenees and in the type locality of

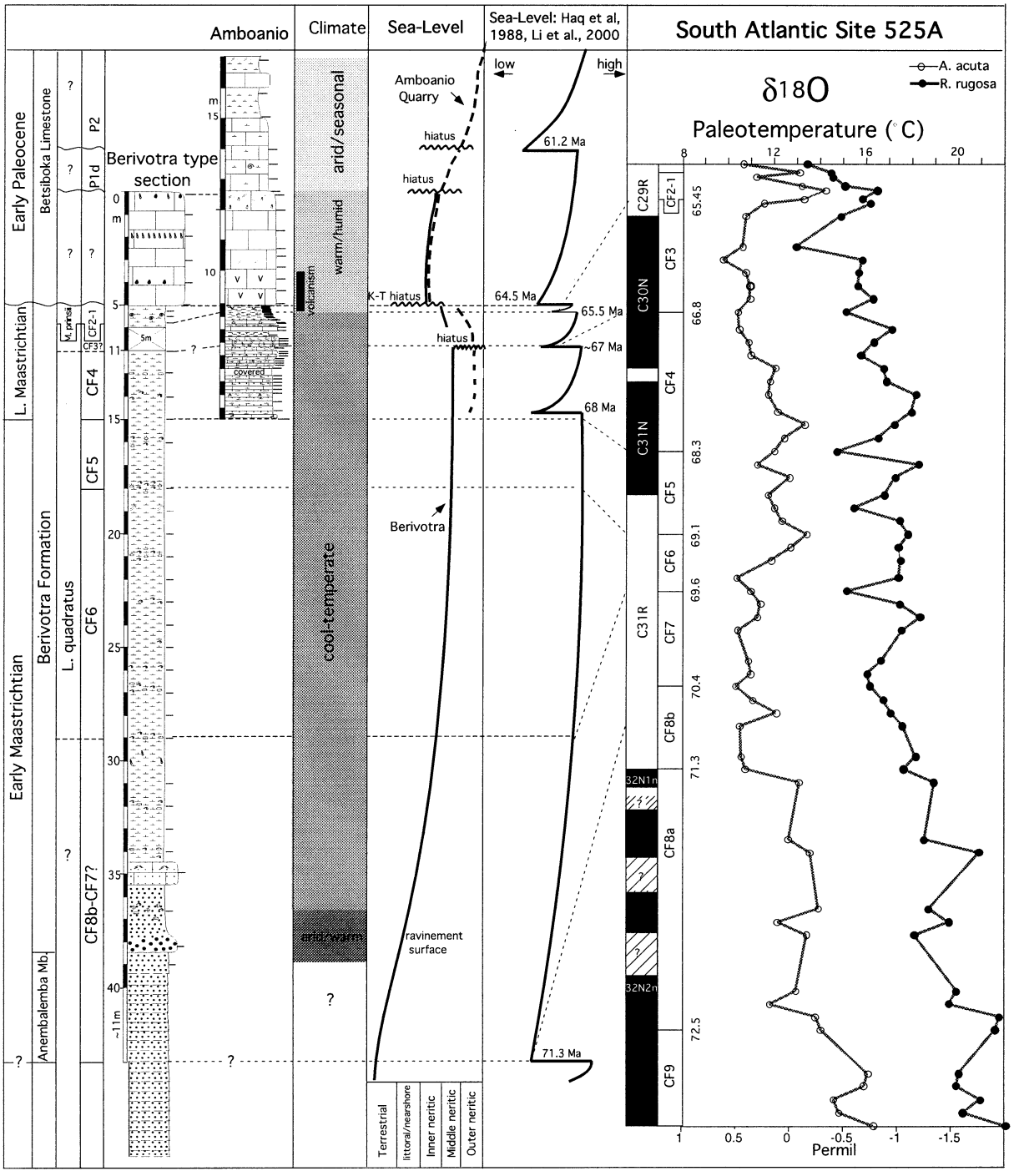
Amboanio
Climate
Sea-Level
Sea-Level: Haq et al, 1988, Li et al., 2000
South Atlantic Site 525A
Early Paleocene
Early Maastrichtian
L. Maastrichtian
Betsiboka Limestone
Berivotra Formation
Anembalemba Mb.
L. quadratus
P2
P1d
CF4
CF5
CF6
CF8b-CF7?
CF2-1
Berivotra type section
covered
5m
~11m
arid/seasonal
warm/humid
volcanism
cool-temperate
arid/warm
Amboanio Quarry
hiatus
K-T hiatus
Berivotra
ravinement surface
low
high
61.2 Ma
64.5 Ma
65.5 Ma
67 Ma
68 Ma
71.3 Ma
Terrestrial
littoral/nearshore
Inner neritic
Middle neritic
Outer neritic
δ18O
A. acuta
R. rugosa
Paleotemperature (°C)
Permil
C29R
C30N
C31N
C31R
CF3
CF4
CF5
CF6
CF7
CF8b
CF8a
CF9
32N1n
32N2n
65.45
66.8
68.3
69.1
69.6
70.4
71.3
72.5

the Maastrichtian in southern Limburg. Their relations to the Caribbean realm remain obscure. Consequently, the benthic late Cretaceous fauna of Madagascar is not endemic, though it clearly shows a lower than usual diversity hampering to some extent the paleoecological interpretation.

7. Stable isotopes

Stable isotope analysis was conducted on the planktic foraminifer *Rugoglobigerina rugosa* and benthic foraminifer *Cibicidoides pseudoacuta* from the Amboanio section. The preservation of species is generally good, although foraminiferal tests are partly recrystallized, which can alter the original test calcite and significantly affect $\delta^{18}O$ values (Barrera and Huber, 1990; Killingley, 1983). Constancy in isotopic differentiation between species can be used as indicator of the degree of diagenetic alteration. As diagenetic alteration increases, interspecific isotopic differences become smaller and disappear as diagenetic calcite approaches 100% (Barrera and Huber, 1990). Interspecific isotopic differences at Amboanio are relatively constant (Fig. 18), suggesting that diagenetic alteration was modest and that temperature trends are preserved (Schrag et al., 1995).

Oxygen isotope values are relatively constant through most of zone CF4 with a 1.5‰-surface-to-deep gradient. In the upper part of zone CF4, benthic and planktic $\delta^{18}O$ values increase and the surface-to-deep gradient is reduced. This suggests cooler temperatures that abruptly terminate at the CF4/CF3 hiatus (Fig. 18). Above the hiatus benthic and planktic $\delta^{18}O$ values decrease marking a return to warmer temperatures through zone CF3. A reduced surface-to-deep gradient in the upper part of zone CF3 and lower part of the CF2–CF1 interval suggests warmer bottom water temperatures and possibly a shallower environment (Figs. 4 and 18). $\delta^{18}O$ values in the zone CF2–CF1 interval show erratic fluctuations in planktic values that are likely due to post-depositional alteration and dissolution linked to subaerial exposure. Above the K–T boundary hiatus, whole rock $\delta^{18}O$ values of the Betsiboka limestone gradually decrease.

Carbon isotope values for the benthic species *Cibicidoides pseudoacuta* at Amboanio average about 1.2‰ during zone CF4, but gradually decrease during the upper part of CF4 to a low of 0.2‰ at the CF4/CF3 hiatus. Above the hiatus in zone CF3, $\delta^{13}C$ values average of 0.8‰ (Fig. 18). Planktic (*Rugoglobigerina rugosa*) $\delta^{13}C$ values show similar trends. The absence, or near-absence of a surface-to-deep carbon gradient at Amboanio is probably due to the shallow neritic depositional environment (deposition within photic zone). In the early Paleocene, whole rock carbon isotope values are 2‰ lighter. The 1‰ fluctuations may be related to hiatuses, subaerial exposure and karstification evident within the Betsiboka limestone sequence.

The successively lighter $\delta^{13}C$ trends from zone CF4 to CF3 of the late Maastrichtian suggest decreasing productivity beginning before the CF4/CF3 hiatus, or increased terrestrial organic influx. However, the latter is unlikely because measured TOC values are very low (average 0.6%) and decrease in CF3 (Fig. 8). The drop in $\delta^{13}C$ values in the early Paleocene above the K–T hiatus reflects the reduced surface productivity worldwide. Similar post-K–T negative $\delta^{13}C$ excursions have been observed in marine shelf and slope environments of Israel (Magaritz et al.,

Fig. 19. Maastrichtian to early Paleocene paleoenvironment of Madagascar and correlation with South Atlantic DSDP Site 525A located at similar paleolatitude. Sea level and climate changes based on Madagascar are shown in relationship with the global sea-level curve and the stable isotope record of Site 525A (Li and Keller, 1998a). Note that the global sea-level transgression began about 71 Ma. In the Berivotra type area a marine transgression is noted by the agradational Anembalemba Member followed by deposition of marine sediments of the Berivotra Formation. A conglomerate layer marks littoral high-energy conditions (ravinement surface), followed by fully marine conditions in zone CF6. Major hiatuses recognized at the CF3–CF4, the K–T, and early Paleocene (P1d, P2) may correspond to global sea-level lowstands. Relatively cool–temperate climate prevailed through most of the Maastrichtian, Mahajanga and Site 525A. The latest Maastrichtian short-term warm event (zone CF2–CF1) was not observed in Madagascar probably because this interval is incomplete due to an unconformity, subareal exposure and karstification.

1992), Tunisia (Keller and Lindinger, 1989), Bulgaria (Adatte et al., 2002), Denmark (Schmitz et al., 1992; Keller et al., 1993), Texas (Barrera and Keller, 1990), and various deep-sea localities (e.g. Boersma, 1984; Zachos et al., 1989; Alcalá-Herrera et al., 1992; Barrera and Keller, 1994).

8. Discussion

8.1. Biostratigraphy and age

The absence of systematic biostratigraphic, chronologic, and faunal studies in the Mahajanga Basin has hampered paleoenvironmental reconstruction of the region and correlation to the global climate regime. Marine deposits of the Berivotra Formation have generally been considered as of undifferentiated Maastrichtian, or late Maastrichtian age, followed by the Betsiboka limestone of Danian age (e.g. Janin et al., 1996; Bignot et al., 1996, 1998; Papini and Benvenuti, 1998; Rogers et al., 2000). Our detailed biostratigraphic study of planktic foraminifera augmented by calcareous nannofossils at the Berivotra type section and Amboanio provides good age control and permits correlation with sections in the Tethys and middle latitude South Atlantic DSDP Site 525A which was deposited at a similar paleolatitude.

Marine sediments of the Berivotra type section with age diagnostic microfossil assemblages span from the early Maastrichtian (~69.6 Ma; zone CF6) through the late Maastrichtian (zones CF2–CF1, *Micula prinsii*; Figs. 7 and 19). This interval is represented by seven planktic foraminiferal biozones defined by Li and Keller (1998a,b), six of which can be recognized in the Berivotra section. This high-resolution age control together with faunal, sedimentary and stratigraphic characteristics allows the identification of major hiatuses and disconformities, i.e. (1) the disconformity marked by the earliest Maastrichtian microconglomerate between the Anembalemba Member and Berivotra Formation; (2) the hiatus between planktic foraminiferal zones CF4/CF3 around 66.8 Ma; (3) the unconformity at the K–T boundary that spans part or all of the early Danian zones P0–Plc and part of the latest Maastrichtian (upper part of CF2–CF1, *M. prinsii*); (4) the disconformity and hardground in the lower Pld zone; and (5) the hiatus between zones P1d/P2 (Fig. 19). The ages of the CF4/CF3, K–T, and early Danian P1d/P2 hiatuses may correspond with major global sea-level drops at 67, 64.5, and 61.2 Ma, as noted by Haq et al. (1987) and by Li et al. (1999, 2000) based on continental shelf sequences in Tunisia (Fig. 19).

Age determinations for the terrestrial strata of the Anembalemba Member are more tentative and based on paleoclimatic and paleoenvironmental inferences, as well as the assumption of slow depositional rates, rather than major multi-million year hiatuses. In the Berivotra Formation type area, the terrestrial sediments of the Anembalemba Member are older than the early Maastrichtian zone CF6 (69.6 Ma) marine sediments of the overlying Berivotra Formation, and possibly as old as CF7–CF8b (71–69.6 Ma).

Rogers et al. (2000) assigned a late Maastrichtian age to the upper boundary of the Anembalemba Member in the Berivotra type area (Fig. 13), based largely on the assumption that the unit is time transgressive and hence younger to the southeast. They further concluded that the most vertebrate-rich faunas present in the Anembalemba Member (Krause et al., 1999) are of late Maastrichtian age and coeval with the dinosaur-bearing strata of the Deccan basalt province of India (65–67.5 Ma). Our age control of the Berivotra Formation in the type area, where most of the dinosaur-rich fossil assemblages were collected, rules out an age younger than earliest Maastrichtian. It is possible, however, that due to the southeast progressing marine transgression, the vertebrate fauna also migrated southeast in the early to late Maastrichtian, though no similar vertebrate-rich fossils assemblages have been reported to date from the Miadana Member to the southeast.

8.2. Paleoenvironment

During the early Maastrichtian a seasonally arid climate prevailed leading to mechanical erosion of the crystalline highlands to the southeast

and sediment accumulation in an alluvial plain populated by dinosaur-rich vertebrate faunas in the Berivotra Formation type area (Rogers et al., 2000; Fig. 19). Paleoclimatic information for this interval can also be obtained from the stable isotope record of DSDP Site 525A, located at a similar paleolatitude in the South Atlantic (Fig. 1). At Site 525A surface water temperatures decreased from 19 to 16°C during this time and bottom water temperatures reached maximum cooling by 71.3 Ma, coincident with a major global sea-level lowstand (Fig. 19; Barrera et al., 1997; Li and Keller, 1998a, 1999; Barrera and Savin, 1999).

A subsequent transgression (~71 Ma) appears to have reached the Berivotra type area during the earliest Maastrichtian, as first indicated by aggradational deposition of the Anembalemba Member, and later by the onset of marine conditions indicated by a microconglomerate (ravinement surface) at the base of the Berivotra Formation. From this time onward gradual deepening reached fully marine conditions by ~69.6 Ma, as indicated by well-developed marine plankton assemblages. Deepening continued through most of the late Maastrichtian, but was terminated at the hiatus at the CF4/CF3 zone boundary hiatus at about 66.8 Ma. Mineralogical data suggest a seasonally cool temperate climate in the Mahajanga Basin, similar to the cool climatic conditions indicated by the stable isotope data from DSDP Site 525A (Fig. 19).

The latest Maastrichtian at Site 525A is characterized by maximum cooling and a sea-level lowstand at 65.5 Ma (Li and Keller, 1998c). This event was followed by a short warm event between 65.2–65.4 Ma that has been recognized across latitudes (Li and Keller, 1998c; Kucera and Malmgren, 1998; Pardo et al., 1999), and may be related to the major Deccan volcanism between 65.2 and 65.4 Ma (Hoffmann et al., 2000). These events could not be identified in the Amboanio and Berivotra sections because of poor outcrop exposure, hiatuses, and poor preservation. However, volcanic ash is abundantly present in the uppermost 10 cm of the Maastrichtian at Amboanio and also in the lower part of the Betsiboka limestone (1.2 m) which is barren of microfossils and represents a very shallow early Danian environment as indicated by characteristic early Danian $\delta^{13}C$ values. Clay mineralogy indicates a warm and seasonally humid climate at this time. The marine environment deepened in the upper part of the Betsiboka limestone accompanied by seasonally arid climates.

9. Conclusions

Integrated microfossil biostratigraphy, based on quantitative and qualitative microfossil and macrofossil studies and sedimentologic, mineralogic and stable isotope analyses, provides new insights into the age, faunal changes, climate and sea-level fluctuations of the Maastrichtian to early Paleocene of the Mahajanga Basin of Madagascar. The following conclusions can be reached from this study.

(1) The terrestrial deposits and dinosaur-rich vertebrate fossils of the Anembalemba Member in the Berivotra type area are probably of earliest Maastrichtian age and predate ~69.6 Ma (zone CF6).

(2) Age control based on planktic foraminifera augmented by calcareous nannofossils indicates that the Berivotra Formation in the type area spans the early and late Maastrichtian. The overlying Betsiboka limestone is of early Danian age, as indicated by the characteristically low carbon isotope values relative to the underlying late Maastrichtian, and the presence of early Danian Pld planktic foraminiferal assemblages beginning 3.8 m above the base of the Betsiboka limestone

(3) The K–T boundary coincides with an unconformity between the brown marl at the top of the Berivotra Formation and the overlying white Betsiboka limestone. The K–T boundary is missing, and the hiatus spans the early Danian (zones P0, Pla, Plb and possibly Plc?), and part of the latest Maastrichtian CF2–CF1 or *Micula prinsii* zone interval.

(4) Sediments in the top 10 cm of the Berivotra Formation and the base of the Betsiboka limestone are rich in volcanic ash that may be related to the Deccan volcanic province.

(5) The early Maastrichtian marine transgres-

sion reached the Berivotra type area around ~71 Ma, gradually rising to middle neritic depths by 69.6 Ma (zone CF6). Very shallow marine environments mark the lower 3.8 m of the Betsiboka limestone, and represent a new sedimentary cycle with gradual deepening to fully marine conditions in the upper Danian.

Acknowledgements

We are greatly indebted to N. Wells who patiently introduced us to the geology, culture and politics of Madagascar. We thank J. Hartman, D. Krause, R. Rogers and S. Sampson for many discussions on the geology of the Mahajanga Basin, R. Rogers and S. Sampson for showing us around the Berivotra type area. We also thank M. Papini and M. Benvenuti for early discussions and advice, students from the University of Mahajanga for field support, and T. Fresquet, Technical Director of SANCA, for kindly authorizing the sampling of the Amboanio Quarry. We are grateful to Steven Culver and Chaim Benjamini for critical review, many helpful suggestions and discussions of the manuscript. This study was supported by National Geographic Society Grant 6121-98 (G.K.), BSF Grant 9800425 (G.K.), DFG STU 169/17-1 Grant (D.S.), DFG STI 128/4-1 (W.S.) and the Swiss National Science Fund 8220-028367 (T.A.).

Appendix 1. Abbreviations of taxonomical terms used in Plates III and IV

(Glossary of terms available at www.ucmp.berkeley.edu/people/jlipps/pubs,html.)

al, alar prolongation (of involute spiral chambers); can, canal system (always umbilical); cht, chamberlet lumen; ck, canaliferous keel; csp, canaliferous spine; f, intercamaeral foramen; ff, feathering (of septal sutures); lw, lateral wall (of spiral or orbitidal chambers resp. chamberlets); mw, median wall (between the two layers of orbitoidal chamberlets); per, (spiral) periphery of test; pi, piles (=‘granules’, ‘pillars’ etc.); pl, plate or umbilical wall (of spiral chamber); ppi, peripheral piles; pr, proloculus; s, septum; sa, annular septum (in *Omphalocyclus*); sb, septal bend; scl, spiral chamber lumen; sf, sutural furrow; val, ventral alar extension.

Appendix 2. Taxonomic remarks on illustrated taxa in Plates III and IV

Siderolites denticulatus (Douvillé) (Plate I, figs. 1–3): key reference Wannier (1983). The species is characterized by a keel bearing numerous radial canals and dividing the chamber lumen totally in adult growth stages. Thus, the adult spiral chambers are split in two independent chamberlets of elongate-sigmoidal outline reaching the axial pile in proximal direction.

Siderolites calcitrapoides (Lamarck) (Plate I, figs. 4–6): key reference Wannier (1983).

Omphalocyclus macroporus (Lamarck, 1816) Plate I, figs. 11–13): key reference Hottinger (1981). So far, there is only one species in this genus. Possibly, two successive species may be distinguished by their size of the proloculus, an earlier one in the Campanian, a later one in the Maastrichtian. The exact time-level of the replacement of the former by the latter depends on the concept of the limit Campanian–Maastrichtian. The forms from Madagascar belong to the smaller, earlier unit.

Orbitoides concavatus (Rahaghi) (Plate I, fig. 10): key reference Rahaghi (1976). This is a *Planorbulinella*-like discoidal form with orbitoidal chamberlet cycles. In contrast to *Omphalocyclus*, there is only a single layer of orbitoidal chamberlets. No thickening of the lateral chamberlet walls as observed in the earliest true orbitoids (Hofker, 1967).

Novum genus 1 nova species A (Plate I, figs. 7–9): dorsally evolute, ventrally involute spiral shells with ventral, adaxial alar prolongations similar to the dorsal ones in *Sirtina*. Foramen in marginal–inframarginal position as in *Sirtina* and in *Daviesina*. No tooth-like structure in the foramen, as in *Daviesina*. No folium; nature of the plate doubtful.

Operculina labanae (Visser), key reference is Visser (1951). The specimen is dorsally involute

and seems to lack any adaxial alar prolongations. The position of the foramen and the absence of a folium suggest further investigations on possible relations with the early Tertiary group of *Tremastegina–Amphistegina lopeztrigoi* and consorts.

Sirtina orbitoidiformis (Brönnimann and Wirz) (Plate II, figs. 1–3): key reference is Brönnimann and Wirz (1962). The generic definition produces considerable confusion by identifying the dorsal structures as lateral chamberlets, as in orbitoidiform larger foraminifera. In fact, these structures are long, almost tubular, curved or wavy alar prolongations supported by a series of dorsal piles. In axial sections, these alar prolongations are cut in oblique direction and produce intersections similar to lateral chamberlets. In the Campanian, similar forms with true lateral chamberlets (*Neumannites*, Rahaghi, 1976) are observed.

Sirtina nova species B (Plate II, figs. 4, 11–14): may be identical with *Operculina cretacea* (Reuss) in Hofker (1962, figures 1, 3 and 4) from Maastricht. Hofker (1962) does not show any details of the inner morphology of the test so that the question remains open. This form was interpreted by Hofker (1962) as microspheric generation of *Daviesina fleuriausi* because of its small proloculus. We do not follow this idea because in dimorphic species with shells of operculinid growth the accretion rate of the spiral radius always increases in the microspheric as compared to the megalospheric generation.

Daviesina fleuriausi (d'Orbigny) (Plate II, figs. 5–10): key references Visser (1951) and Hofker (1962). Dorsal alar prolongations as in *Sirtina* and a tooth-like structure partially subdividing the intercameral foramen, as in *Daviesina*. The latter structure has not been observed in the rather poorly preserved material from Madagascar. On the species level, the often angular backward bend of the septa far from the periphery of the test is diagnostic.

References

Abramovich, S., Keller, G., 2002. High stress upper Maastrichtian Paleoenvironment: Inference from planktic foraminifera in Tunisia. Palaeogeogr. Palaeoclimatol. Palaeoecol. in press.

Abramovich, S., Almogi-Labin, A., Benjamini, C., 1998. Decline of the Maastrichtian pelagic ecosystem based on planktic foraminiferal assemblage changes: Implications for the terminal Cretaceous faunal crisis. Geology 26, 63–66.

Adatte, T., Rumley, G., 1989. Sedimentology and mineralogy of Valanginian and Hauterivian in the stratotypic region (Jura mountains, Switzerland). In: Wiedmann, J. (Ed.), Cretaceous of the Western Tethys, Proceedings 3rd International Cretaceous Symposium. Scheizerbart, Stuttgart, pp. 329–351.

Adatte, T., W. Stinnsbeck, G. Keller, 1996. Lithostratigraphic and mineralogic correlations of near K–T boundary clastic sediments in northeastern Mexico: Implications for origin and nature of deposition. Geol. Soc. Am. Spec. Pap. 307, pp. 211–226.

Adatte, T., G. Keller, S. Burns, K.H. Stoykova, M.I. Ivanov, D. Vangelov, U. Kramar, D. Stüben, 2002. Paleoenvironment across the Cretaceous–Tertiary transition in eastern Bulgaria. Geol. Soc. Am. Spec. Pap. 356.

Alcalá-Herrera, J.A., Grossman, E.L., Gartner, S., 1992. Nannofossil diversity and equitability and fine fraction $\delta^{13}C$ across the Cretaceous–Tertiary at Walvis Ridge Leg 74, South Atlantic. Mar. Micropaleontol. 20, 77–88.

Barrera, E., Huber, B.T., 1990. Evolution of Antarctic waters during the Maastrichtian: Foraminifera oxygen and carbon isotope ratios, Leg 113. Proc. ODP Sci. Results 113, 813–827.

Barrera, E., Keller, G., 1990. Stable isotope evidence for gradual environmental changes and species survivorship across the Cretaceous/Tertiary boundary. Paleoceanography 5, 867–890.

Barrera, E., Keller, G., 1994. Productivity across the Cretaceous–Tertiary boundary in high latitudes. Geol. Soc. Am. Bull. 106, 1254–1266.

Barrera, E., Savin, S. M., 1999. Evolution of late Campanian–Maastrichtian marine climates and oceans. In: Barrera, E., Johnson, C.C. (Eds.), Evolution of the Cretaceous ocean–climate system. Geol. Soc. Am. Spec. Publ. 332, 245–282.

Barrera, E., Savin, S.M., Thomas, E., Jones, C.E., 1997. Evidence for thermohaline circulation reversals controlled by sea-level change in the latest Cretaceous. Geology 5, 715–718.

Berggren, W.A., Kent, D.V., Swisher, C.C., Aubry, M.P., 1995. A revised Cenozoic geochronology and chronostratigraphy. SEPM 54, 129–213.

Besairie, H., 1972. Géologie de Madagascar. I. Les terrains sédimentaires. Ann. Geol. Madag. 35, 1–463.

Bignot, G., Janin, M. C., Bellier, J. P., Randriamantenaosa, A., 1996. Modalités du passage K–T dans le region de Mahajanga (Madagascar W): the Cretaceous Tertiary boundary: biological and geological aspects. Séance Spécialisée Soc. Geol. France, Paris, p. 7.

Bignot, G., Bellier, J.P., Janin, M.C., Randriamanantenasoa, A., 1998. Modalités du passage K–T dans le region de Mahajanga (Madagascar W). Rev. Paléobiol., Genève 17, 531–539.

Boersma, A., 1984. Campanian through Paleocene paleotemperature and carbon isotope sequence and the Cretaceous–Tertiary boundary in the Atlantic Ocean. In: Berggren, W. A., Van Couvering, J.A., (Eds.), Catastrophes and Earth history. Princeton Univ. Press, Princeton, NJ, pp. 247–277.

Brönnimann, P., Wirz, A., 1962. New Maastrichtian Rotaliids from Iran and Lybia. Eclogae geol. Hel. 55, 519–528.

Caron, M., 1985. Cretaceous planktic foraminifera. In: Bolli, H. M., Saunders, J. B., Perch-Nielsen, K., (Eds.), Plankton Stratigraphy. Cambridge Univ. Press, Cambridge, pp. 17–86.

Chamley, H., 1989. Clay Sedimentology. Springer, Berlin.

Chamley, H., 1998. Clay mineral sedimentation in the Ocean. In: Paquet., H., Clauer, N. (Eds.), Soils and Sediments (Mineralogy and Geochemistry). Springer, Berlin, pp. 269–302.

Chave, A.D., 1984. Lower Paleocene Upper Cretaceous magnetostratigraphy, Sites 525, 527, 528 and 529, Deep Sea Drilling Project Leg 74. Int. Rep. DSDP 74, 525–531.

Debrabant, P., Fagel, N., Bout, V., Chamley, H., 1992a. Neogene and Quaternary clay mineral supply in the central Indian Basin. Con. Geol. Int. Res. 29, 719.

Debrabant, P., Chamley, H., Deconinck, J.F., Recourt, P., Trouiller, A., 1992b. Clay sedimentology, mineralogy and chemistry of Mesozoic sediments drilled in the northern Paris Basin. Sci. Drilling 3, 138–152.

Deconinck, J.F., 1992. Sédimentologie des argiles dans le Jurassique–Crétacé d'Europe occidentale et du Maroc. Mém. Habilit. Lille.

Deconinck, J.F., Chamley, H., 1995. Diversity of smectite origins in Late Cretaceous sediments; example of chalks from northern France. Clay Miner. 30, 365–379.

D'Hondt, S., Sigurdsson, H., Hanson, A., Carey, S., Pilson, M., 1994. Sulfate volatilization, surface-water acidification, and extinction at the KT boundary. In: K–T event and other catastrophes in Earth history. LPI, Houston, TX, 825, pp. 29–30.

Espitalié, J., Deroo, G., Marquis, F., 1986. La pyrolyse Rock–Eval et ses applications. Partie 3. Rev. Inst. France Petrol. 41, 1.

Forster, C.A., Chiappe, L.M., Krause, D.W., Sampson, S.D., 1996. The first Cretaceous bird from Madagascar. Nature 382, 532–534.

Gradstein, F.M., Agterberg, F. P., Ogg, J. G., Hardenbol, J., Van Veen, P., Thierry, J., Huang, Z., 1995. A Triassic, Jurassic and Cretaceous time scale. In: Berggren, W. A., Kent, D. V., Aubry, M. P., Hardenbol, J. (Eds.), Geochronology, Time Scales and Global Stratigraphic Correlation. SEPM, Spec. Publ. 54, pp. 95–128.

Haq, B.U., Hardenbol, J., Vail, P.R., 1987. Chronology of fluctuating sea levels since the Triassic. Science 235, 1156–1167.

Henriksson, A.S., 1993. Biochronology of the terminal Cretaceous calcareous nannofossil Zone of *Micula prinsii*. Cretac. Res. 14, 59–68.

Hoffmann, C., Feraud, G., Courtillot, V., 2000. 40Ar/39Ar dating of mineral separates and whole rocks from the Western Ghats lava pile: further constraints on duration and age of Deccan traps. Earth Planet Sci. Lett. 180, 13–27.

Hofker, J., Sr., 1962. The evolution of *Daviesina fleuriausi* (d'Orbigny) in the Maestrichtian Tuff Chalk. Natuurh. Maandbl. 51, 79–82.

Hofker, J., Jr., 1967. Primitive Orbitoides from Spain. Micropaleontology 13, 243–249.

Hottinger, L., 1966. Foraminifères benthoniques du bassin côtier de Tarfaya. Mem. Serv. Geol. Morocco 175, 181–232.

Hottinger, L., 1981. Functions of the alternating disposition of chambers in foraminifera and the structure of Omphalocyclus. Cah. Micropaleontol. 4, 45–55.

Hottinger, L., Caus, E., 1993. Praestorrsella roestae (Visser), a foraminiferal index fossil for Late Cretaceous deeper neritic deposits. Zitteliana 20, 213–221.

Janin, M. C., Bignot, G., Bellier, J. P., Randriamantenaosa, A., 1996. Remarques sur la signification biologique du renouvellement des nannofossiles calcaires au passage Cretace/Tertiare: exemple du basin de Mahajanga (Madagascar Ouest). The Cretaceous–Tertiary boundary: biological and geological aspects. Séance Spécialisée Soc. Geol. France, Paris, p. 30.

Keller, G., 1988. Extinction, survivorship and evolution of planktic foraminifera across the Cretaceous/Tertiary boundary at El Kef, Tunisia. Mar. Micropaleontol. 13, 239–263.

Keller, G., 1989. Extended Cretaceous/Tertiary boundary extinctions and delayed population change in planktonic foraminifera from Brazos River, Texas. Paleoceanography 4, 287–332.

Keller, G., 1993. The Cretaceous/Teriary boundary transition in the Antarctic Ocean and its global implications. Mar. Micropaleontol. 21, 1–45.

Keller, G., 2002. *Guembelitria*-dominated late Maastrichtian planktic foraminiferal assemblages mimic early Danian in Central Egypt. Mar. Micropaleontol. X-ref: S0377-8398(02)00116-0.

Keller, G., Lindinger, M., 1989. Stable isotopes, TOC and CaCO3 records across the Cretaceous–Tertiary boundary at El Kef, Tunisia. Palaeogeogr., Palaeoclimatol., Palaeoecol. 73, 243–265.

Keller, G., Benjamini, C., 1991. Paleoenvironment of the eastern Tethys in the Early Paleocene. Palaios 6, 439–464.

Keller, G., Barrera, E., Schmitz, B., Matsson, E., 1993. Gradual mass extinction, species survivorship, and long term environmental changes across the Cretaceous–Tertiary boundariy in high latitudes. Geol. Soc. Am. Bull. 105, 979–997.

Keller, G., Li, L., MacLeod, N., 1995. The Cretaceous/Tertiary boundary stratotype section at El Kef, Tunisia: How catastrophic was the mass extinction? Palaeogeogr. Palaeoclimatol. Palaeoecol. 119, 221–254.

Keller, G., Adatte, T., Stinnesbeck, W., Stuben, D., Kramar, U., Berner, Z., Li, L., von Salis Perch-Nielsen, K., 1998. The Cretaceous–Teriary transition on the shallow Sharan platform of southern Tunisia. Geobios 30, 951–975.

Keller, G., Adatte, T., Stinnesbeck, W., Luciani, V., Karoui-Yaakoub, N., Zaghbib-Turki, D., 2002. Paleoecology of the Cretaceous–Tertiary mass extinction in planktic foraminifera. Palaeogeogr. Palaeoclimatol. Palaeoecol. 178, 257–297.

Killingley, J.S., 1983. Effect of diagenetic recrystallization on $^{18}O/^{16}O$ values of deep sea sediments. Nature 301, 594–597.

Krause, D.W., Hartman, J.H., 1996. Late Cretaceous fossils from Madagascar and their implications for biogeographic relationships with the Indian subcontinent. In: Sahni, A., (Ed.), Cretaceous Stratigraphy and Palaeoenvironments. Mem. Geol. Soc. India 37, pp. 135–154.

Krause, D.W., Hartman, J.H., Wells, N.A., 1997. Late Cretaceous vertebrates from Madagascar: implications for biotic changes in deep time. In: Goodman, S.D., Patterson, B.D. (Eds.), Natural change and human impact in Madagascar. Smithsonian Inst., Washington, DC, pp. 3–43.

Krause, D.W., Rogers, R.R., Forster, C.A., Hartman, J.H., Buckley, G.A., Sampson, S.D., 1999. The late Cretaceous vertebrate fauna of Madagascar: implications for Gondwana paleobiogeography. GSA Today 8, 1–7.

Kucera, M., Malmgren, B.A., 1998. Terminal Cretaceous warming event in the mid-latitude South Atlantic Ocean: evidence from poleward migration of Contusotruncana contusa (planktonic foraminifera) morphotypes. Palaeogeogr. Palaeoclimatol. Palaeoecol. 138, 1–15.

Kübler, B., 1983. Dosage quantitatif des mineraux majeurs des roches sedimentaires par diffraction X. Cahiers l'Institut de Geologie de Neuchatel, Suisse, Serie ADX 1, p. 12.

Kübler, B., 1987. Crisallinite de l'illite, methodes normalisées de preparations, methodes normalisees de mesures. Cahiers l'Institut de Geologie de Neuchatel, Suisse, Serie ADX 1, p. 13.

Lafargue, E., Espitalié, J., Marquis, F., Pillot, D., 1996. Rocal–Eval 6, Applications in Hydrocarbon Exploration, Production and Soil Contamination Studies. Vinci Technologies, Rock-Eval.

Li, L., Keller, G., 1998a. Maastrichtian climate, productivity and faunal turnovers in planktic foraminifera in south Atlantic DSDP Sites 525 and 21. Mar. Micropaleontol. 33, 55–86.

Li, L., Keller, G., 1998b. Diversification and extinction in Campanian–Maastrichtian planktic foraminifera of Northwestern Tunisia. Eclogae geol. Helv. 91, 75–102.

Li, L., Keller, G., 1998c. Abrupt deep-sea warming at the end of the Cretaceous. Geology 26, 995–999.

Li, L., Keller, G., 1999. Variability in late Cretaceous climate and deep waters: evidence from stable isotopes. Mar. Geol. 161, 171–190.

Li, L., Keller, G., Stinnesbeck, W., 1999. The Late Campanian and Maastrichtian in northern Tunisia: palaeoenvironmental inferences from lithology, macrofauna and benthic foraminifera. Cretac. Res. 20, 231–252.

Li, L., Keller, G., Adatte, T., Stinnesbeck, W., 2000. Late Cretaceous sea-level changes in Tunisia: a multi-disciplinary approach. J. Geol. Soc. London 157, 447–458.

Luciani, V., 1997. Planktonic foraminiferal turnover across the Cretaceous–Tertiary boundary in the Vajont valley (Southern Alps, northern Italy). Cretac. Res. 18, 799–821.

Luciani, V., 2002. High resolution planktonic foraminiferal analysis from the Cretaceous/Tertiary boundary at Ain Settara (Tunisia): Evidence of an extended mass extinction. Palaeogeogr. Palaeoclimatol. Palaeoecol. (in press).

MacLeod, N., 1993. The Maastrichtian–Danian radiation of triserial and biserial planktic foraminifera: Testing phylogenetic and adaptational hypotheses in the (micro) fossil record. Mar. Micropaleontol. 21, 47–100.

MacLeod, N., Keller, G., 1991a. Hiatus distribution and mass extinction at the Cretaceous/Tertiary boundary. Geology 19, 497–501.

MacLeod, N., Keller, G., 1991b. How complete are the K–T boundary sections? Geol. Soc. Am. Bull. 103, 1439–1457.

Magaritz, M., Benjamini, C., Keller, G., Moshkovitz, S., 1992. Early diagenetic isotopic signal at the Cretaceous/Tertiary boundary, Israel. Palaeogeogr. Palaeoclimatol. Palaeoecol. 91, 291–304.

Manivit, H., 1984. Paleocene and upper Cretaceous calcareous nannofossils from Deep Sea Drilling Project Leg 74. Init. Rep. DSDP 74, 475–501.

Martini, E., 1971. Standard Tertiary and Quaternary calcareous nannoplankton zonation. Proc. II Planktonic Conf. Roma, 1970, 2, pp. 739–785.

Millot, G., 1970. Geology of Clays. Springer, Berlin.

Monaco, A., Mear, Y., Murat, A., Fernandez, J.M., 1982. Critères mineralogiques pour la reconnaissance des turbidites fines. C.R. Acad. Sci. Paris 295, 43–46.

Nederbragt, A., 1991. Late Cretaceous biostratigraphy and development of *Heterohelicidae* (planktic foraminifera). Micropaleontology 37, 329–372.

Odin, G.S., 2001. The Campanian–Maastrichtian boundary: correlation from Tercis (Lades, SW France) to Europe and other continents. In: Odin, G.S. (Ed.), The Campanian–Maastrichtian Stage Boundary. Characterization at Tercis les Bains (France) and Correlation with Europe and Other Continents. Elsevier, Amsterdam, pp. 805–819.

Papini, M., Benvenuti, M., 1998. Lithostratigraphy, sedimentology and facies architecture of the Late Cretaceous succession in the central Mahajanga Basin, Madagascar. J. Afr. Earth Sci. 26, 229–247.

Pardo, A., Ortiz, N., Keller, G., 1996. Latest Maastrichtian foraminiferal turnover and its environmental implications at Agost, Spain. In: MacLeod, N., Keller, G., (Eds.), Cretaceous–Tertiary Boundary Mass Extinction: Biotic and Environmental Changes. Norton, New York, pp. 139–172.

Pardo, A., Adatte, T., Keller, G., Oberhaensli, H., 1999. Paleoenvironmental changes across the Cretaceous–Tertiary boundary at Koshak, Kazakhstan, based on planktic foraminifera and clay mineralogy. Palaeogeogr. Palaeoclimatol. Palaeoecol. 154, 247–273.

Perch-Nielsen, K., Pomerol, Ch., 1973. Nannoplancton calcaire à la limite K–T dans le basin de Majunga (Madagascar). C.R. Acad. Sci. Paris, 276, pp. 2435–2438.

Rahaghi, A., 1976. Nummulites and Assilina from northern Iran. Eclogae geol. Helv. 69, 765–782.

Reiss, Z., Hottinger, L., 1984. The Gulf of Aqaba–Ecological Micropaleontology. Ecol. Stud. 50, 1–345.

Robaszynski, F., Caron, M., Gonzales Donoso, J.M., Wonders, A.A.H., 1983. Atlas of Late Cretaceous Globotruncanids. Rev. Micropaleontol. 26, 145–305.

Robert, C., Chamley, H., 1991. Development of early Eocene

warm climates as inferred from clay mineral variations in oceanic sediments. Glob. Planet. Change 89, 315–331.

Robert, C., Kennett, J.P., 1994. Antarctic subtropical humid episode at the Paleocene–Eocene boundary: Clay mineral evidence. Geology 22, 211–214.

Rogers, R.R., Hartman, J.H., Krause, D.W., 2000. Stratigraphic analysis of upper Cretaceous rocks in the Mahajanga Basin, northwestern Madagascar: Implications for ancient and modern faunas. J. Geol. 108, 275–301.

Rögl, F., Von Salis, K., Preisinger, A., Aslanian, S., Summesberger, H., 1996. Stratigraphy across the Cretaceous/Paleogene boundary near Bjala, Bulgaria. Bull. Centres. Rech. Explo.-Prod. Elf. Aquitaine Mem. 16, 673–683.

Sampson, D.S., Witmer, L.M., Forster, C.A., Krause, D.W., O'Connor, P.M., Dodson, F.R., 1998. Predatory dinosaur remains from Madagascar: implications for the Cretaceous biogeography of Gondwana. Science 280, 1048–1051.

Schmitz, B., Keller, G., Stenvall, O., 1992. Stable isotope and foraminiferal changes across the Cretaceous–Teriary boundary at Stevens Klint, Denmark: Arguments for long term oceanic instability before and after bolide impact event. Palaeogeogr. Palaeoclimatol. Palaeoecol. 96, 233–260.

Schrag, D.P., DePaolo, D.J., Richter, F.M., 1995. Reconstructing past sea surface temperatures; correcting for diagenesis of bulk marine carbon. Geochim. Cosmochim. Acta 59, 2265–2278.

Smit, J., 1982. Extinction and evolution of planktic foraminifera after a major impact at the Cretaceous/Tertiary boundary. Earth Planet. Sci. Lett. 74, 155–170.

Smit, J., 1990. Meteorite impact, extinctions and the Cretaceous/Tertiary boundary. Geol. Mijnb. 69, 187–204.

Smith, C.C., Pessagno, E.A. Jr., 1973. Planktonic foraminifera and stratigraphy of Corsicana Formation (Maastrichtian) north–central Texas.. Contr. Cushman Found. Foraminiferal Res. Spec. Publ. 12, 5–66.

Stinnesbeck, W., Keller, G., de la Cruz, J., de León, C., MacLeod, N., Whittaker, J.E., 1997. The Cretaceous–Tertiary transition in Guatemala: limestone breccia deposits from the South Petén basin. Geol. Rundsch. 86, 686–709.

Storey, M., Mahoney, J.J., Saunderes, A.D., 1997. Cretaceous basalts in Madagascar and the transition between plume and continental lithosphere mantle sources. Large Igneous Provinces continental, oceanic, and planetary flood volcanism. Am. Geophys. Union Geophys. Monogr. 100, 95–122.

Tantawy, A. A., Keller, G., Adatte, T., Stinnesbeck, W., Kassab, A., Schulte, P., 2002. Maastrichtian to Paleocene (Dakhla Formation) depositional environment of the Western Desert in Egypt: Sedimentology, Mineralogy, and integrated micro- and macrofossil biostratigraphies. Cretaceous Res. (in press).

Thiry, M., 2000. Palaeoclimatic interpretation of clay minerals in marine deposits; an outlook from the continental origin. Earth Sci. Rev. 49, 201–221.

Visser, A. M., 1951. Monograph on the Foraminifera of the type-locality of the Maestrichtian (South-Limburg, Netherlands). Leidse Geologische Mededelingen, Rijksmuseum van Geologie en Mineralogie, Leiden, pp. 197–331.

Wannier, M., 1983. Evolution, biostratigraphie et systematique des Siderolitinae (foraminifers). Rev. Esp. Micropaleontol. 15, 5–37.

Weaver, C.E., 1989. Clays, muds and shales, Development in sedimentology, 44. Elsevier, Amsterdam.

Zachos, J.C., Arthur, M.A., Dean, W.E., 1989. Geochemical evidence for suppression of pelagic marine productivity at the Cretaceous/Tertiary boundary. Nature 337, 61–67.